I. INTRODUCTION

The need for more accurate microstrip circuit simulations has become apparent with the recent interest in millimeter-wave and near millimeter-wave frequencies. The development of more accurate microstrip discontinuity models is very important in improving high frequency circuit simulations. In most applications, the circuits are enclosed in a shielding cavity as shown in Figure 1. This cavity may be considered as a section of a waveguide terminated at both ends. The presence of the shielding cavity affects the performance of the circuit (shielding effects) and has to be taken into consideration.

It has been shown [1] - [2] that one condition where shielding effects are significant is when the frequency approaches the cut-off frequency of the waveguide's dominant mode. In most cases, microstrip circuits including active devices are printed on multilayer structures which consist of a combination of dielectric and semi-conducting materials. The existance of these conducting layers can affect the characteristicts of the loaded cavity and, therefore, of the printed circuits. As it has been pointed out by many authors [3] - [5], the propagation characteristics of higher-order shielded-microstrip modes are very similar to those of the shielding cavity. Consequently, a good understanding of how microstrip modes propagate may be gained by just studying the dielectric-slab loaded waveguide.

In this report we consider the case of a single semi-conducting layer with a dopping density N_D which varies from

10^{14} to 10^{16} and we study the effect of this variation on the cutoff frequencies of the waveguide modes. Conclusions drawn from this study show a very interesting behavior in the propagation characteristics of the modes and may be extended to the case of the shielded microstrip.

II. THEORETICAL FORMULATION

Figure 1 in Appendix I shows a basic description of the loaded waveguide. The modes excited in this structure are LSE and LSM and their characteristic equations which may be derived by applying the transverse resonance condition [6] are shown below:

$$\frac{k_{x1}}{\varepsilon_1} \tan (k_{x1} h) = - \frac{k_{x2}}{\varepsilon_2} \tan \left[k_{x2} (a-h) \right] \qquad \text{LSM} \qquad (1)$$

$$\frac{k_{x1}}{\mu_1} \cot (k_{x1} h) = - \frac{k_{x2}}{\mu_2} \cot \left[k_{x2} (a-h) \right] \qquad \text{LSE} \qquad (2)$$

The eigenvalues k_{x1} and k_{x2} are given by

$$k_{x1}^2 + k_y^2 + k_z^2 = \omega^2 \varepsilon_1 \mu_1 \qquad (3)$$

$$k_{x2}^2 + k_y^2 + k_z^2 = \omega^2 \varepsilon_2 \mu_2 \qquad (4)$$

with

$$k_y = \frac{n\pi}{b}$$

$$\varepsilon_1 = \varepsilon_1' (1 - j\tan\delta_1) \qquad (5)$$

$$\varepsilon_2 = \varepsilon_2' (1 - j\tan\delta_2) \qquad (6)$$

and

$$\tan\delta_2 = 0$$

$$\tan\delta_1 = \frac{eN_D}{w\varepsilon_1'} \quad . \tag{7}$$

In equation (7), e is the charge of an electron and N_D is the doping density of the material. For the case a perfect dielectric layer, cut-off is defined by $k_z=0$. However, when $\tan\delta$ is different than zero, the cut-off condition is modified to the following

$$\mathrm{Re}\ (k_z) = 0 \tag{8}$$

This condition imposed on equations (3), (4) can give:

$$k_{x1}^2 = \omega^2\varepsilon_1'\mu_1\ (1 - j\tan\delta_1) - a_z^2 - k_y^2 \tag{9}$$

and

$$k_{x2}^2 = \omega^2\varepsilon_2\mu_2 - a_z^2 - k_y^2 \tag{10}$$

By substracting equation (9) from (10) we can derive a relation between k_{x1} and k_{x2} which does not include the eigenvalue k_y and the attenuation constant at cut-off a_z:

$$k_{x1}^2 - k_{x2}^2 = \omega^2\left[\varepsilon_1'\mu_1\ (1 - j\tan\delta_1) - \varepsilon_2\mu_2\right] \tag{11}$$

The solution of the sets ((1),(11)) or ((2),(11)) can be performed only numerically and results in infinite many but descrete

eigenvalue pairs $(k_{x1}, k_{x2})_m$ which vary with ω and n. The frequency which satisfies (8) for a given pair $(k_{x1}, k_{x2})_m$ and $k_y = n\pi/b$ is the cut-off frequency of the mn mode. This procedure is rather complicated and requires extensive computation. To avoid this shortcoming the cut-off condition is modified to

$$k_z = 0 \tag{12}$$

Equation (12) together with (3) and (4) transforms the characteristic equation into a complex equation for ω resulting in complex cut-off frequencies. The real part of this cut-off frequency will be exactly equal to the one that condition (8) would give. However, the imaginary part which, in general, is about an order of magnitude smaller than the real, compensates for the neglected attenuation at cut-off and is disregarded. The results derived during this study are based on the second condition.

III. NUMERICAL SOLUTION

Numerical solution of the characteristic equation was achieved with Muller's Method [7] which is iterative in nature and requires a good initial guess for fast convergence. Furthermore, when solving for cut-off frequencies there may be a number of solutions to the characteristic equation in a relatively narrow frequency space. To overcome this problem, a method was developed to track a given mode through increasting doping densities. That

is, the solution for the cut-off for a given mode is determined first for no losses where zeros are spread further apart and this solution is used as the initial guess as the tanδ is slightly increased. The numerical solution for the lossless case proved to be much more simple than the lossy one. The characteristic equation was solved with the bistatic method [7].

IV. RESULTS AND CONCLUSION

The results derived using the technique described above are plotted in figures (1) - (34) and are for the waveguide geometries of Table 1 in Appendix II. From these results it can be concluded that the effect of the conductivity in the dielectric layer can be tremendous. In some cases, as the doping density increases from 10^{14} to 10^{16} there seems to be a switching of dominant modes. That is, higher order modes tend to exhibit a lower cut-off than the mode which was dominant at lower N_D resulting in much lower cut-off frequencies. In addition, for other geometries, increasing conductivity seems to have an opposite effect.

Presently, we are trying to investigate the effect of the presence of semi-conducting materials on the modes of a shielded microstrip printed on single, as well as multi-layer substrates.

APPENDIX I

Computation of the cut-off frequencies for the case of a non-conducting layer:

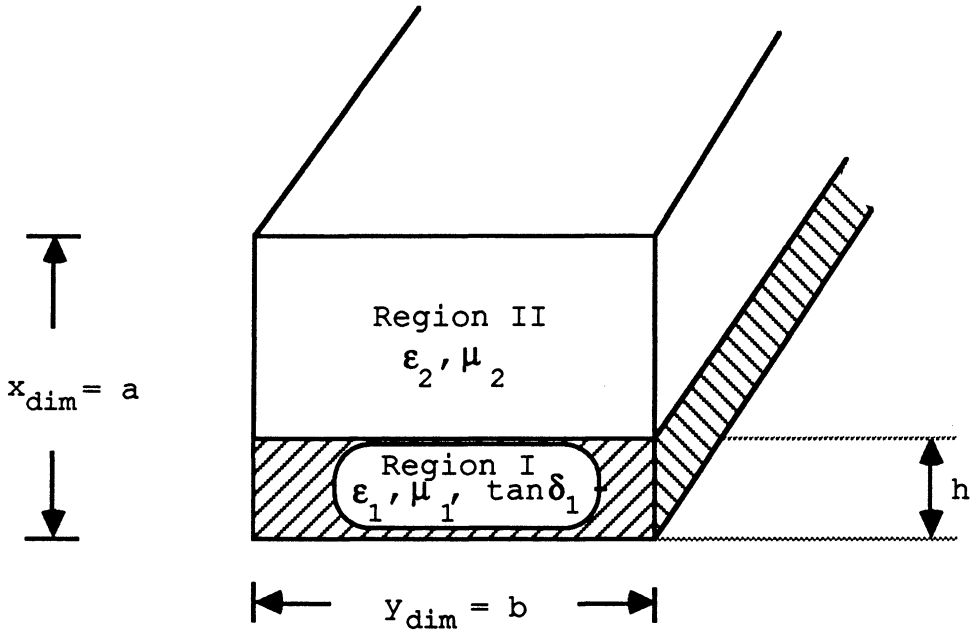

$$d = a-h$$

$$k_{x1}^2 + k_y^2 + k_z^2 = \omega^2 \varepsilon_1 \mu_1$$

$$k_{x2}^2 + k_y^2 + k_z^2 = \omega^2 \varepsilon_2 \mu_2$$

For LSM, LSE k_z is set to zero to determine the cut-off frequency.

The dominant LSM mode corresponds to TE_{01} $\therefore$ $k_y = \pi/b$

The dominant LSE mode corresponds to TE_{10} $\therefore$ $k_y \triangleq 0.0$

Determining the next higher order mode:

LSM: Interation begins assuming a lower bound which was the cut-off frequency for the dominant mode.

Two possibilities are tested:

(i) $M = 0, \quad N = 2$
$(i.e., \; k_y = 2\pi/b)$

(ii) $M = 1, \quad N = 1$
$(i.e., \; k_y = \pi/b)$

whichever case yields the lowest f_c is taken as the next higher mode.

LSE: Similar to the above, using instead the following two cases:

(i) $M = 2, \quad N = 0$
$(i.e., \; k_y = 0.0)$

(ii) $M = 1, \quad N = 1$
$(i.e., \; k_y = \pi/b)$

Iteration for dominant mode solution:
(Lossless dielectric)

LSM: A lower bound is determined by the following:

$F_{o_{01}} = c/Zb \triangleq TE_{01}$ cut-off for air-filled WG.

with c the velocity of light in free space.

$$F_{d_{01}} = \frac{F_{o_{01}}}{\sqrt{\varepsilon_{r1}}} \triangleq TE_{01} \text{ cut-off for completely filled WG.}$$

$F_{d_{01}}$ is used as the lower bound.

LSE: Similar to the above, using

$F_{o_{01}} = c/Za \triangleq TE_{10}$ cut-off for air-filled WG.

APPENDIX II

Group A Plots

Symbol definition:

Symbol	Mode
	LSM1
*	LSM2
Δ	LSE1
+	LSE2

TABLE 1

Waveguide Parameters:			Substrate Parameters	
Plot #	a (in)	b (in)	h (in)	ε_{r1}
1	.305	.305	.15	3.0
2	.305	.305	.08	3.0
3	.305	.305	.025	3.0
4	.305	.305	.025	12.0
5	.305	.305	.025	16.0
6	.25	.305	.08	3.0
7	.25	.305	.08	12.0
8	.25	.305	.08	16.0
9	.305	.25	.08	3.0
10	.305	.25	.08	12.0
11	.305	.25	.08	16.0

GROUP A

"Cut-off frequencies vs. tanδ for LSE and LSM modes"

CUTOFF FREQUENCY .VS. LOSS TANGENT #1

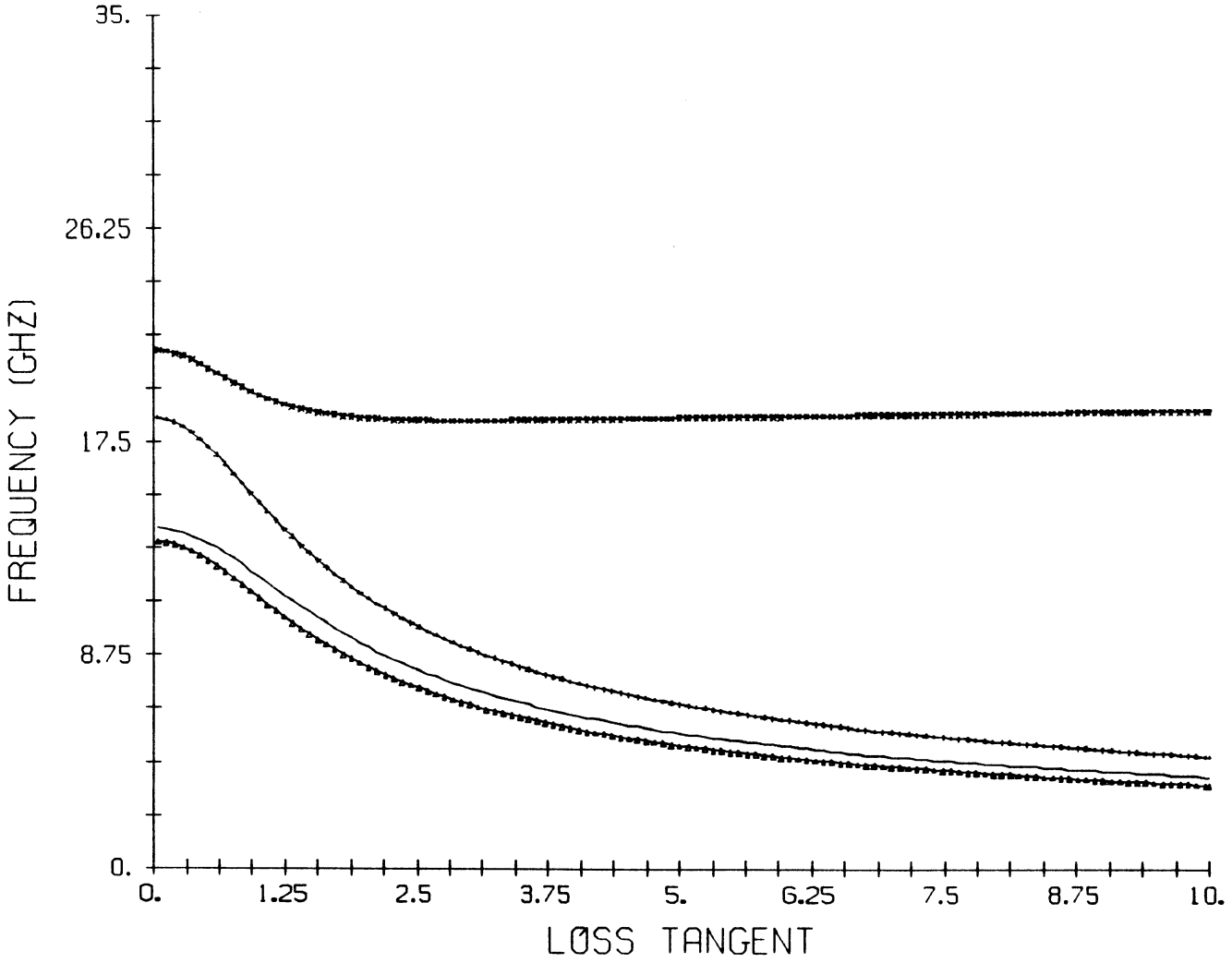

21-APR-88
20:11:34

CUTØFF (REAL AND IMAG) .VS. LØSS TANGENT FØR LSM #1

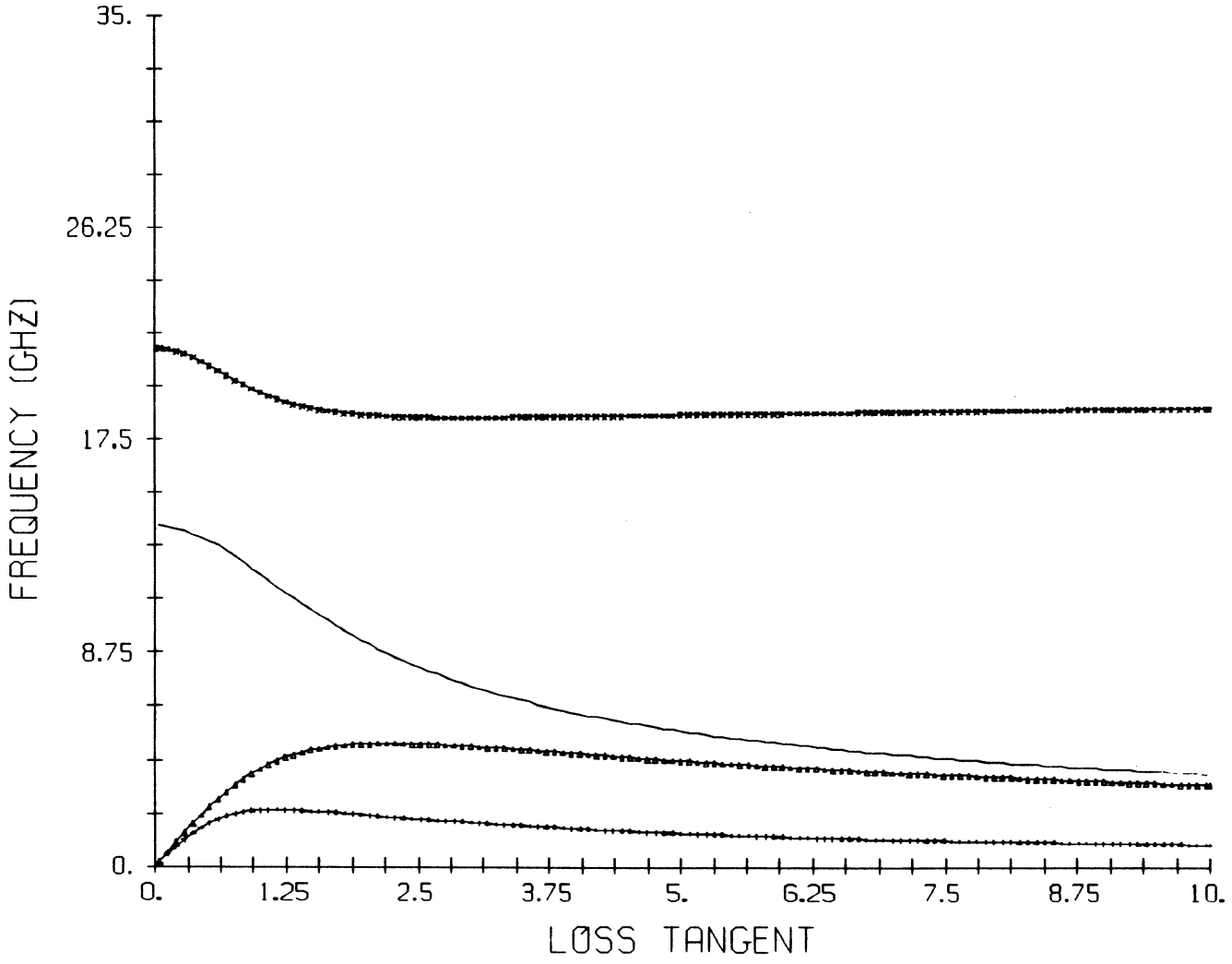

21-APR-88
20:11:52

CUTØFF (REAL AND IMAG) .VS. LØSS TANGENT FØR LSE #1

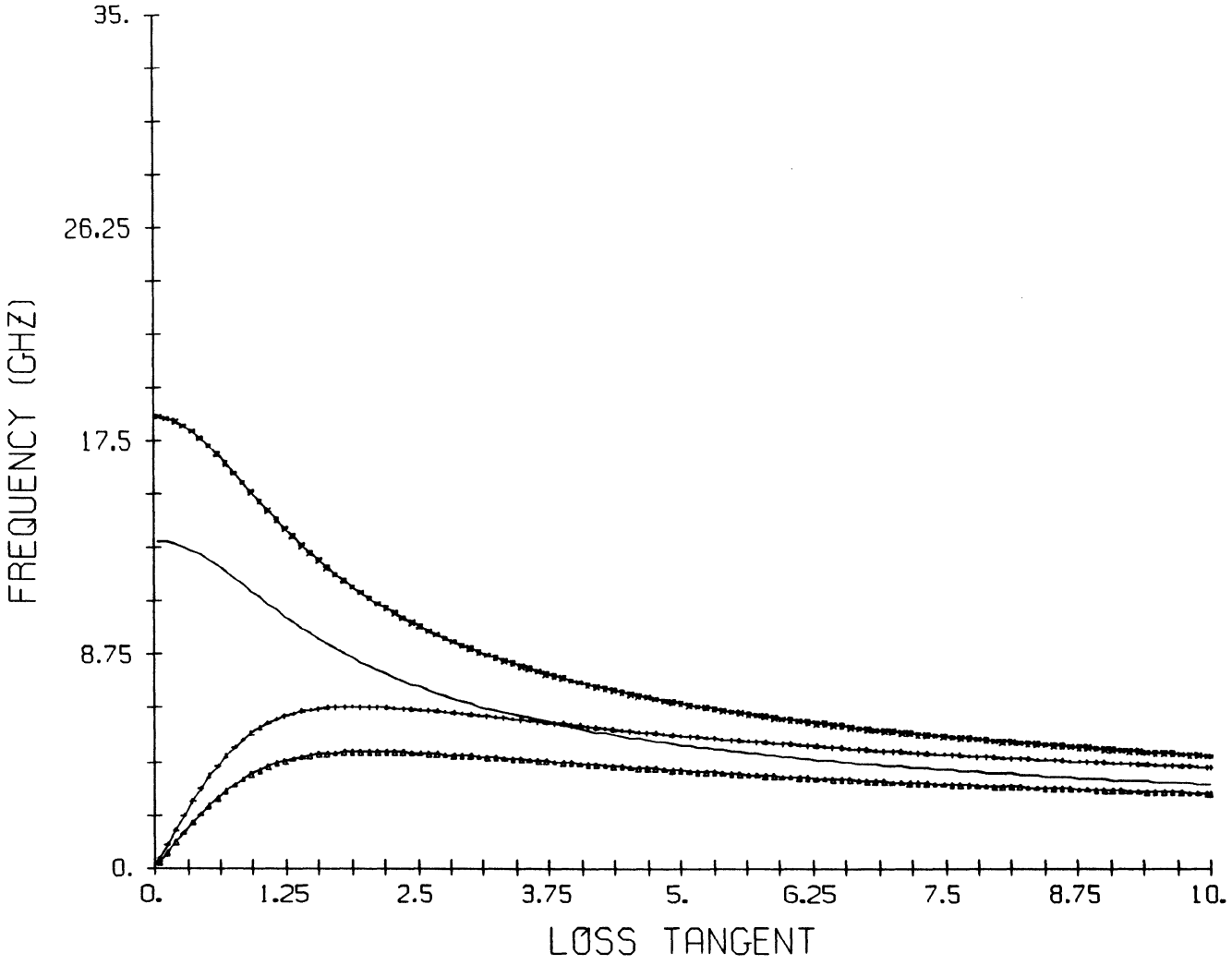

21-APR-88
20:18:56

CUTØFF FREQUENCY .VS. LØSS TANGENT #2

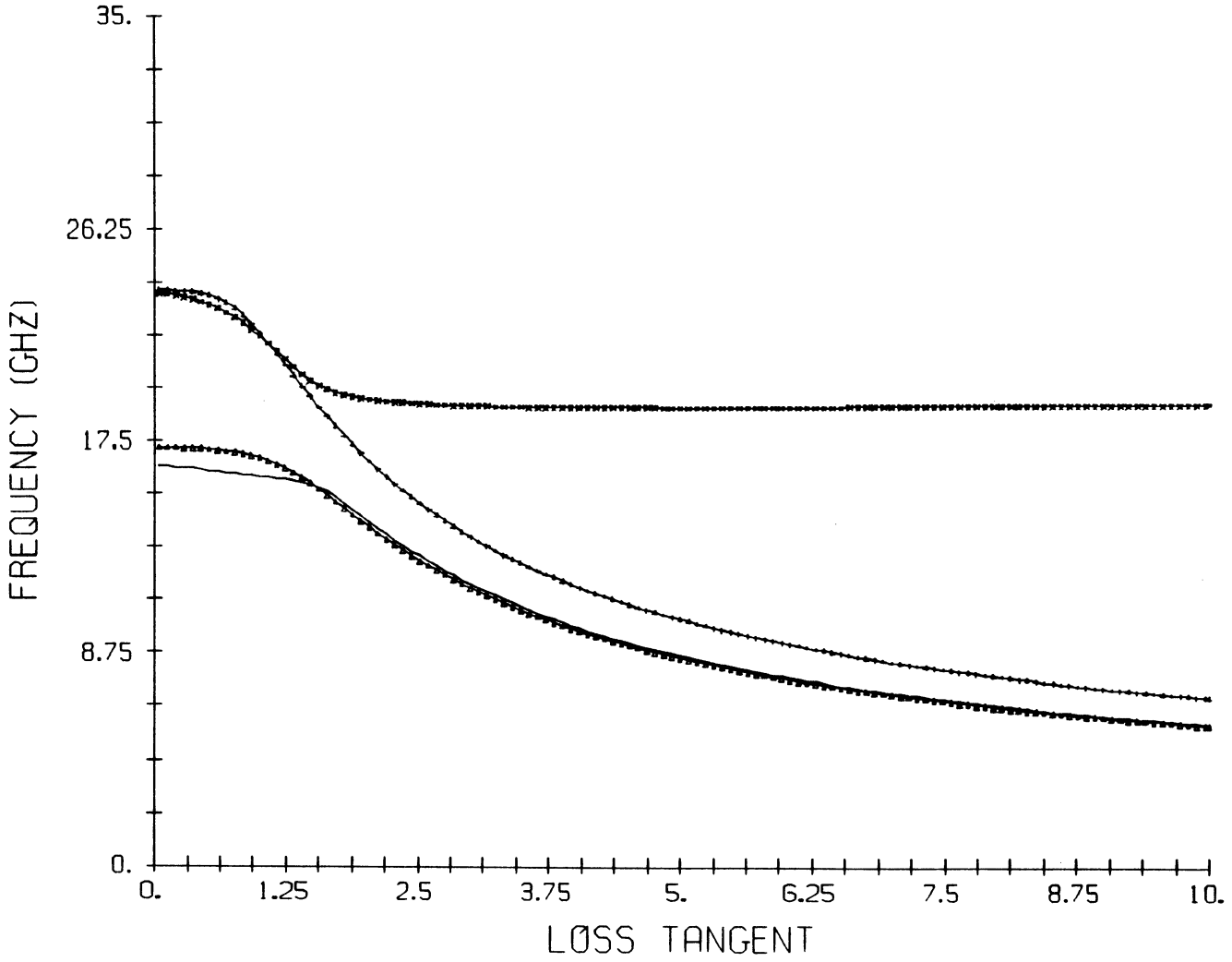

21-APR-88
20:19:10

CUTØFF (REAL AND IMAG) .VS. LØSS TANGENT FØR LSM #2

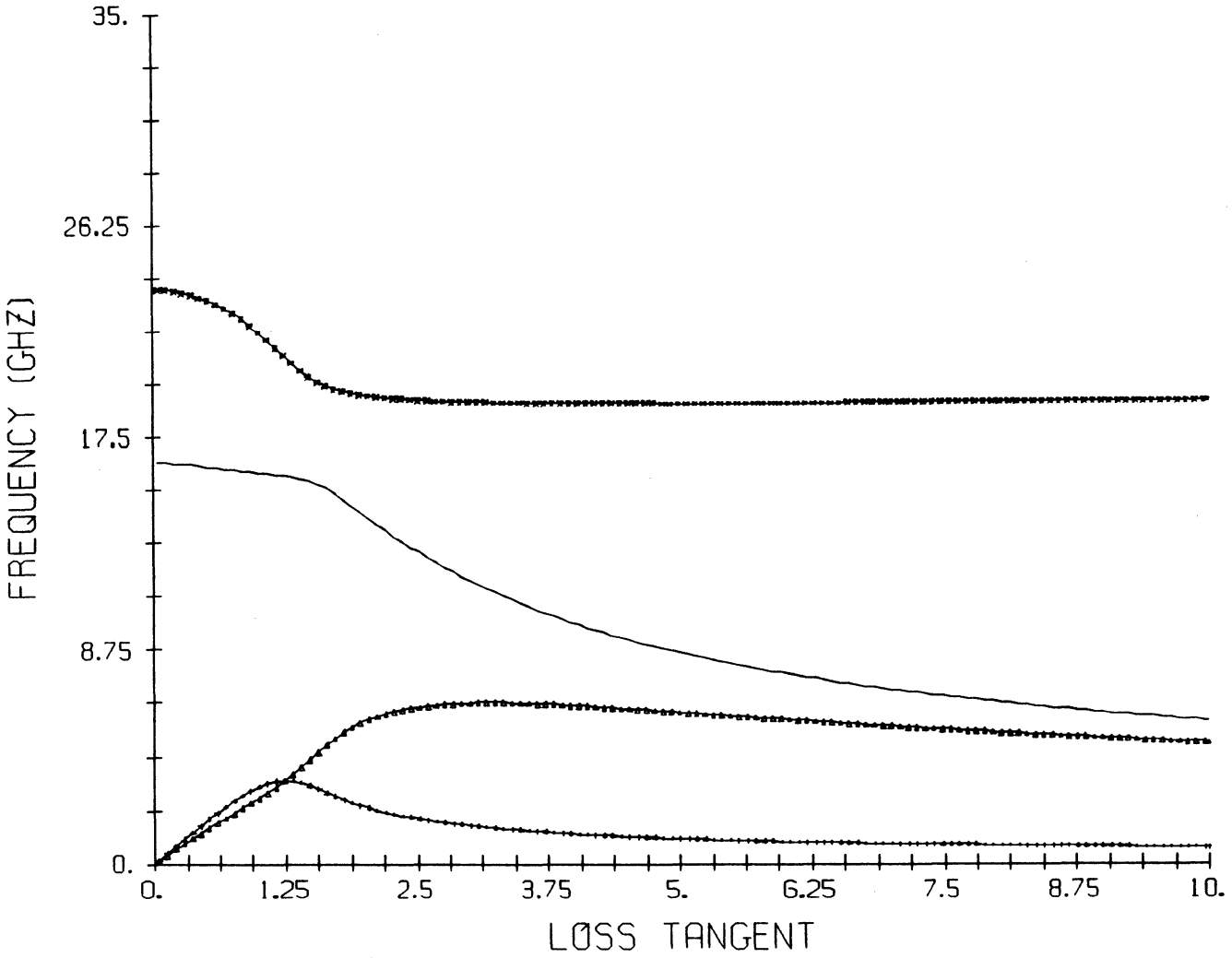

21-APR-88
20:19:21

CUTØFF (REAL AND IMAG) .VS. LØSS TANGENT FØR LSE #2

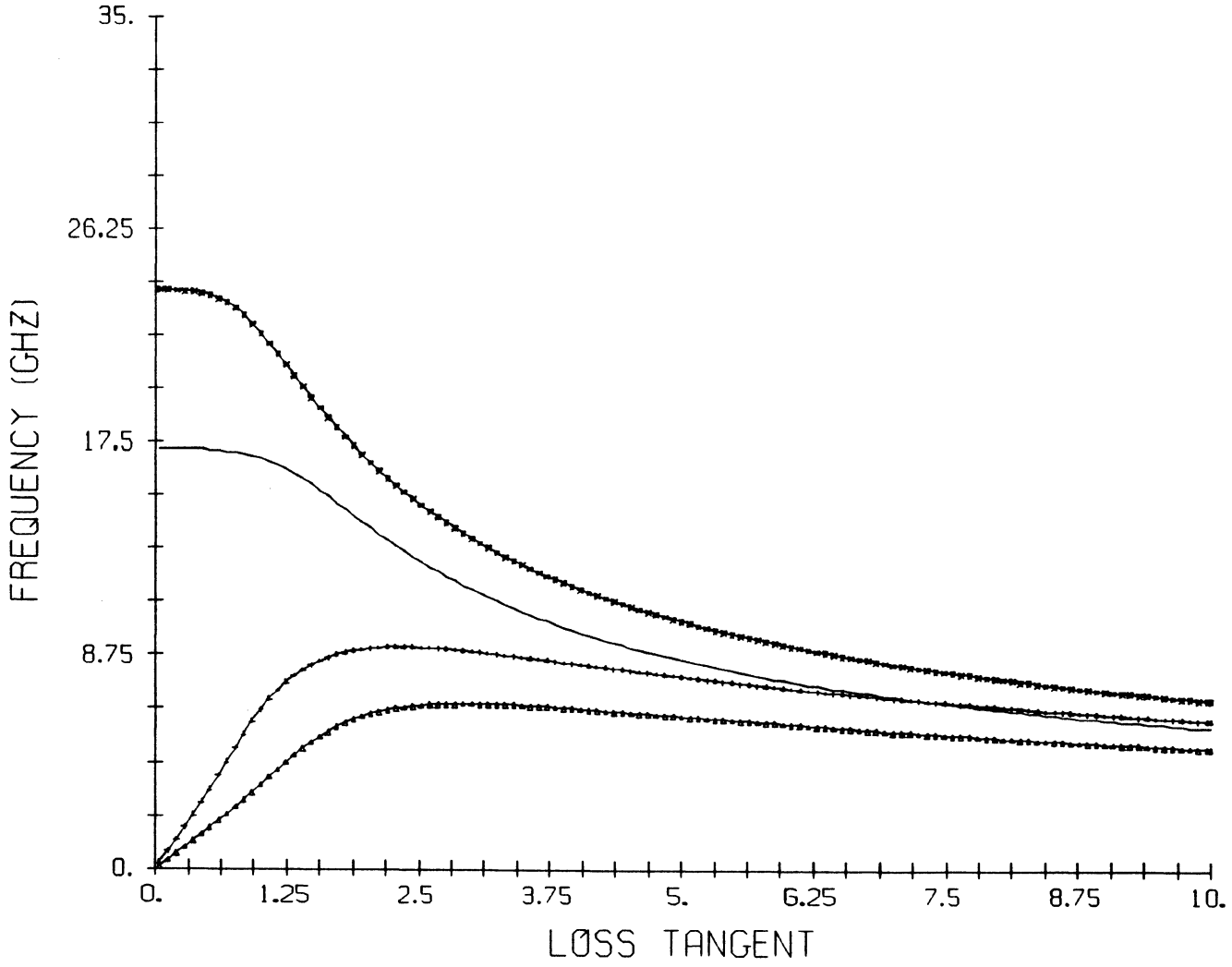

21-APR-88
20:21:45

CUTØFF FREQUENCY .VS. LØSS TANGENT #3

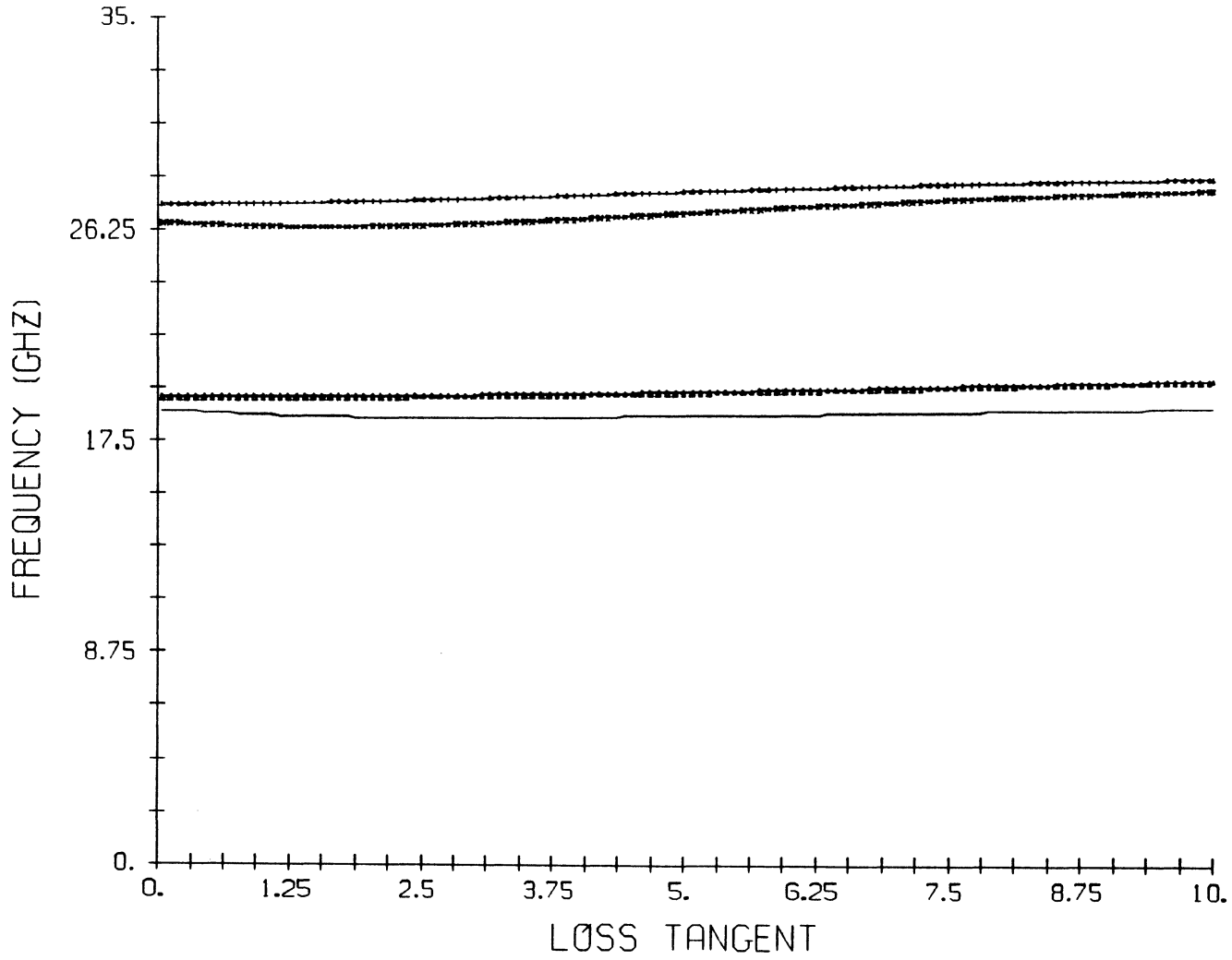

21-APR-88
20:22:01

CUTØFF (REAL AND IMAG) .VS. LØSS TANGENT FØR LSM #3

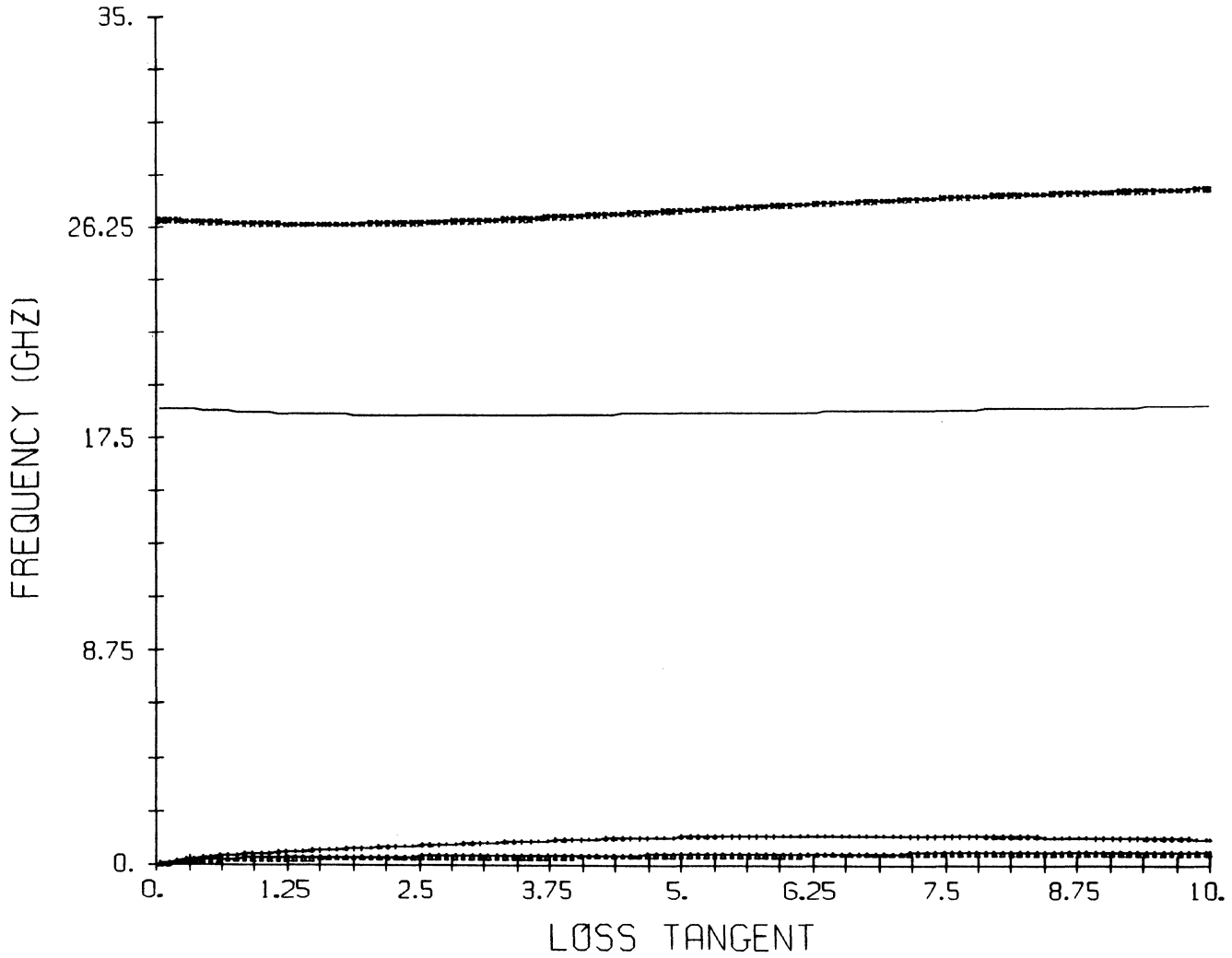

21-APR-88
20:22:11

CUTOFF (REAL AND IMAG) .VS. LOSS TANGENT FOR LSE #3

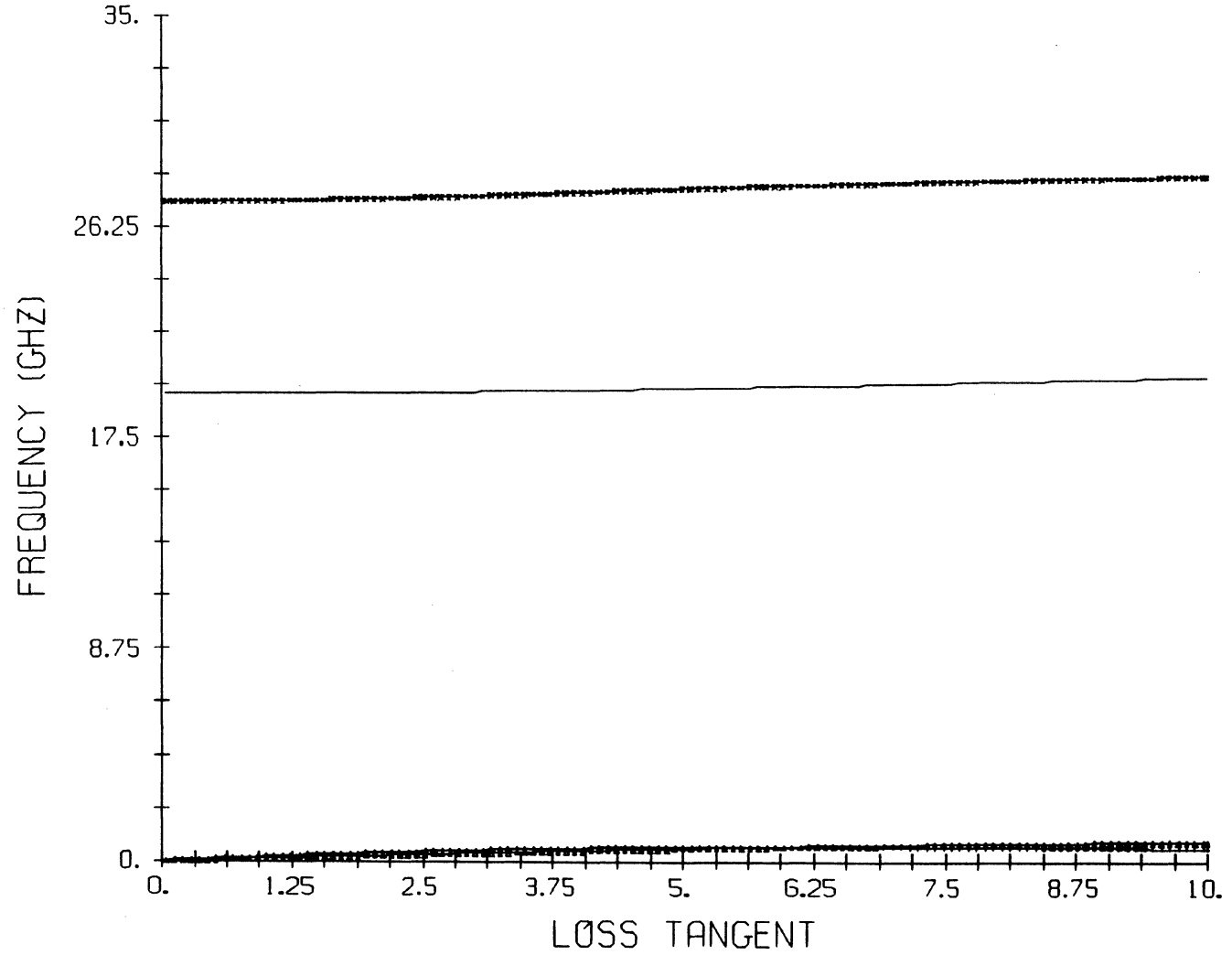

21-APR-88
20:25:20

CUTØFF FREQUENCY .VS. LØSS TANGENT #4

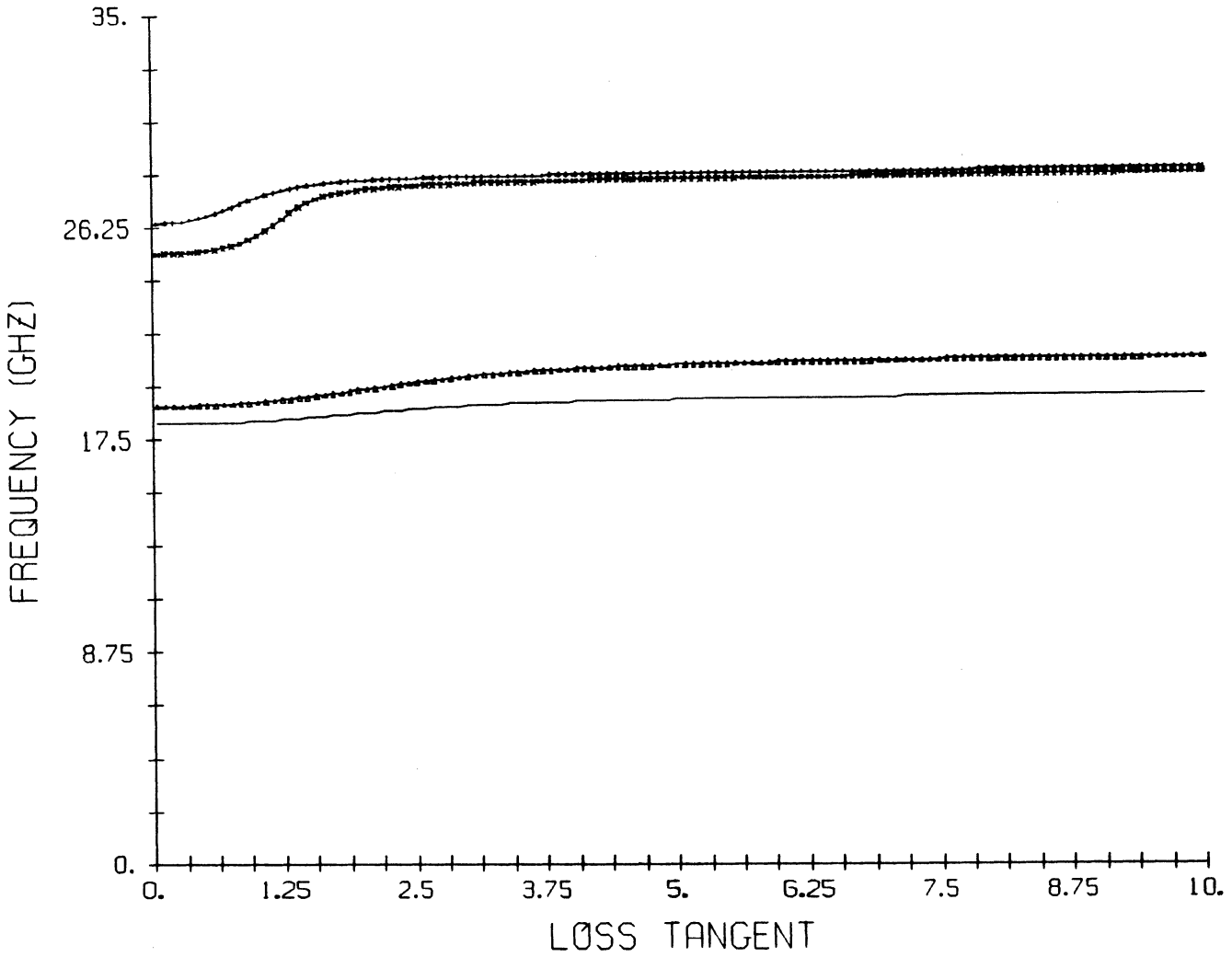

21 APR 88
20:25:32

CUTOFF (REAL AND IMAG) .VS. LOSS TANGENT FOR LSM #4

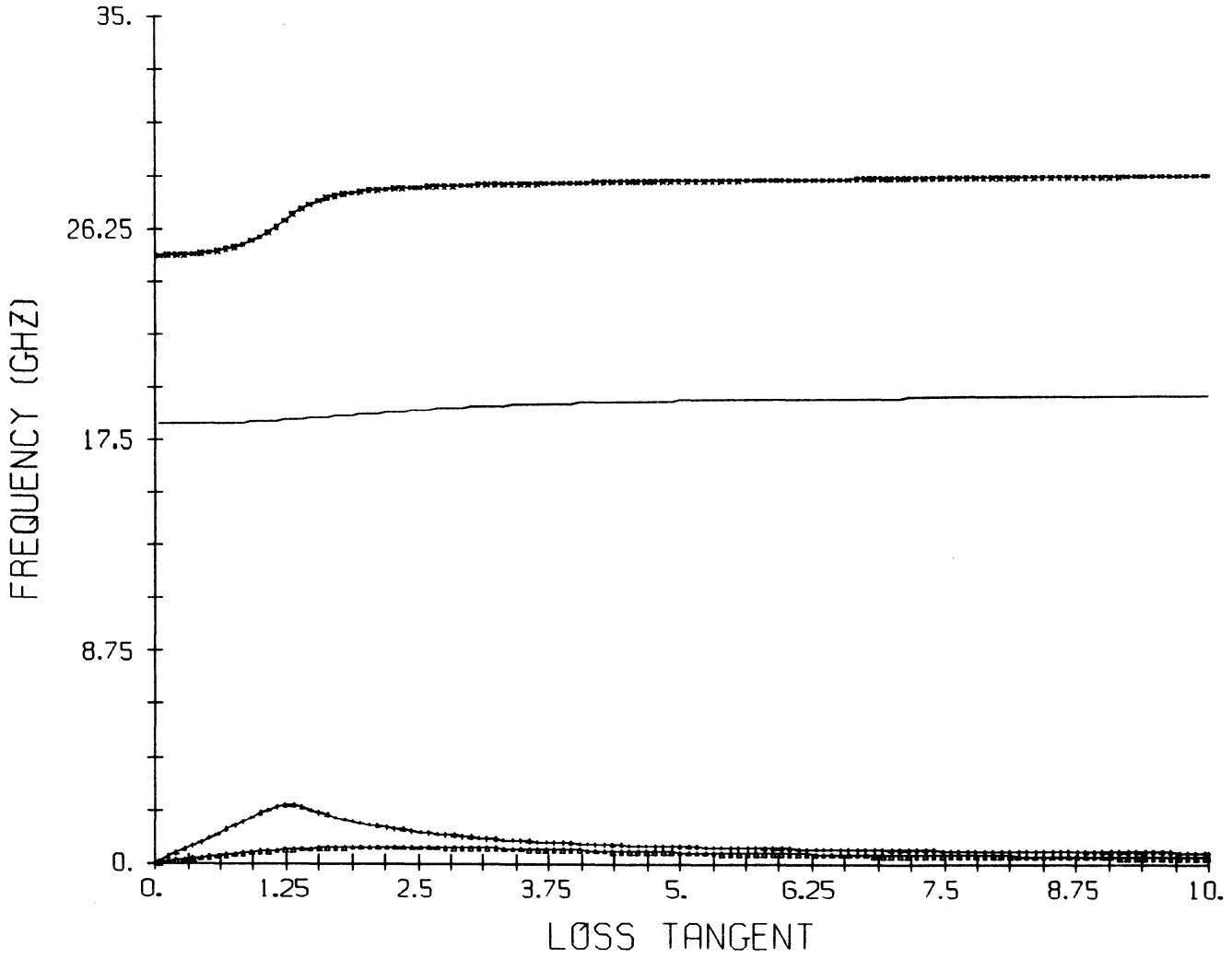

21-APR-88
20:25:42

CUTOFF (REAL AND IMAG) .VS. LOSS TANGENT FOR LSE #4

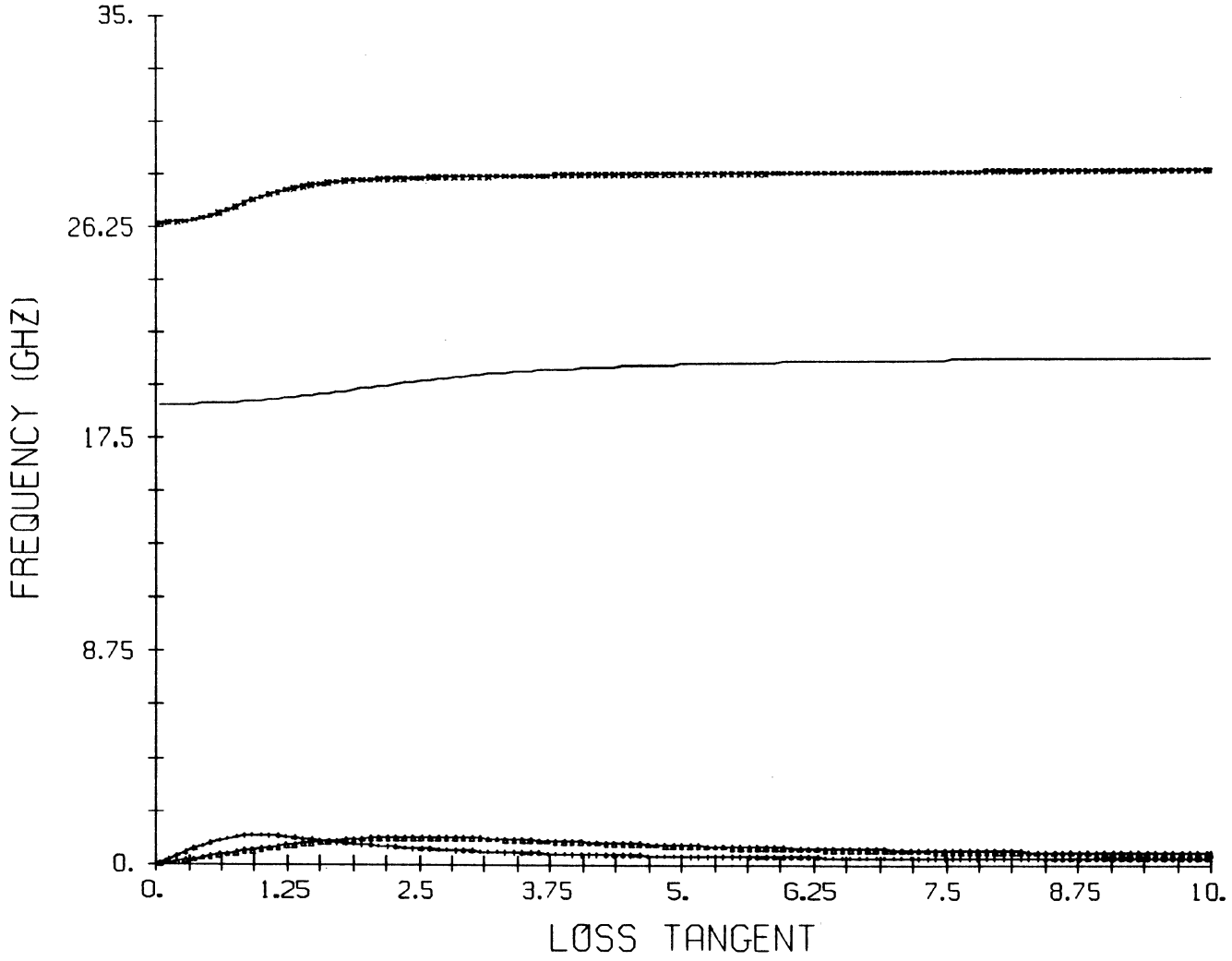

21-APR-88
19:50:42

CUTOFF FREQUENCY .VS. LOSS TANGENT #5

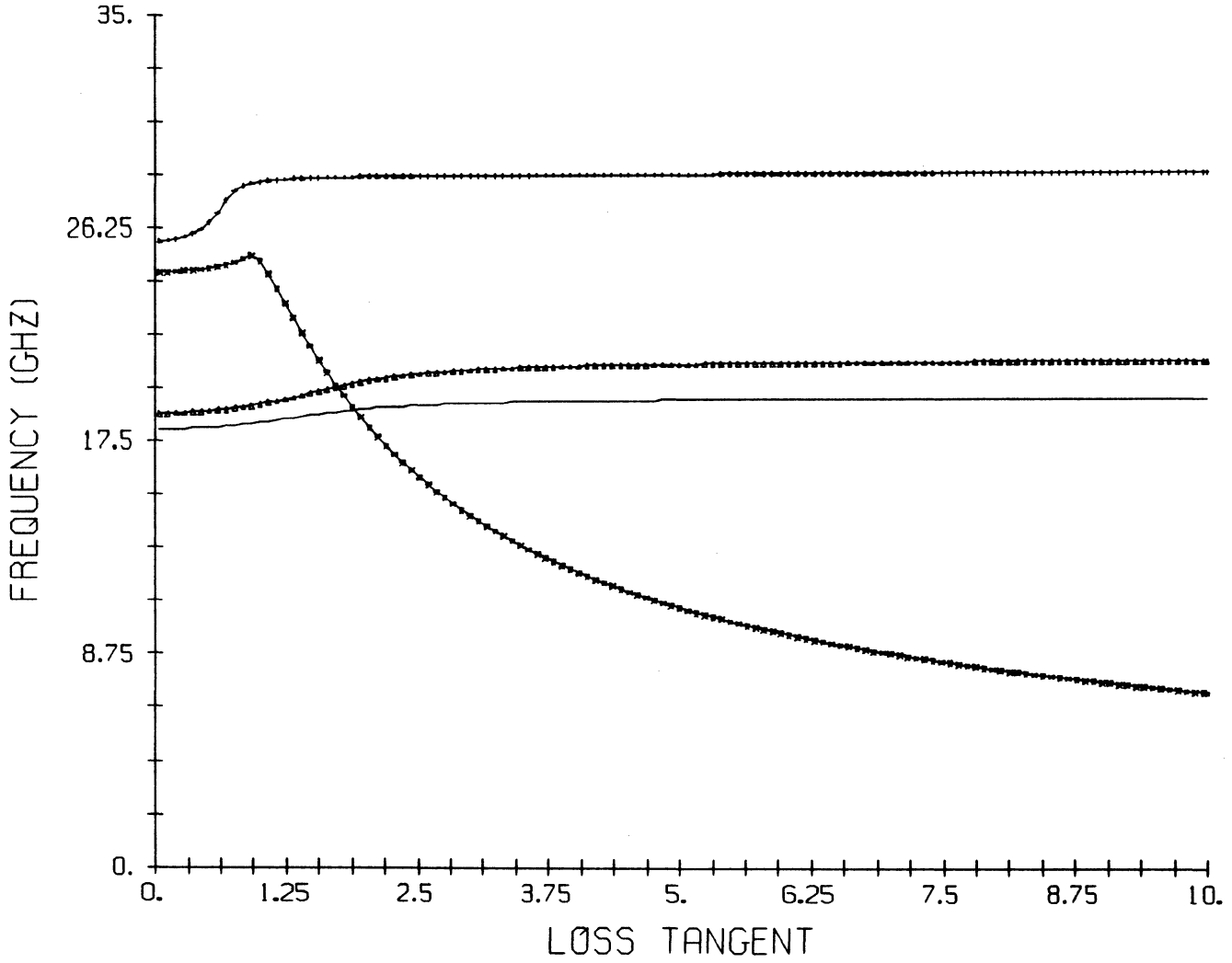

21-APR-88
19:55:27

CUTOFF (REAL AND IMAG) .VS. LOSS TANGENT FOR LSM #5

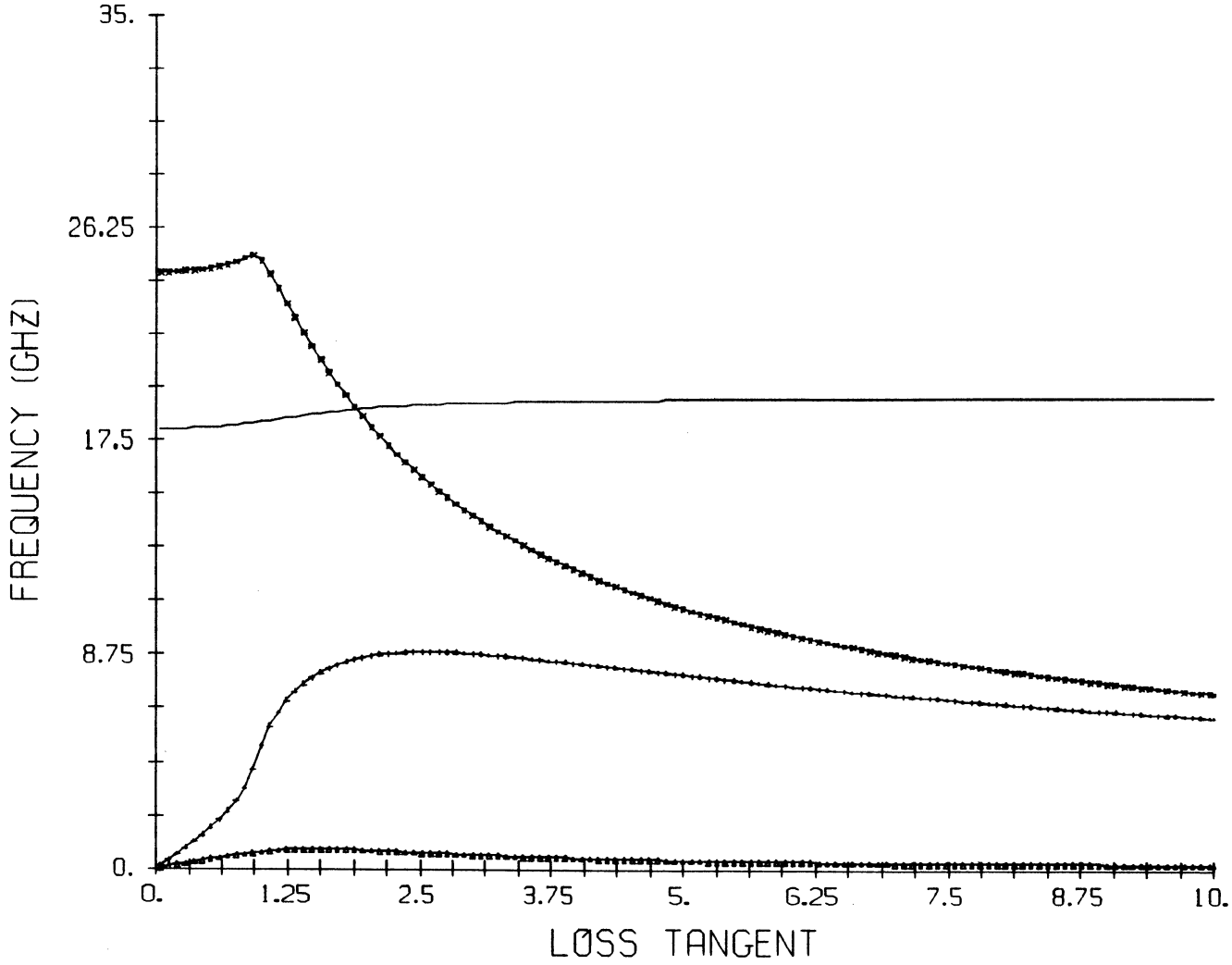

21-APR-88
19:58:26

CUTØFF (REAL AND IMAG) .VS. LØSS TANGENT FØR LSE #5

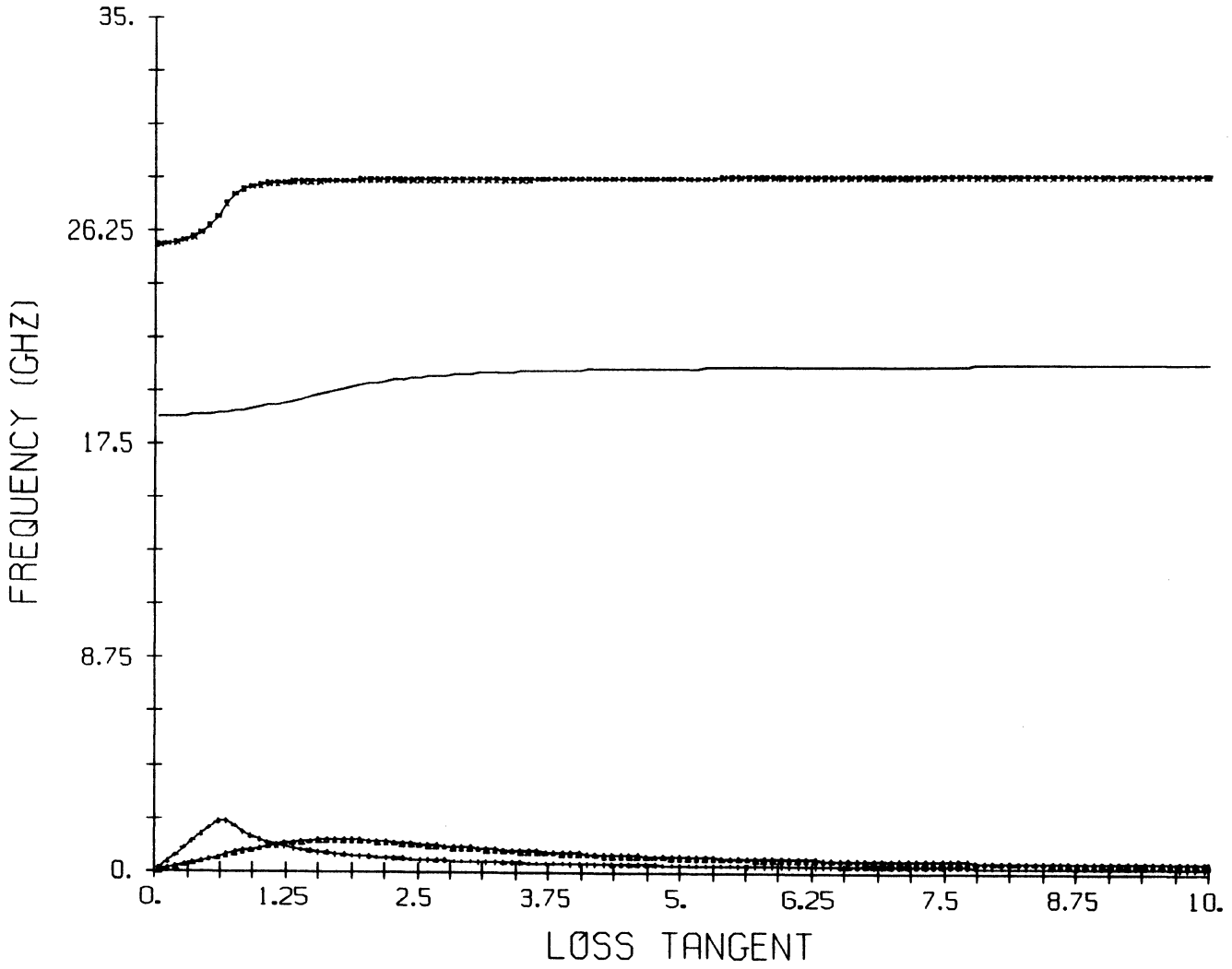

21-APR-88
23:24:32

CUTØFF FREQUENCY .VS. LØSS TANGENT #6

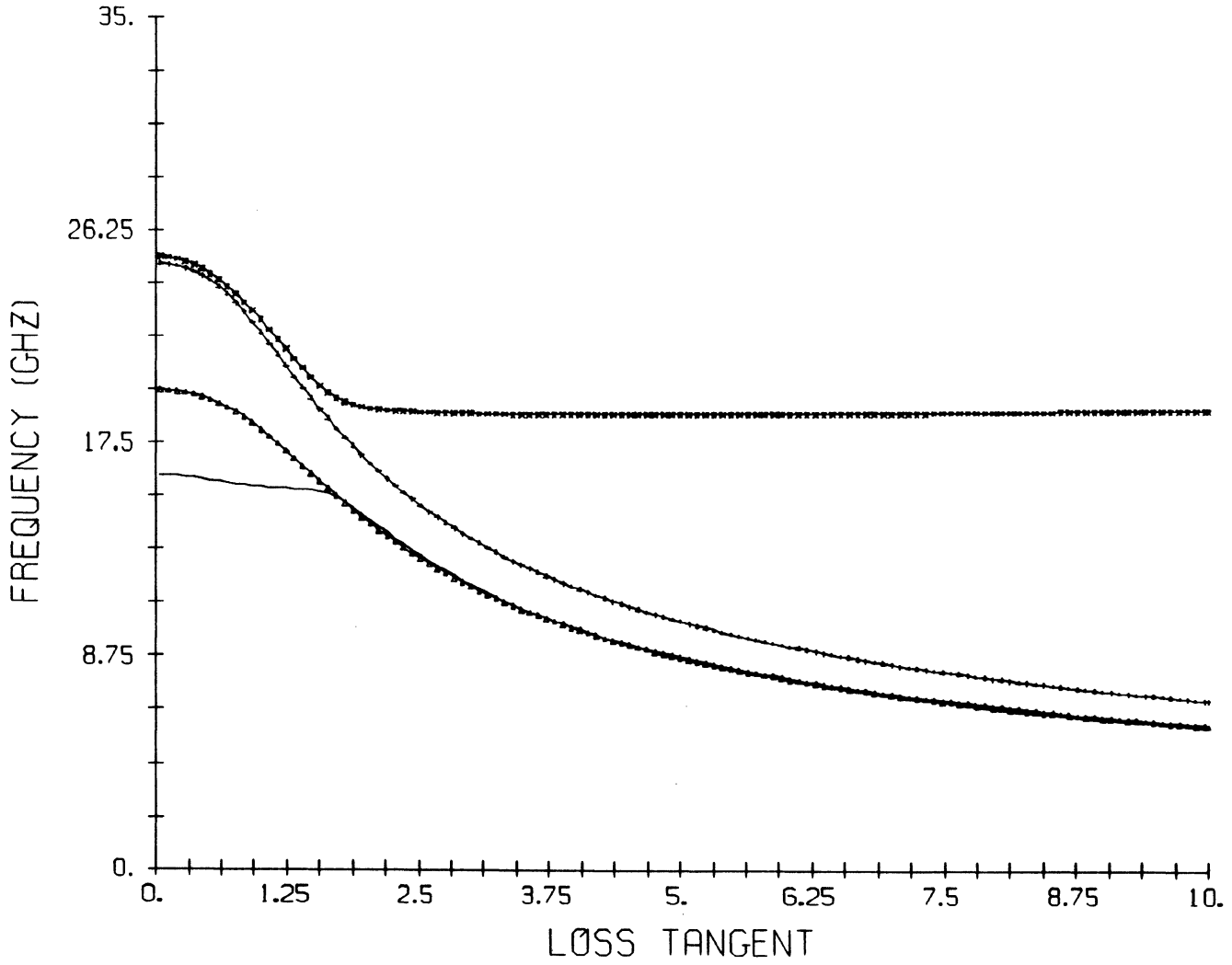

21-APR-88
23:24:46

CUTOFF (REAL AND IMAG) .VS. LOSS TANGENT FOR LSM #6

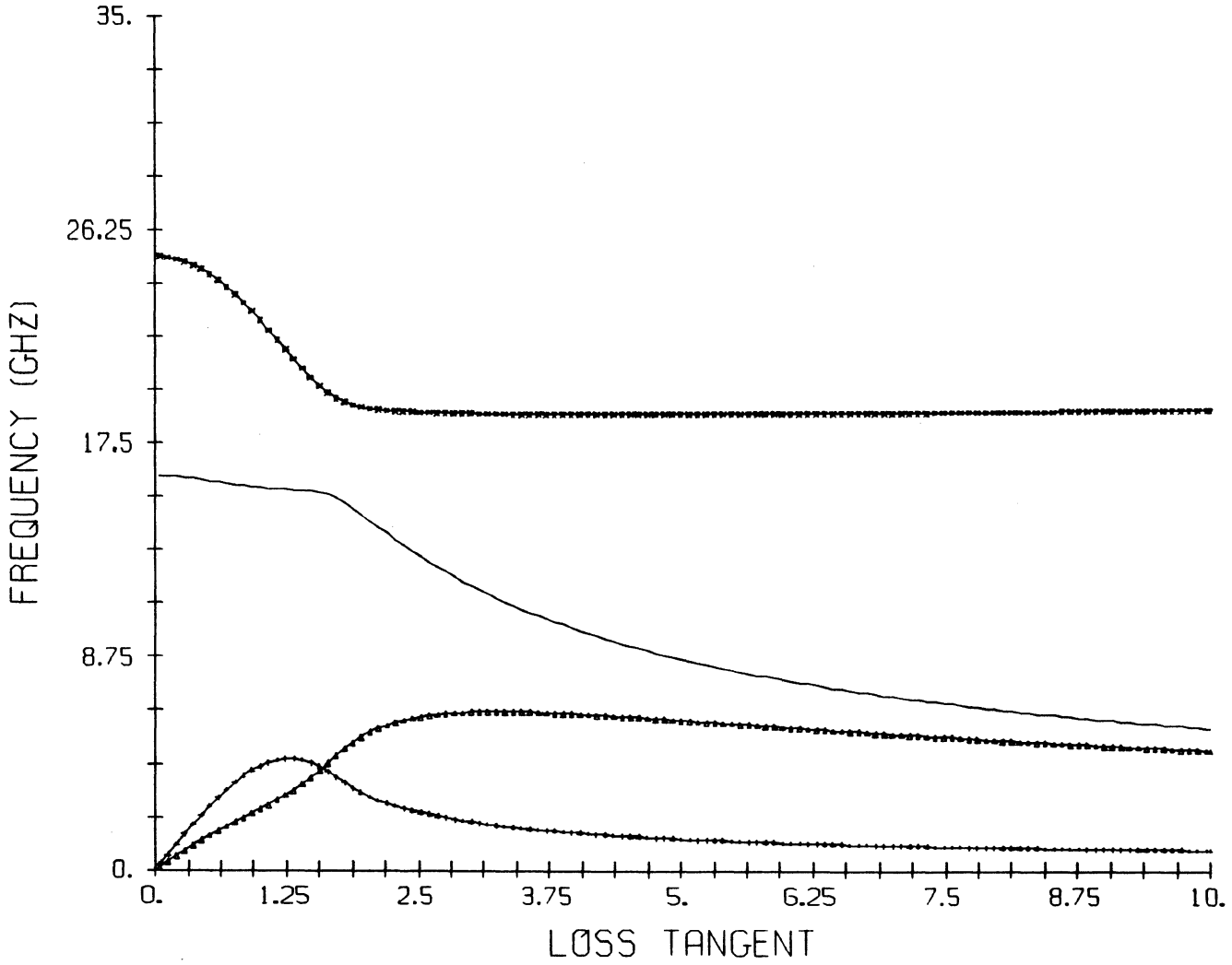

21-APR-88
23:24:56

CUTOFF (REAL AND IMAG) .VS. LOSS TANGENT FOR LSE #6

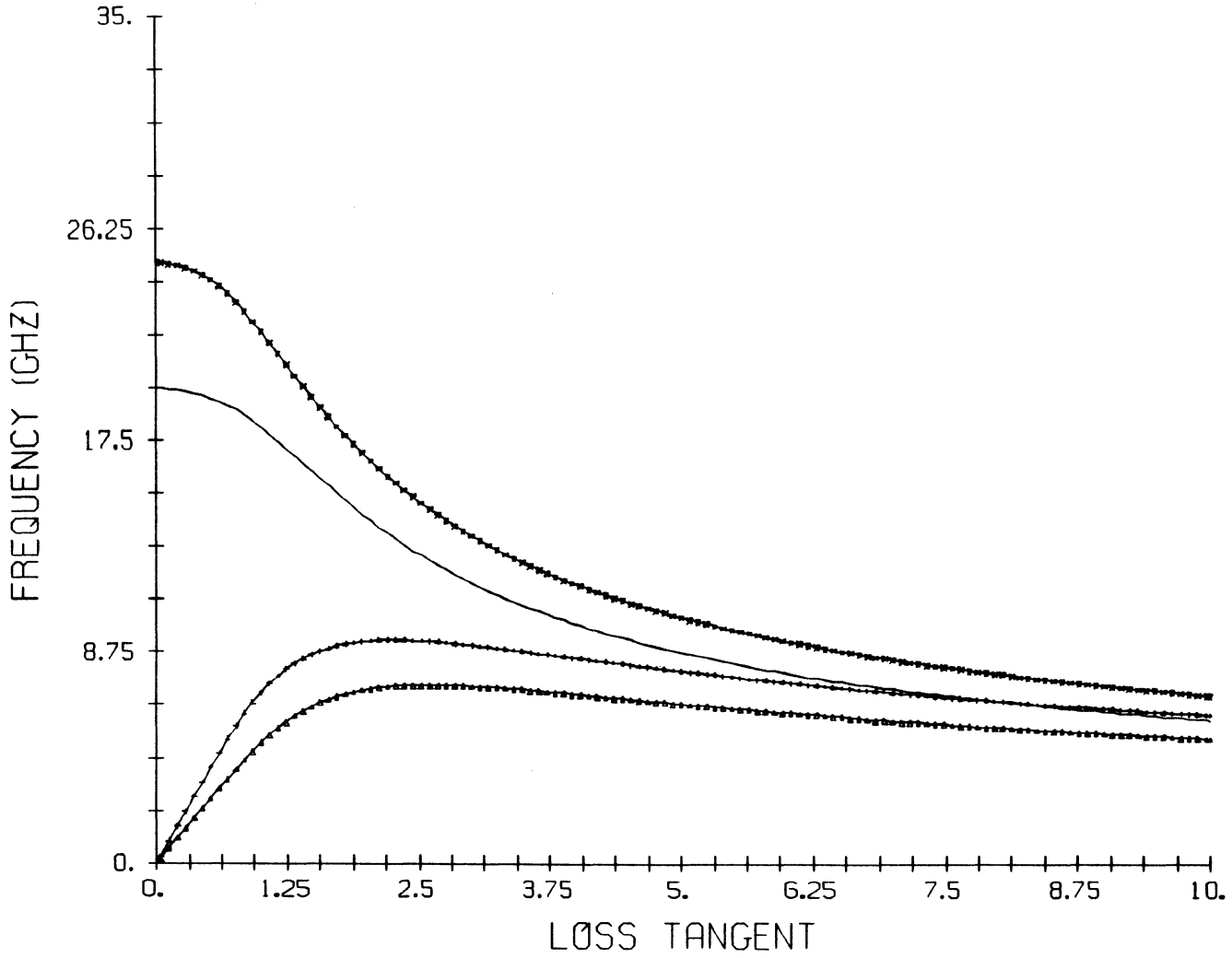

21-APR-88
23:32:42

CUTØFF FREQUENCY .VS. LØSS TANGENT #7

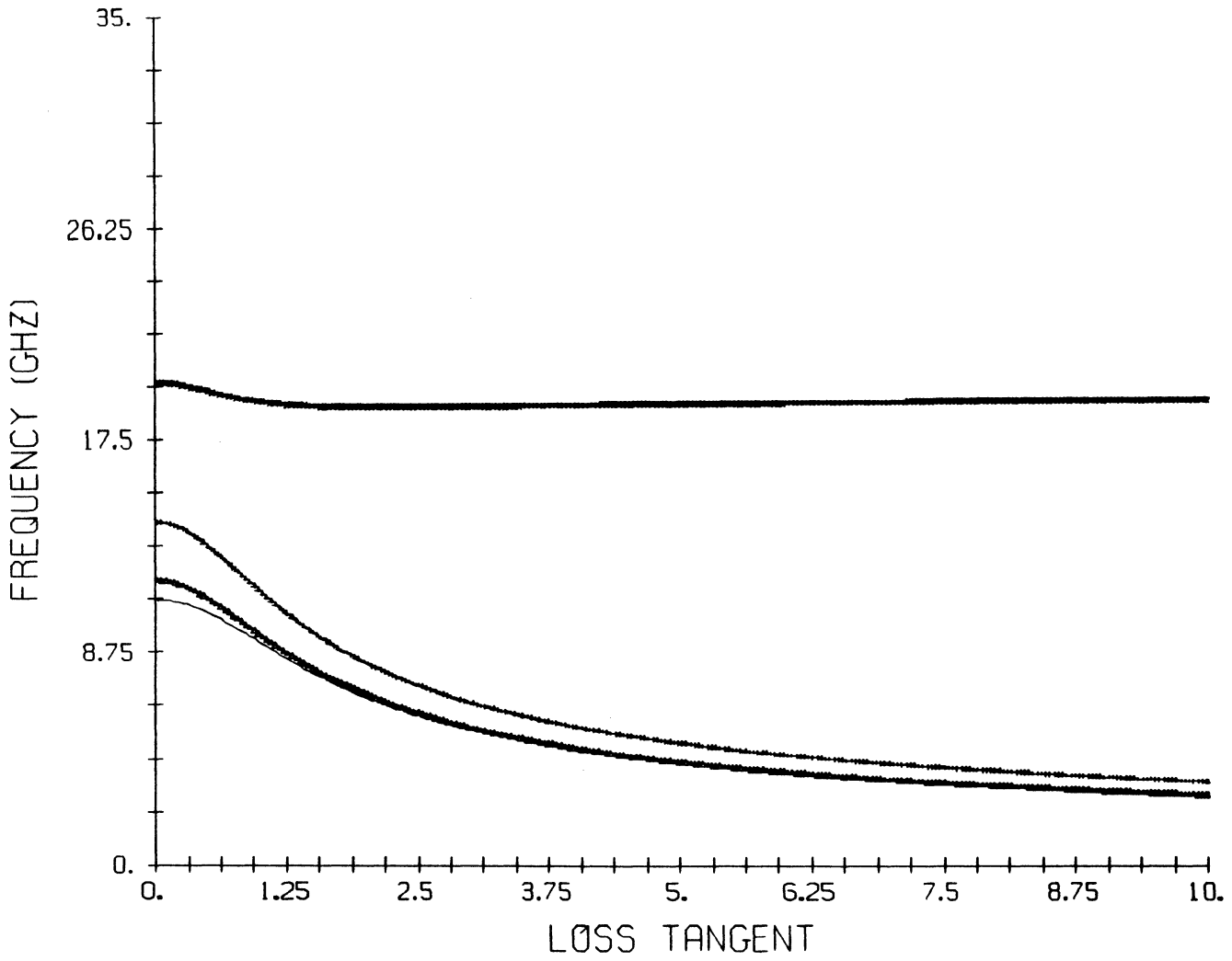

21-APR-88
23:32:53

CUTOFF (REAL AND IMAG) .VS. LOSS TANGENT FOR LSM #7

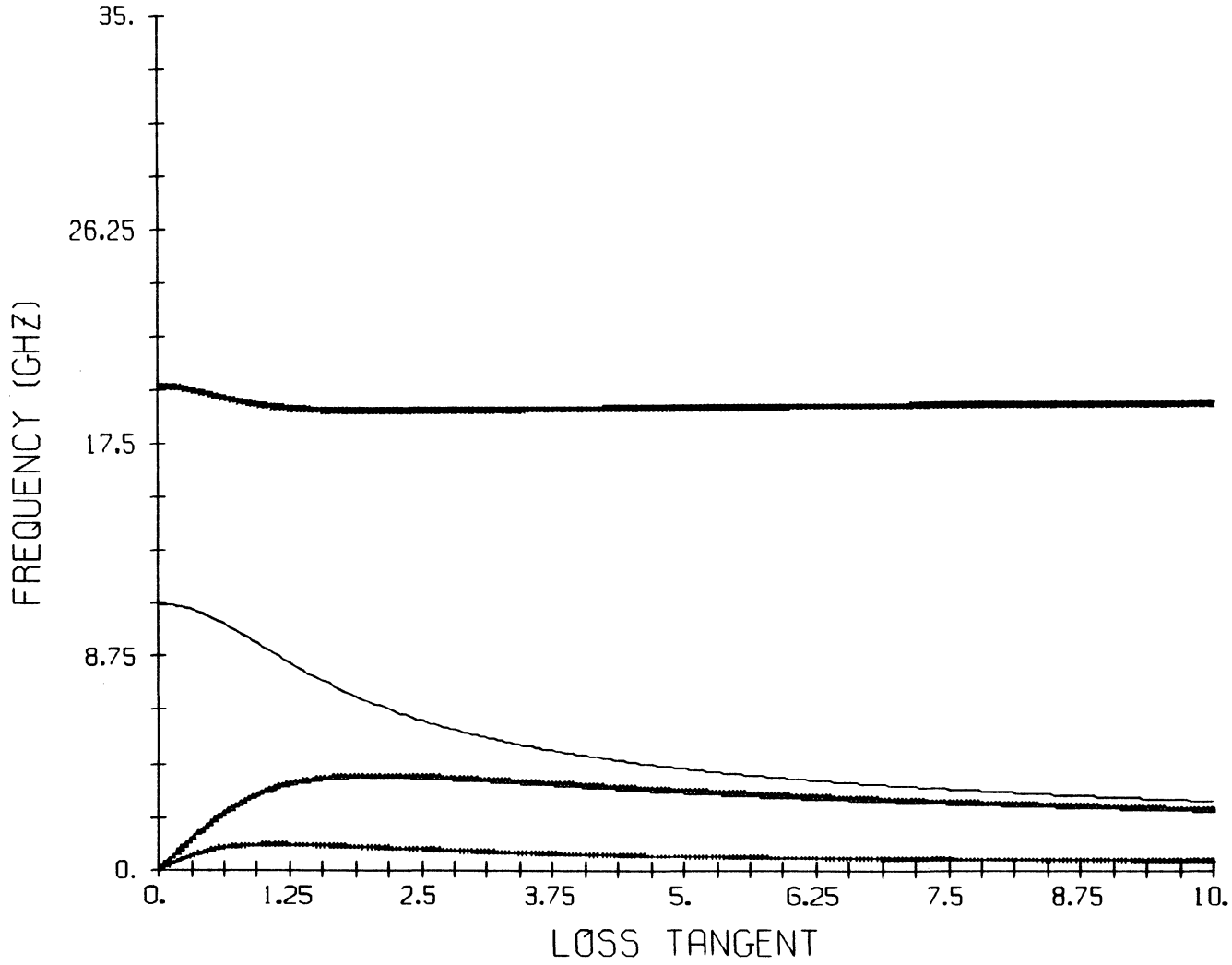

21-APR-88
23:33:04

CUTOFF (REAL AND IMAG) .VS. LOSS TANGENT FOR LSE #7

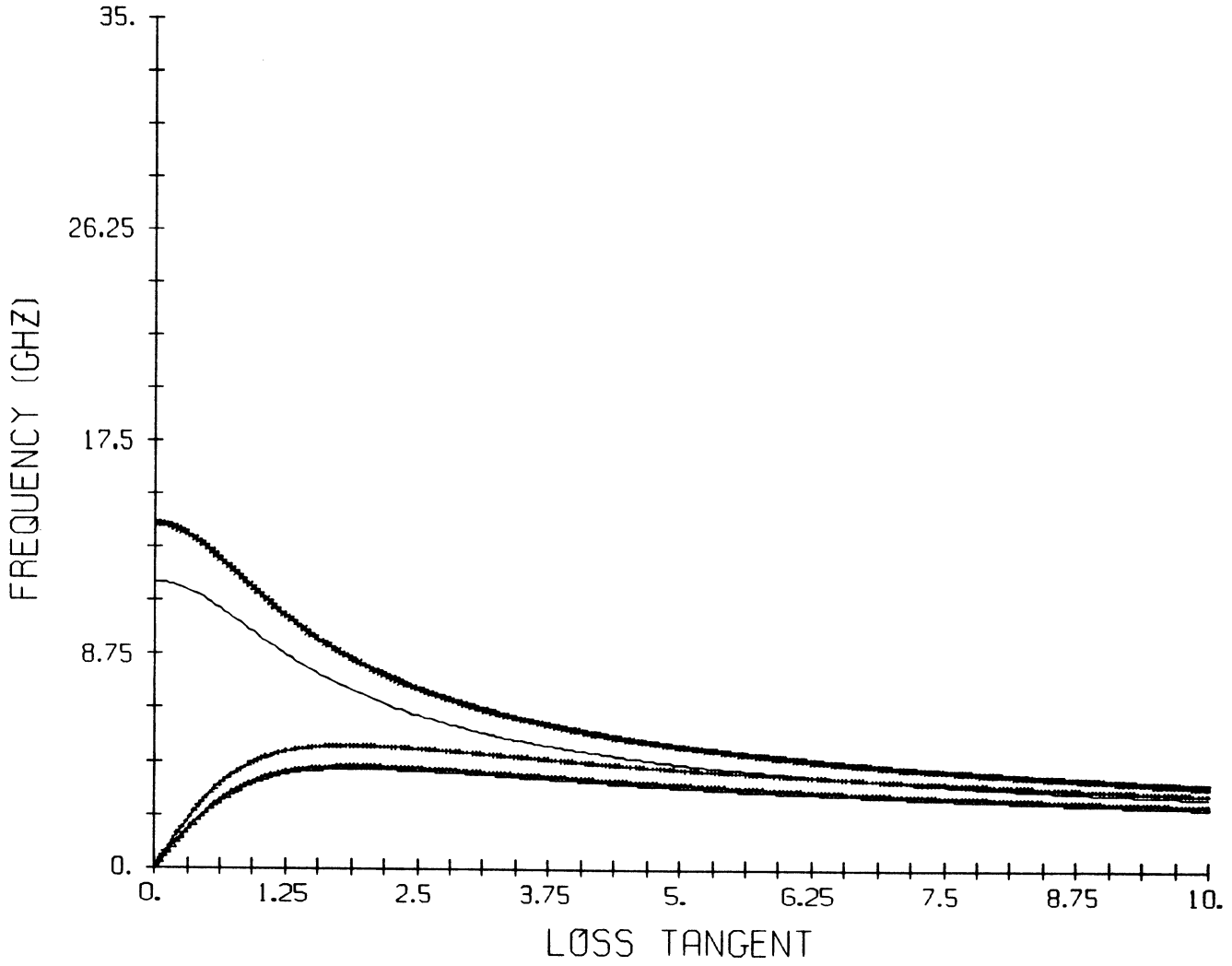

21-APR-88
23:43:56

CUTOFF FREQUENCY .VS. LOSS TANGENT #8

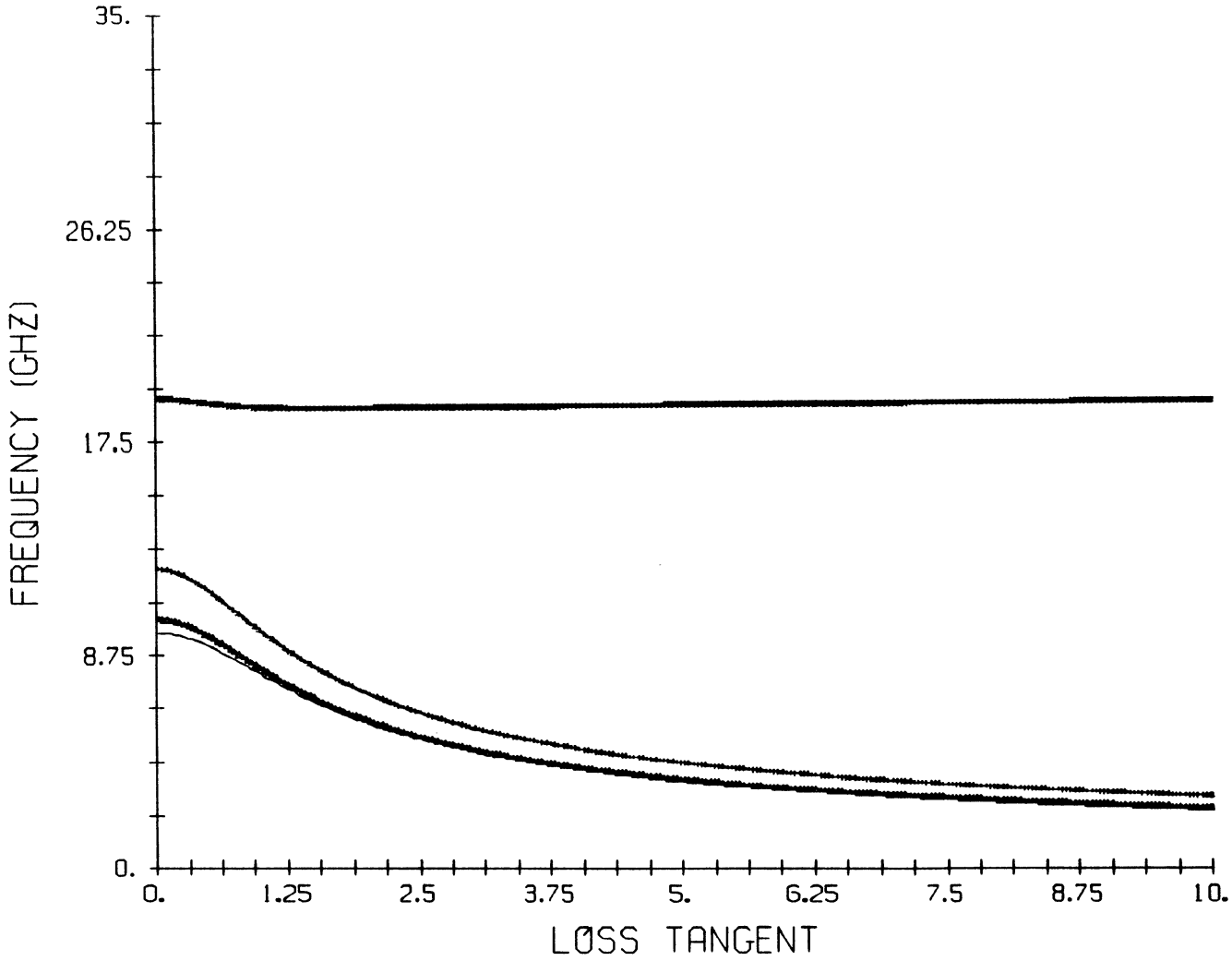

21-APR-88
23:44:07

CUTØFF (REAL AND IMAG) .VS. LØSS TANGENT FØR LSM #8

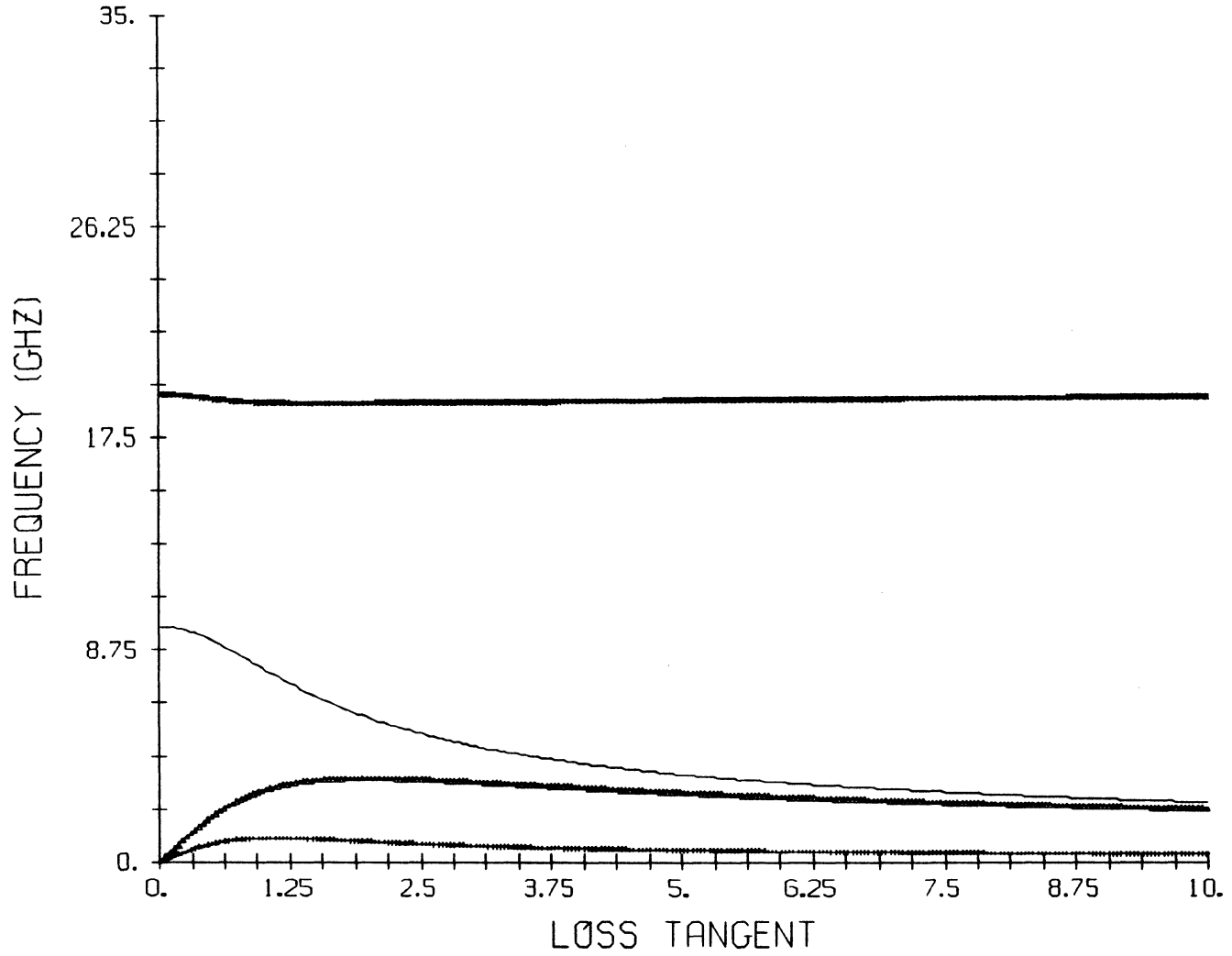

21-APR-88
23:44:16

CUTØFF (REAL AND IMAG) .VS. LØSS TANGENT FØR LSE #8

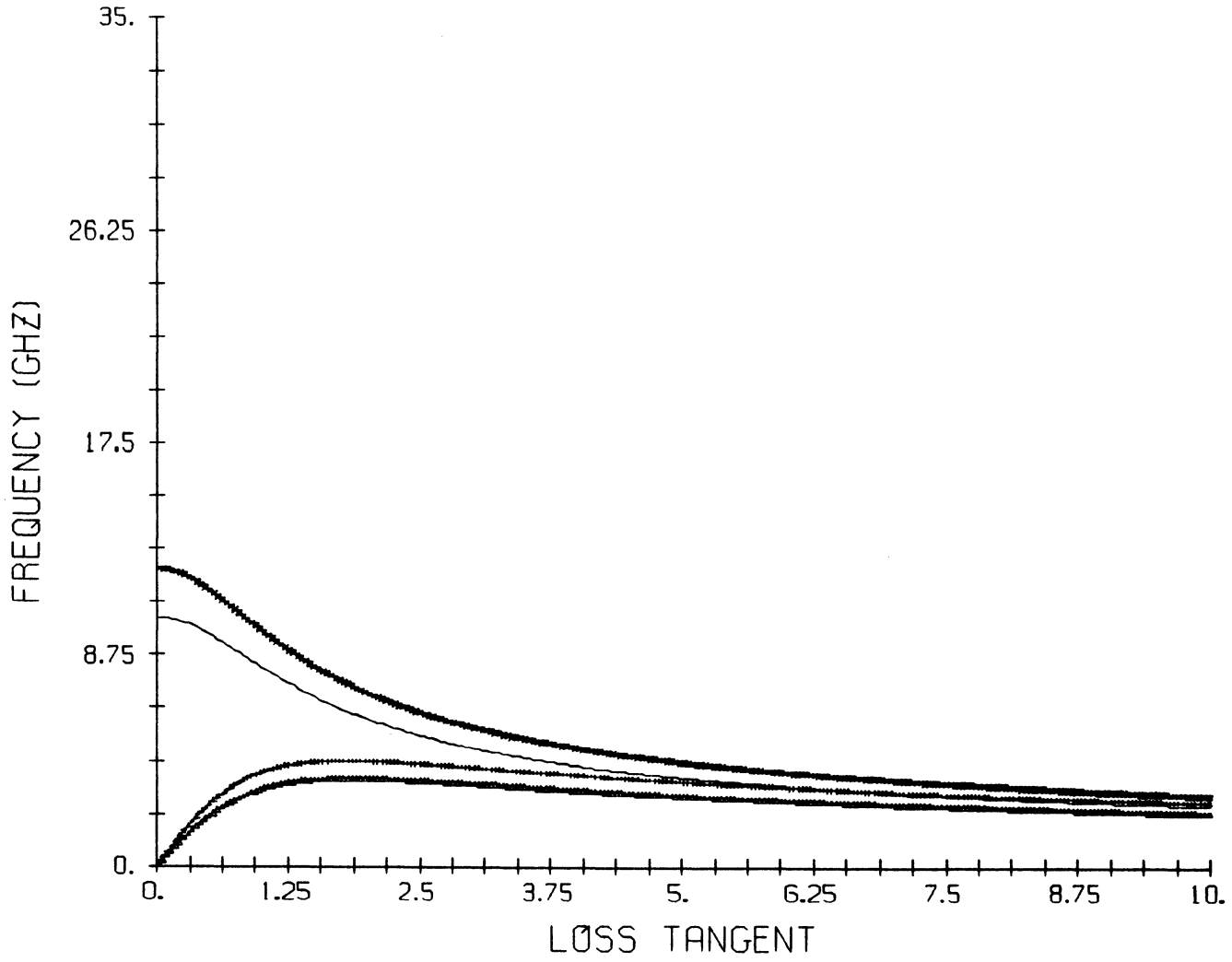

22-APR-88
00:13:16

CUTOFF FREQUENCY .VS. LOSS TANGENT #9

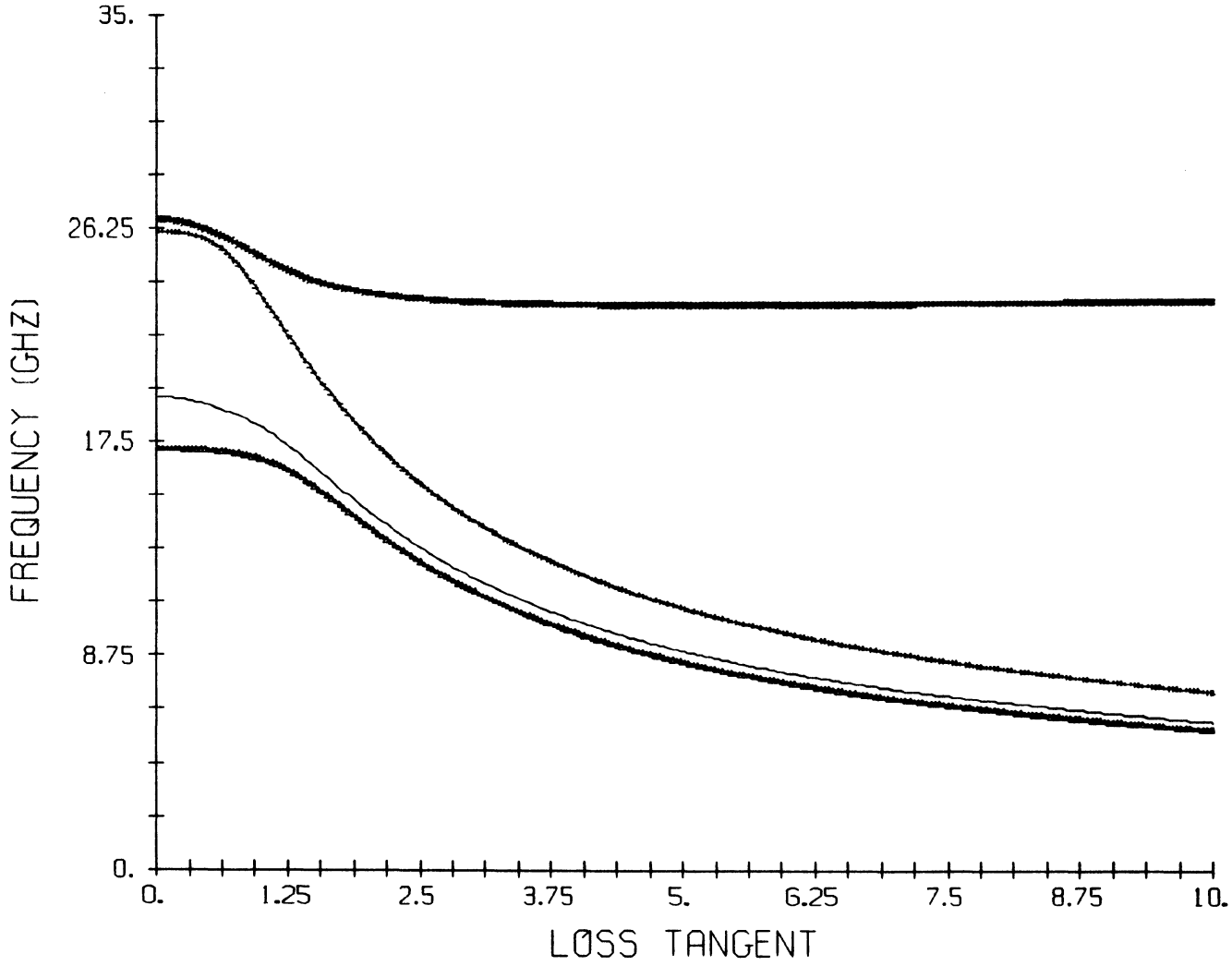

22-APR-88
00:13:26

CUTOFF (REAL AND IMAG) .VS. LOSS TANGENT FOR LSM #9

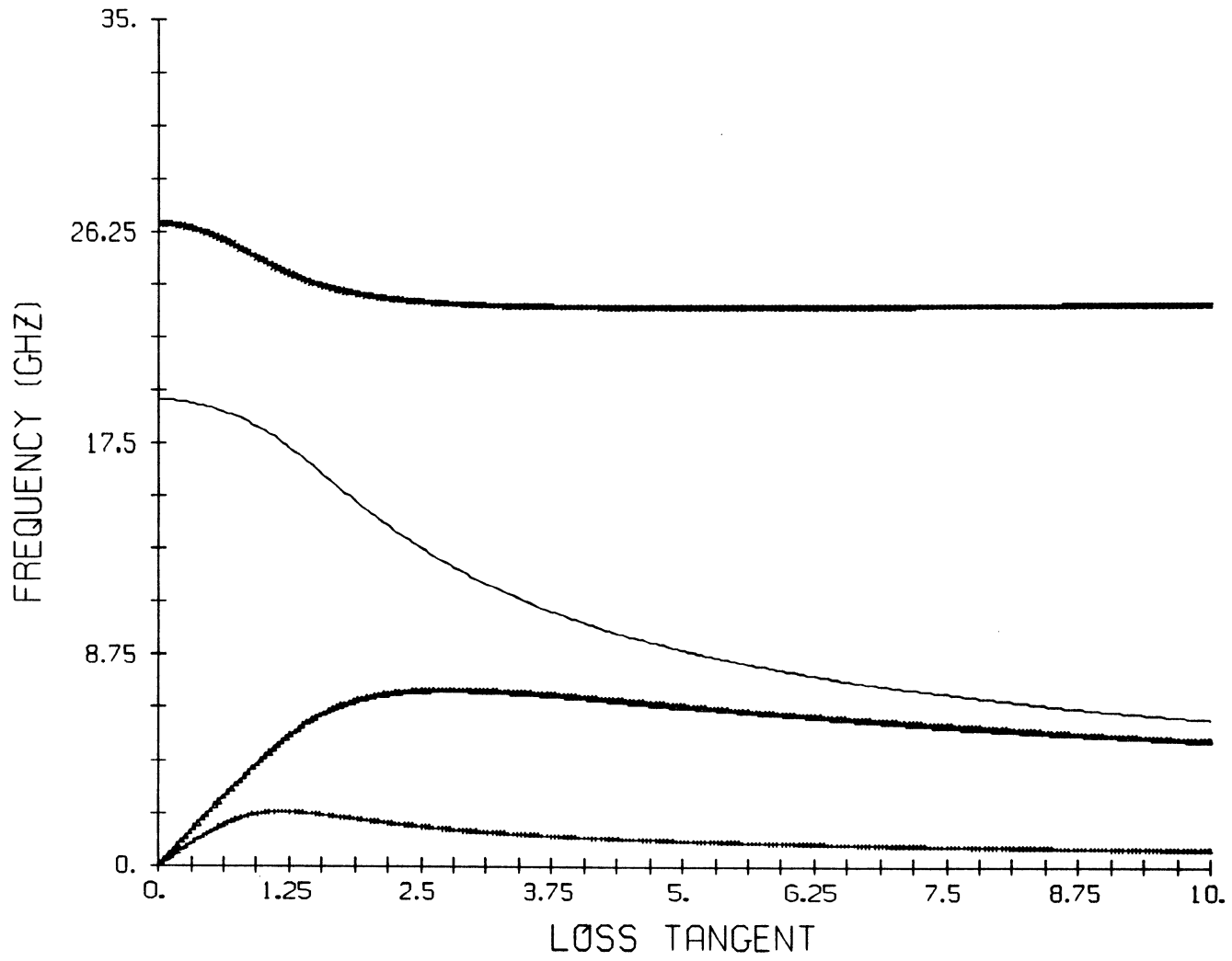

22-APR-88
00:13:35

CUTØFF (REAL AND IMAG) .VS. LØSS TANGENT FØR LSE #9

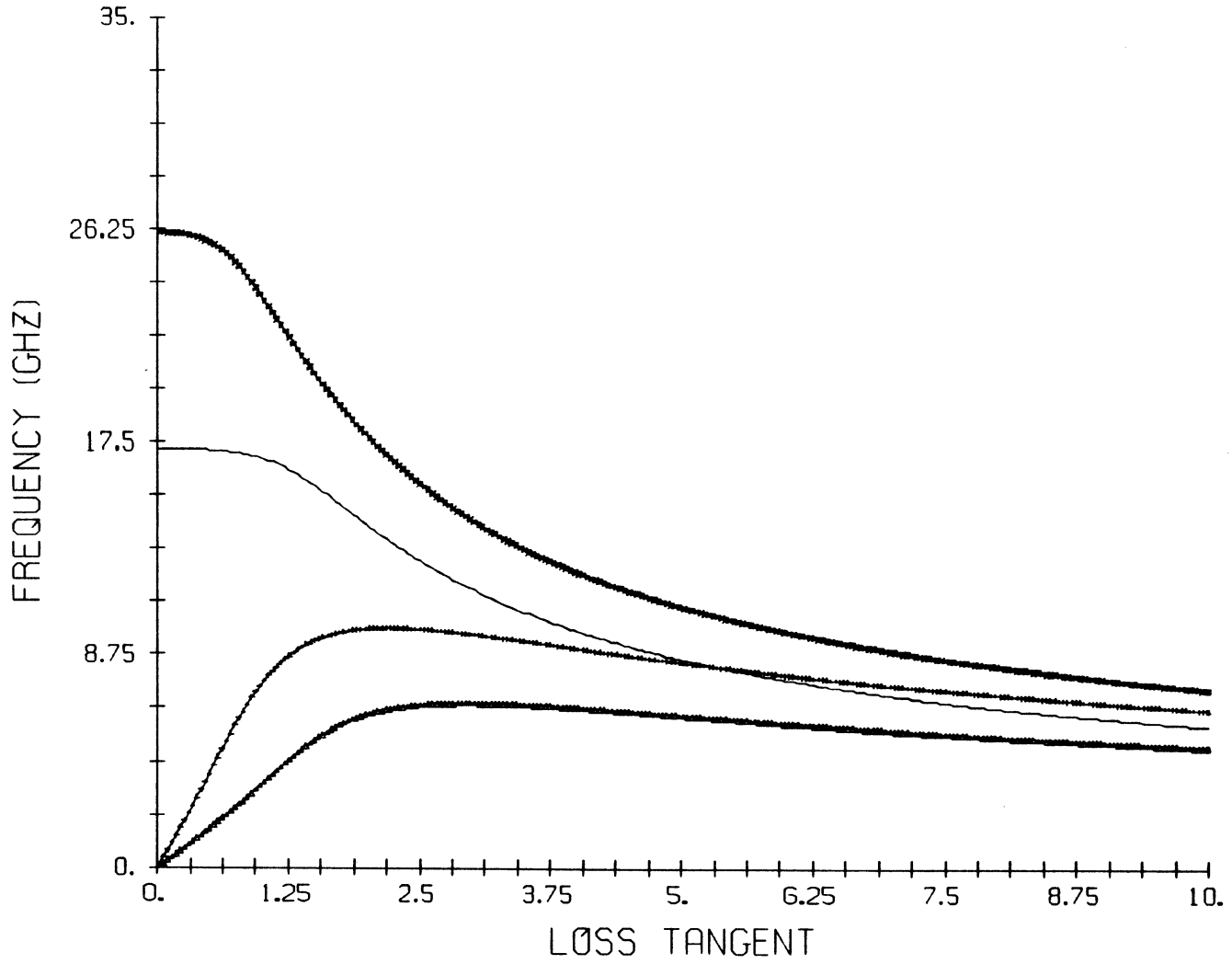

22-APR-88
00:18:32

CUTØFF FREQUENCY .VS. LØSS TANGENT #10

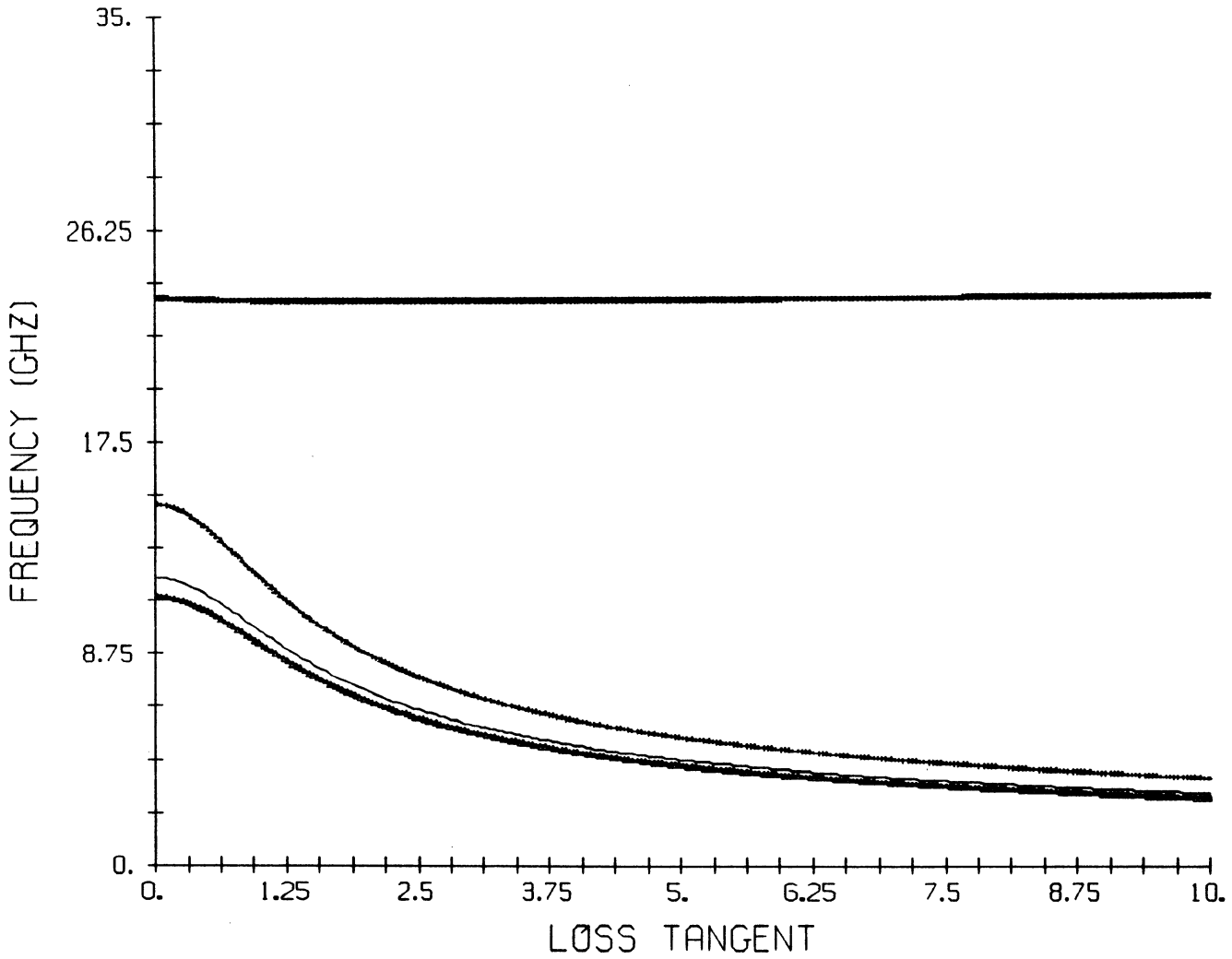

22-APR-88
00:18:39

CUTOFF (REAL AND IMAG) .VS. LOSS TANGENT FOR LSM #10

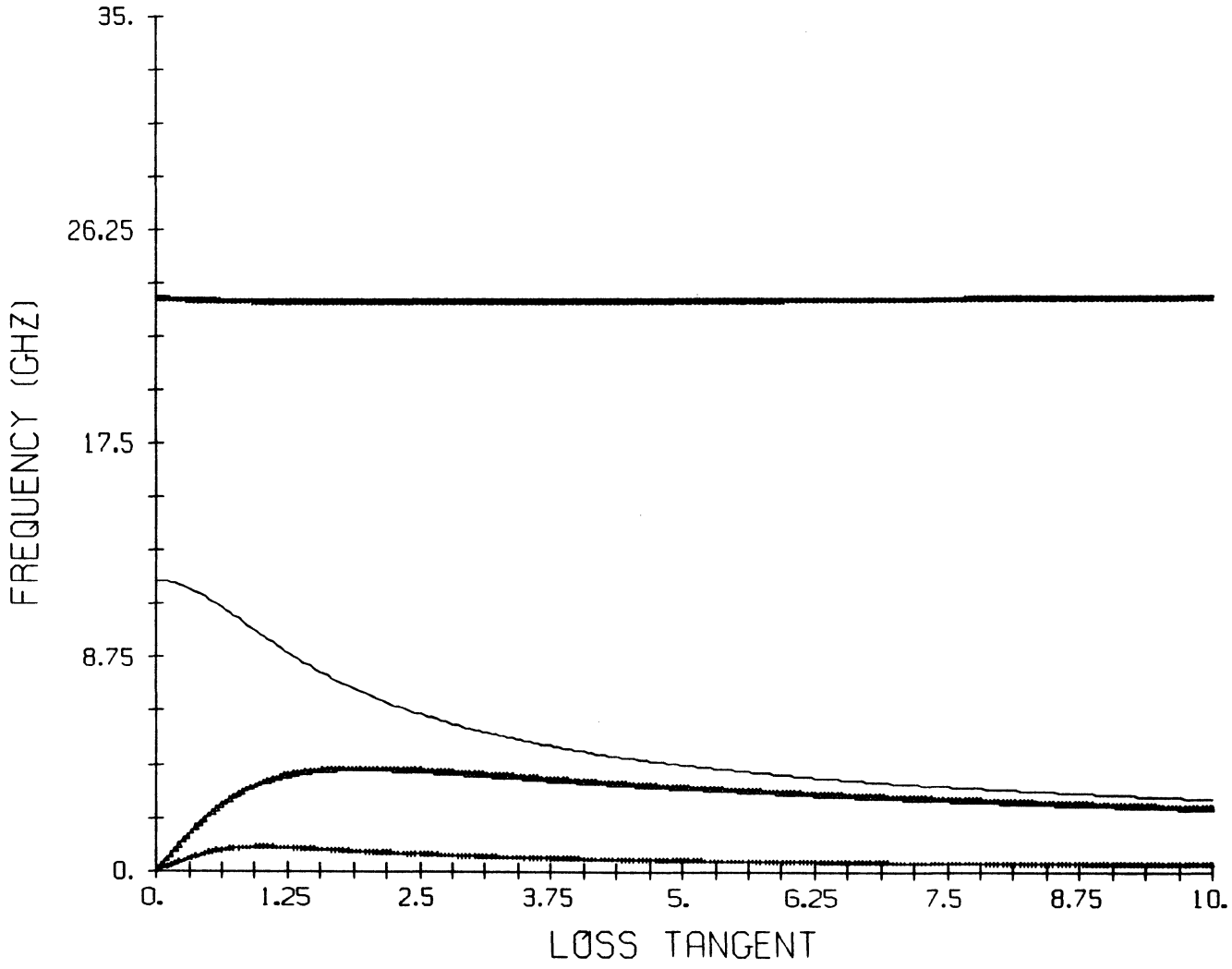

22-APR-88
00:18:47

CUTØFF (REAL AND IMAG) .VS. LØSS TANGENT FØR LSE #10

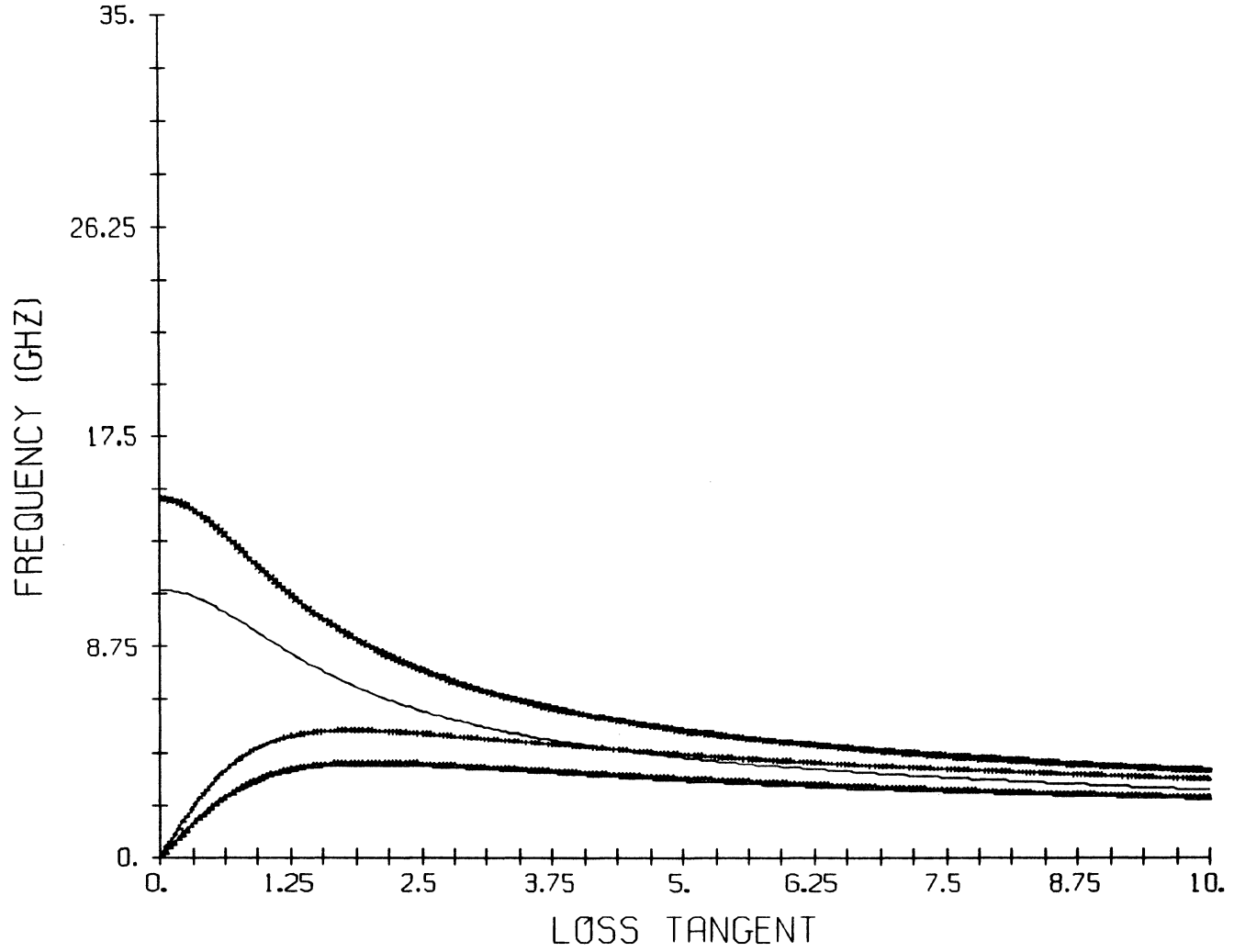

22-APR-88
00:21:02

CUTØFF FREQUENCY .VS. LØSS TANGENT #11

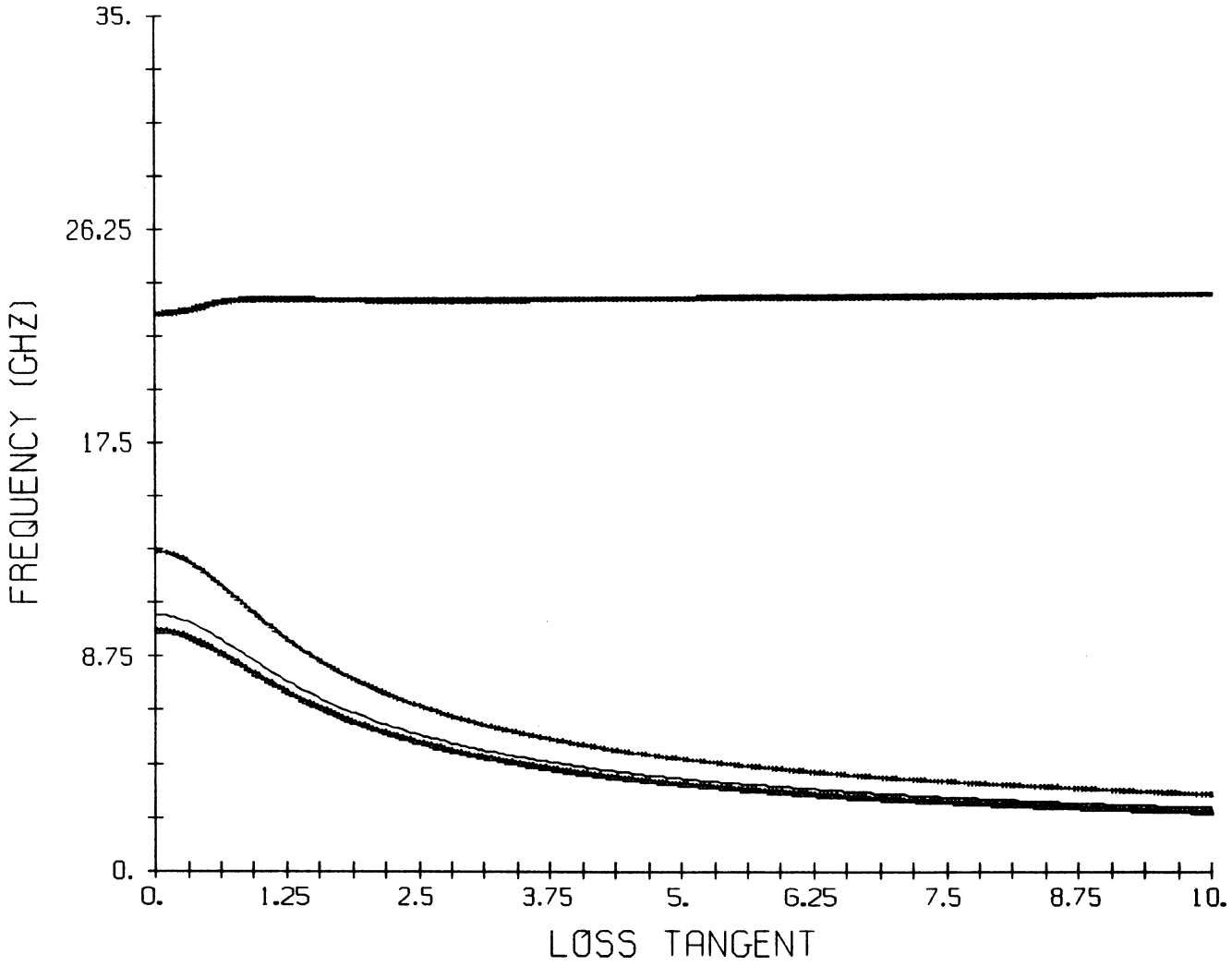

22-APR-88
00:21:09

CUTØFF (REAL AND IMAG) .VS. LØSS TANGENT FØR LSM #11

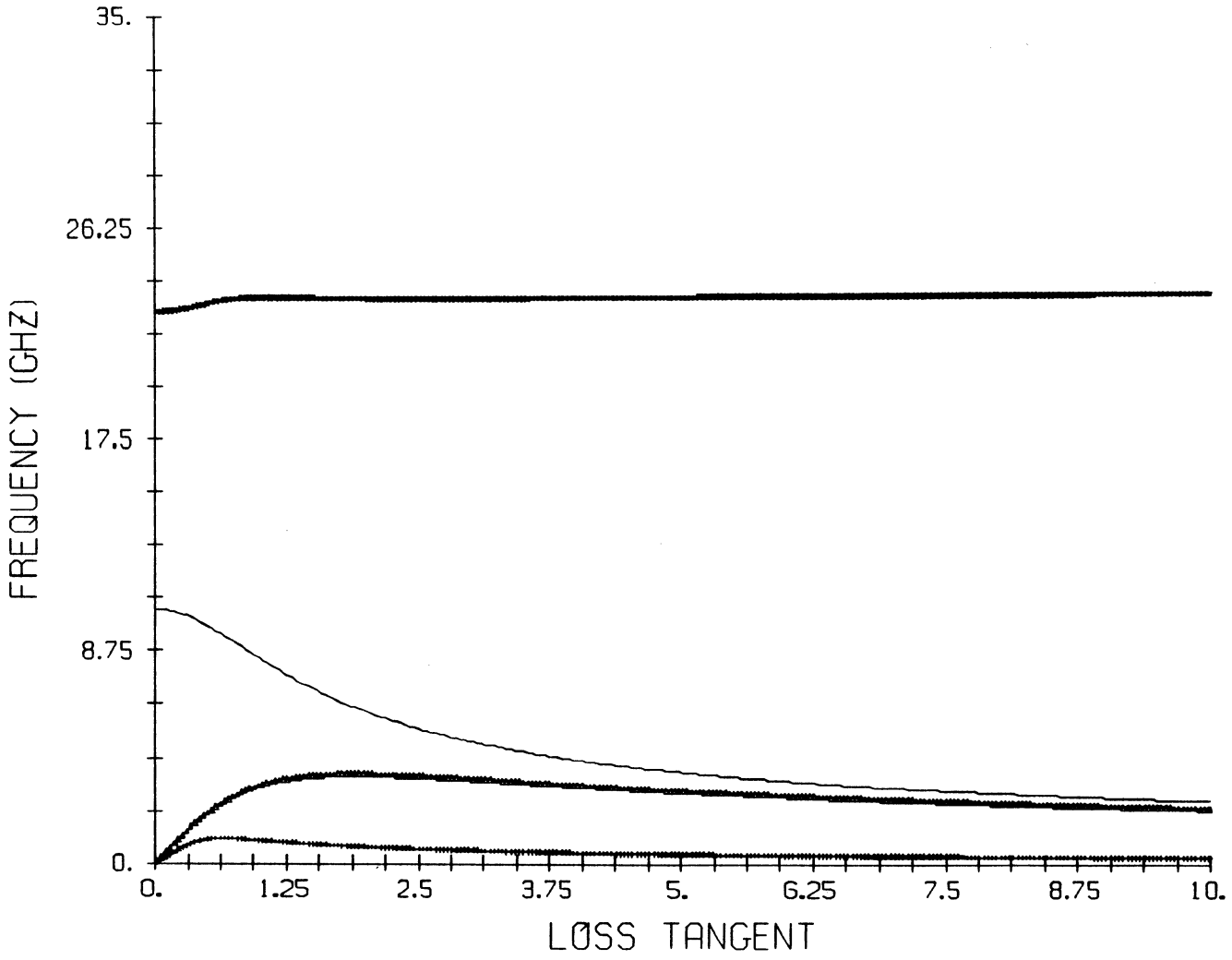

22-APR-88
00:21:27

CUTØFF (REAL AND IMAG) .VS. LØSS TANGENT FØR LSE #11

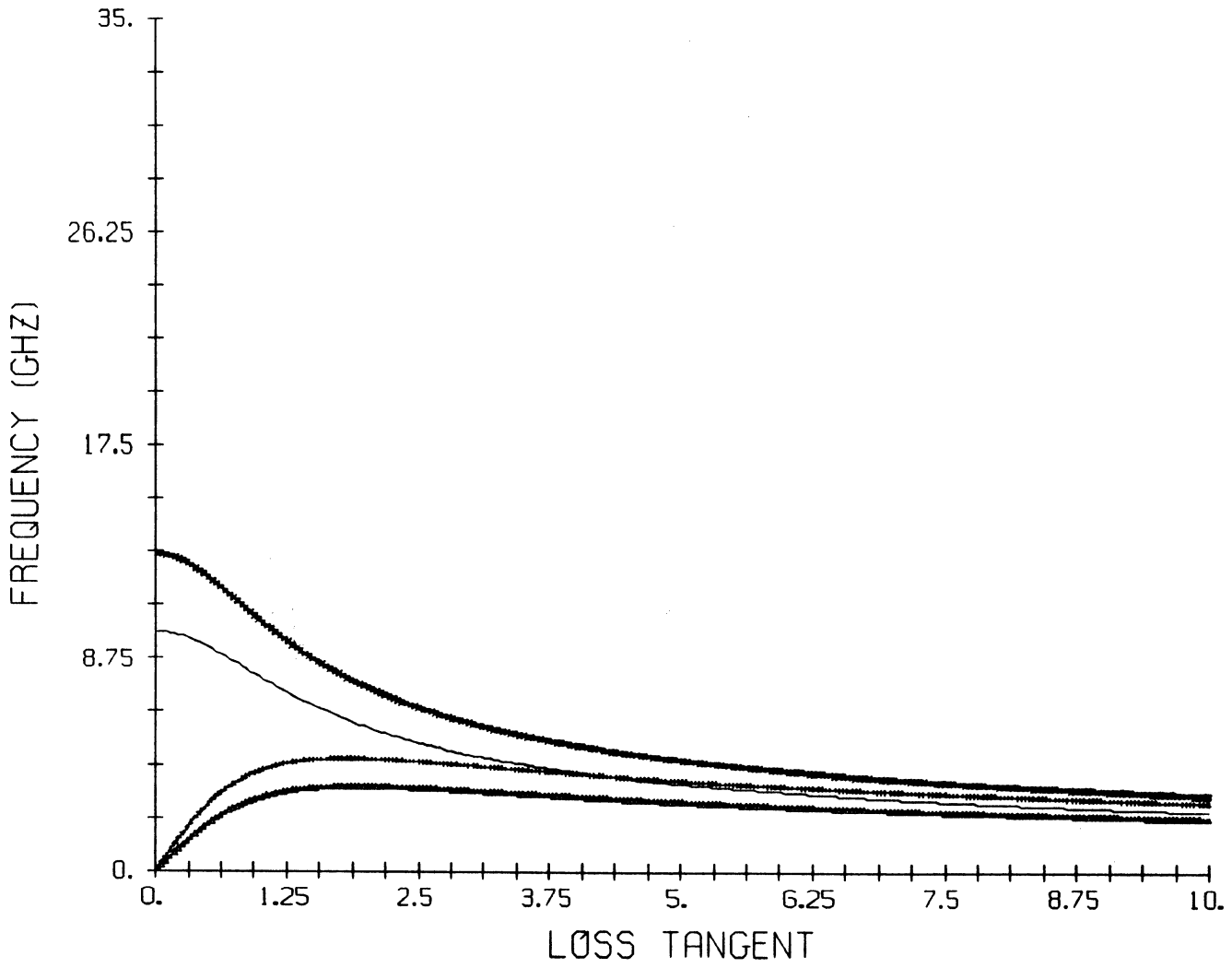

GROUP B

Comments

In this group there are two plots which served as a motivation for generating the plots of groups C-F.

These plots demonstrate the interchange of the mode order (Figure B.1) and the sensitivity of Muller's method to initial guesses (x_i, x_{i-1}, x_{i-2}) (Figure B.2).

17-APR-88
21:32:36

CUTØFF (REAL AND IMAG) VS. LØSS TANGENT

#5, 41

use xi-z values

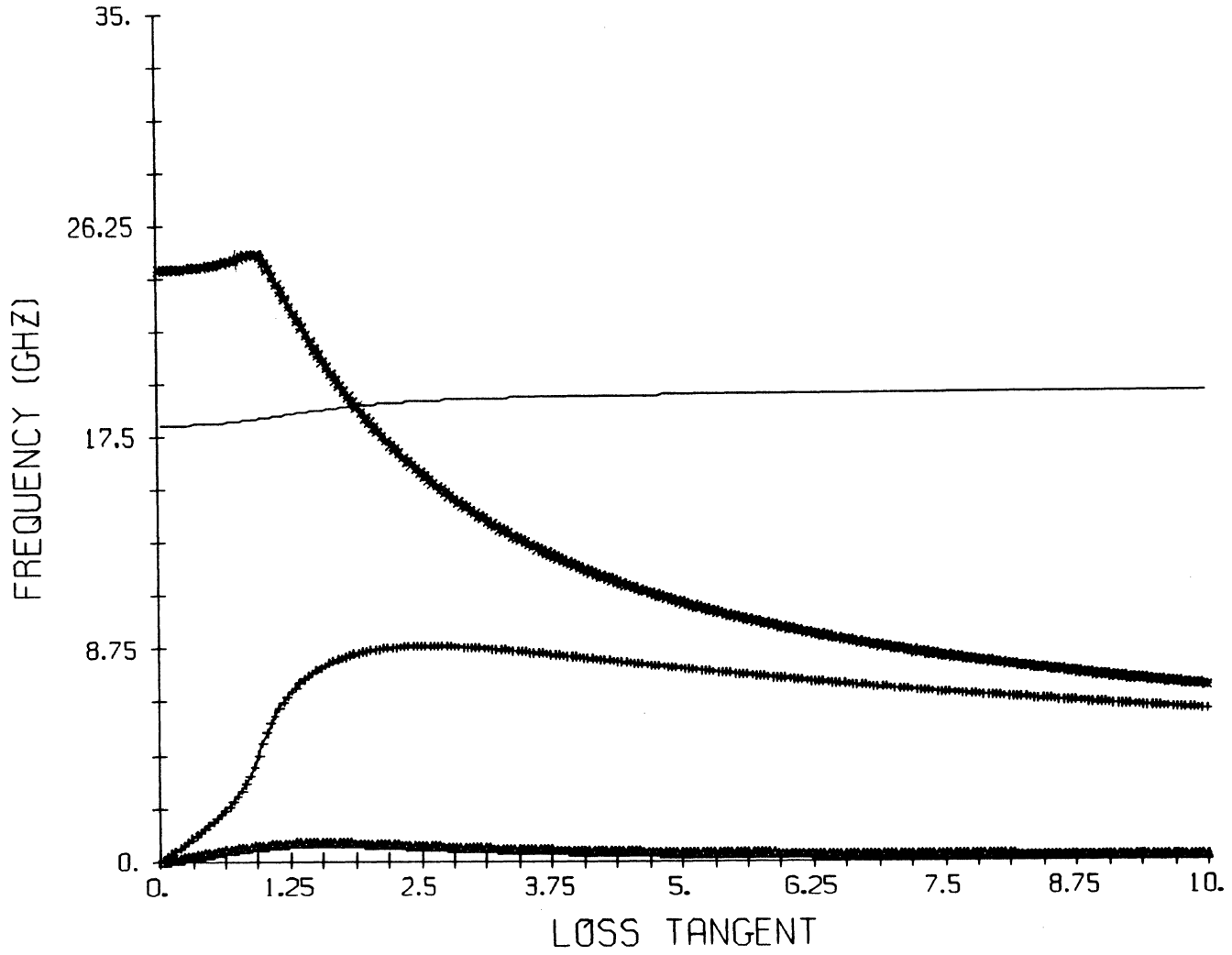

18-APR-88
23:06:22

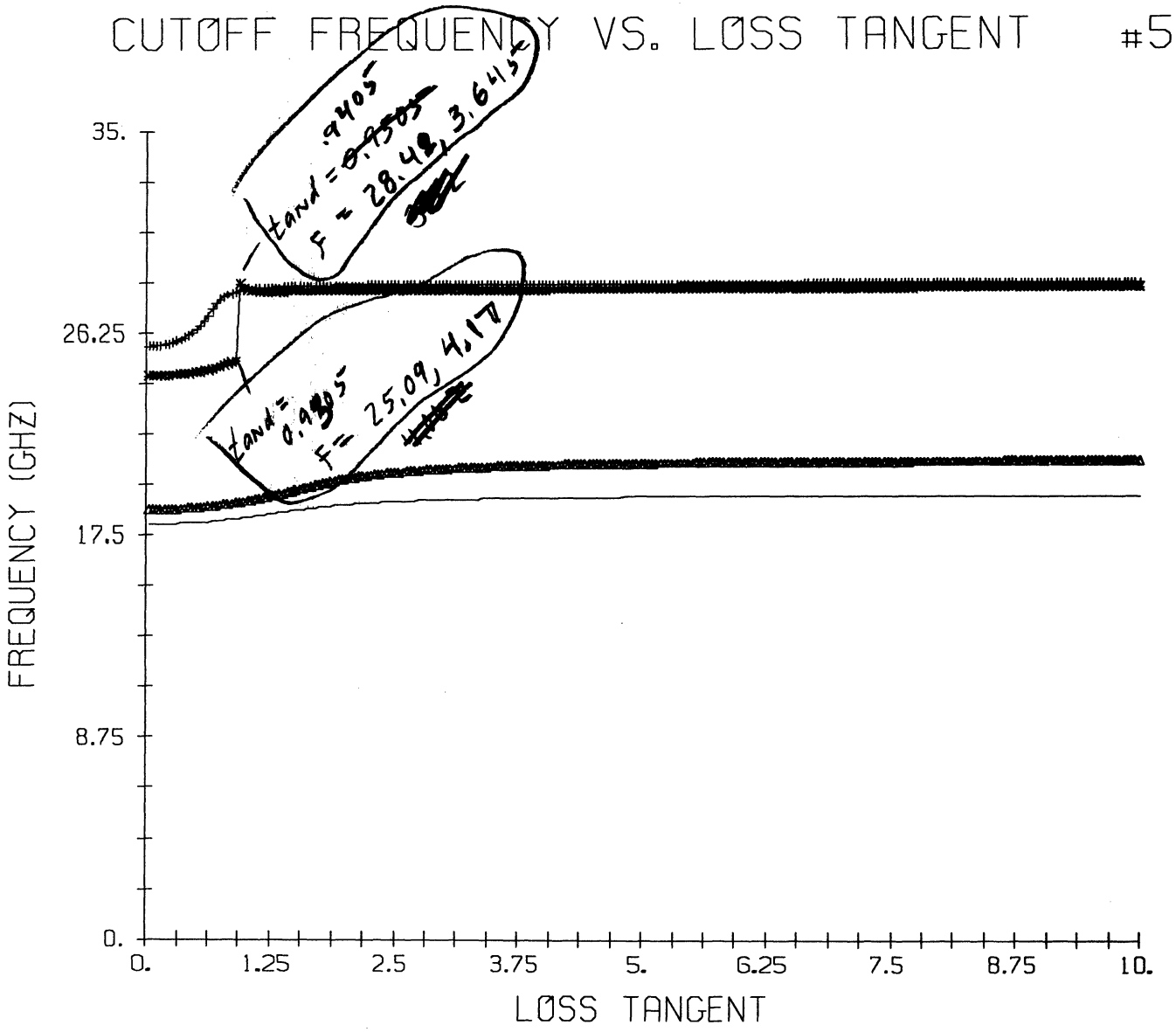

GROUP C

Specs:

Type of Mode = LSM

$k_y = \pi/b$
h = 0.025"
a = 0.305"
b = 0.305"
$\varepsilon_r = 16.0$

Observations:

- It is obvious that there are two LSM modes very close together.
- As tand increases, one can see that the original 2nd order mode has moved to become the dominant.

Equation for Epsr=0.9305

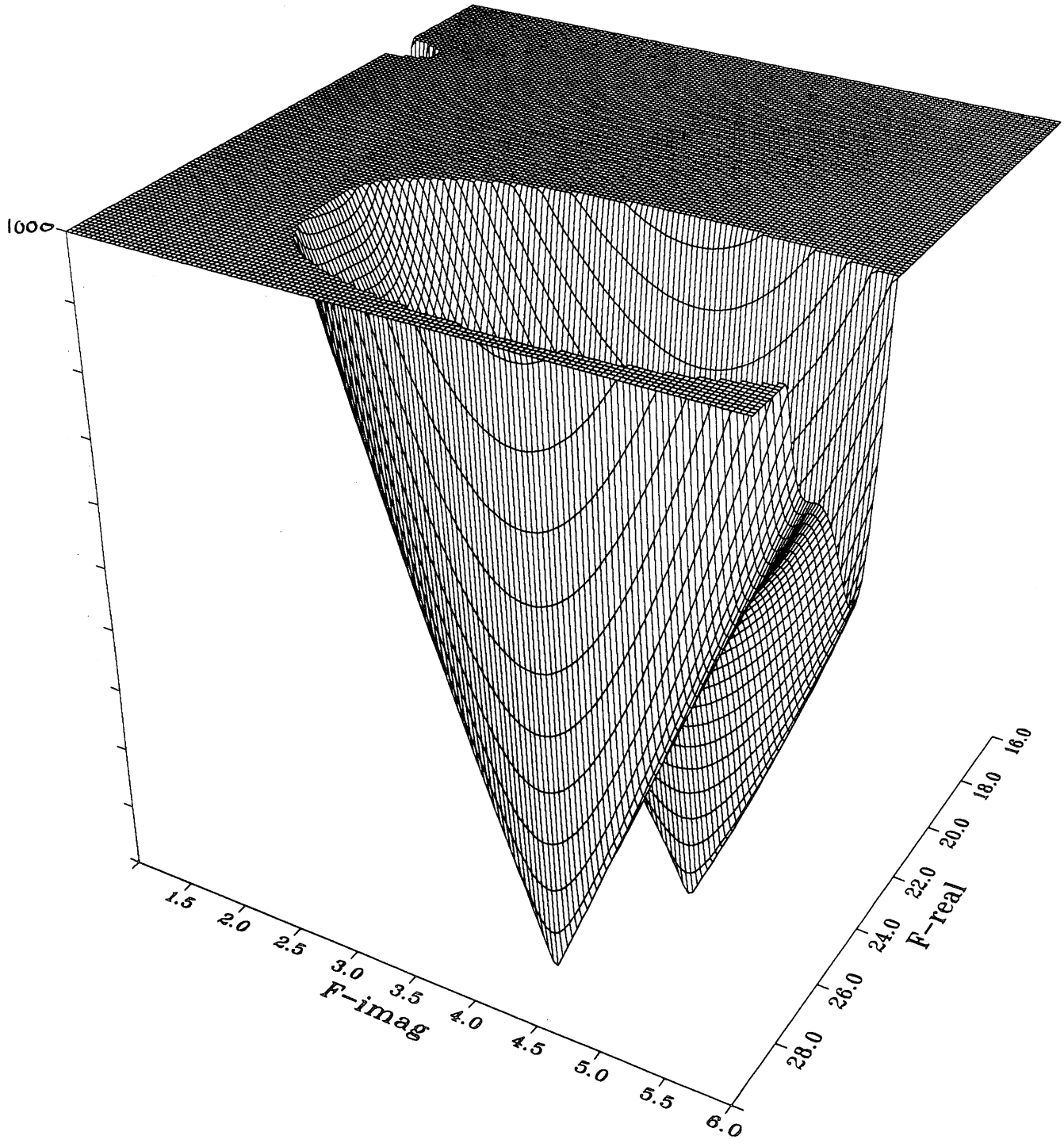

Equation for Epsr=0.9405

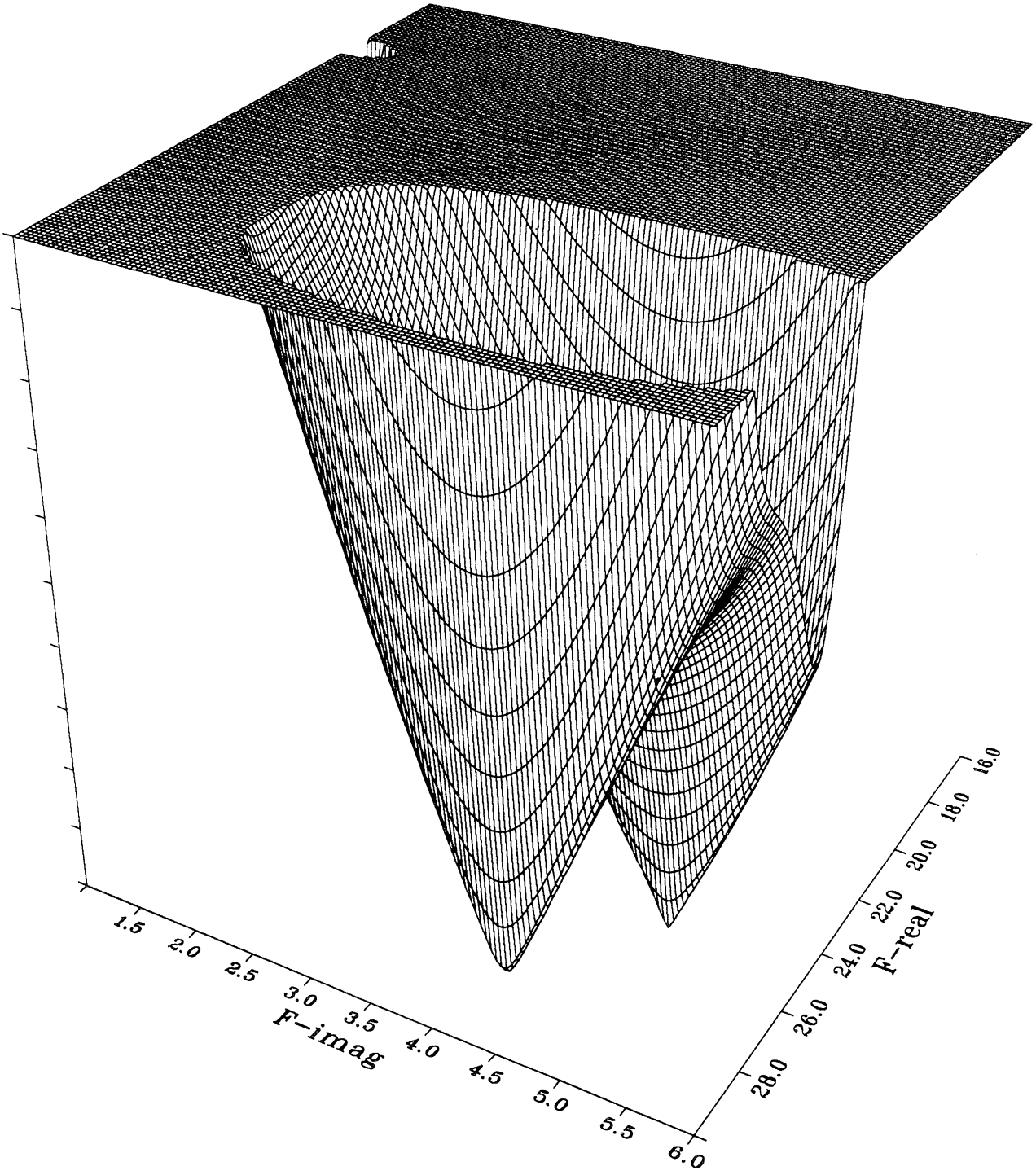

Equation for Epsr=0.9405

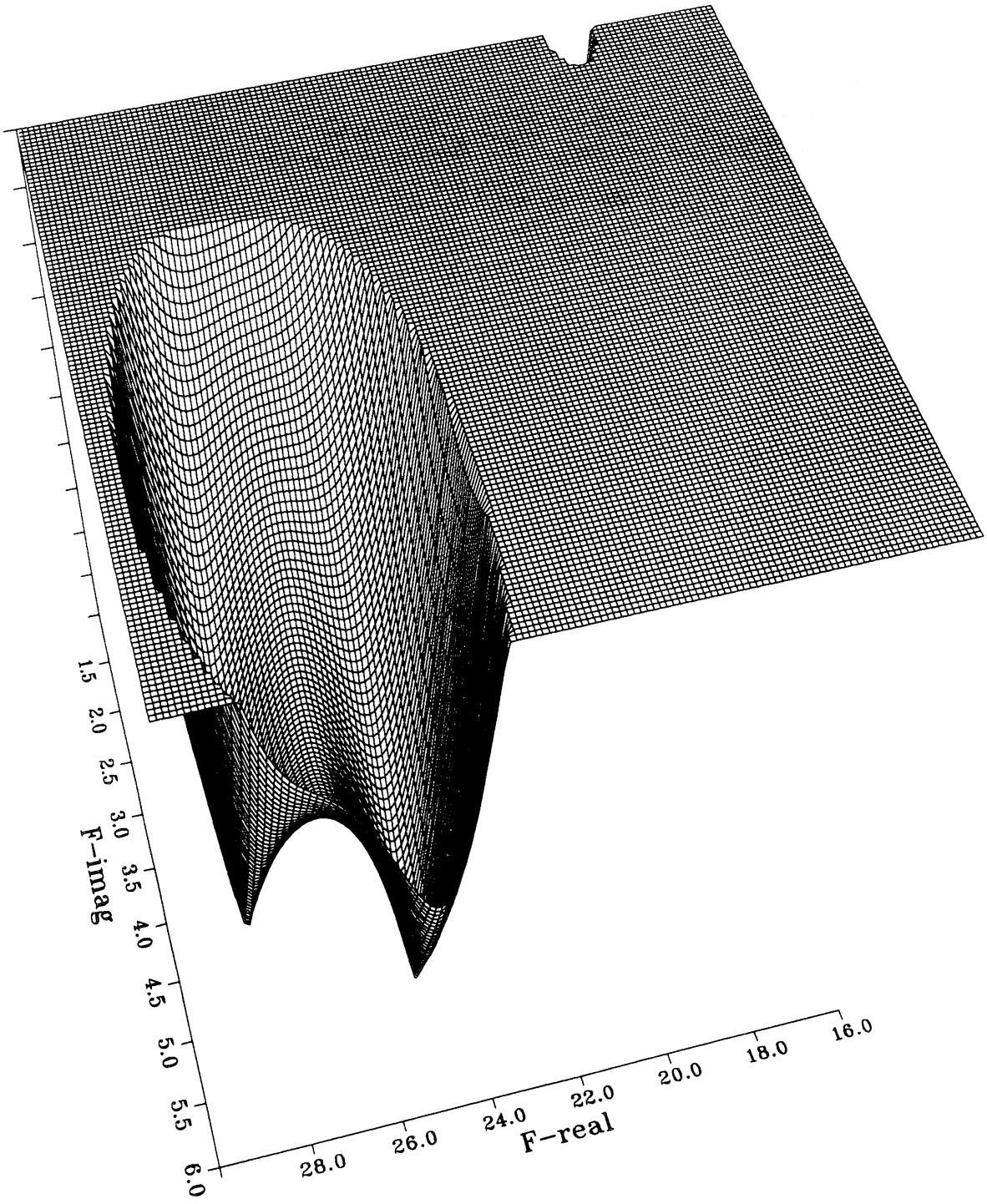

Equation for tand = 0.5

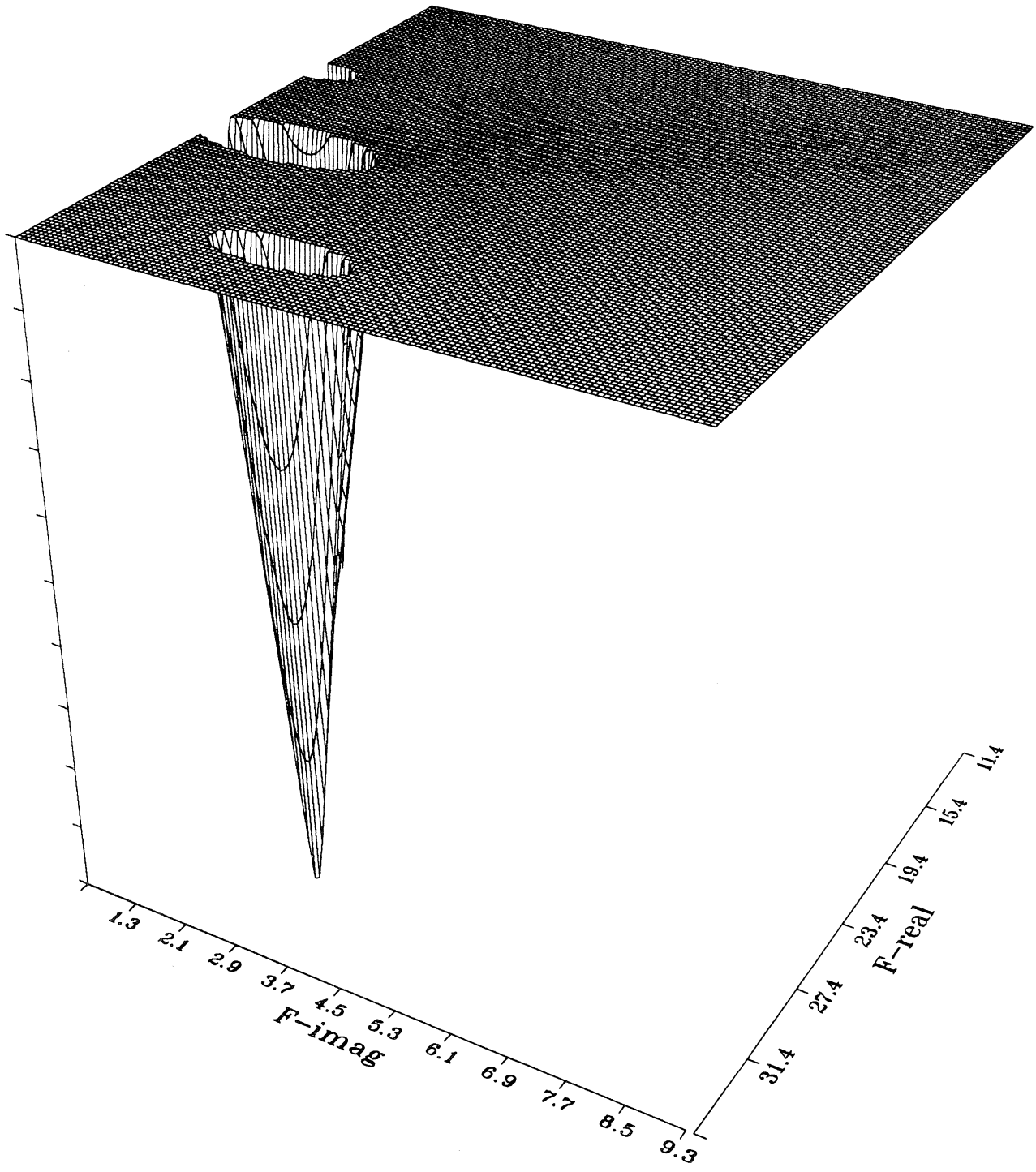

Equation for Epsr=0.5

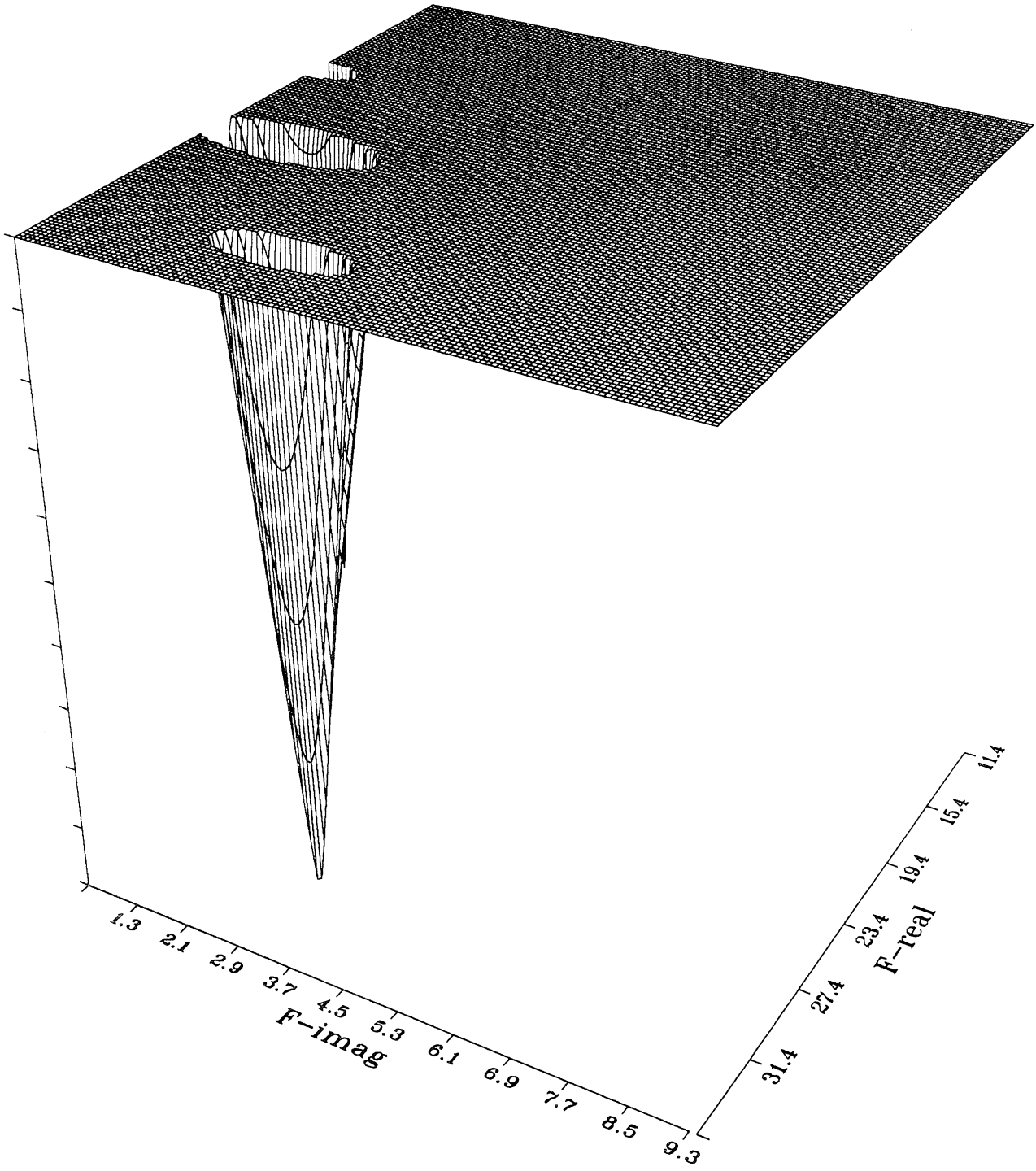

Equation for Epsr=1.0

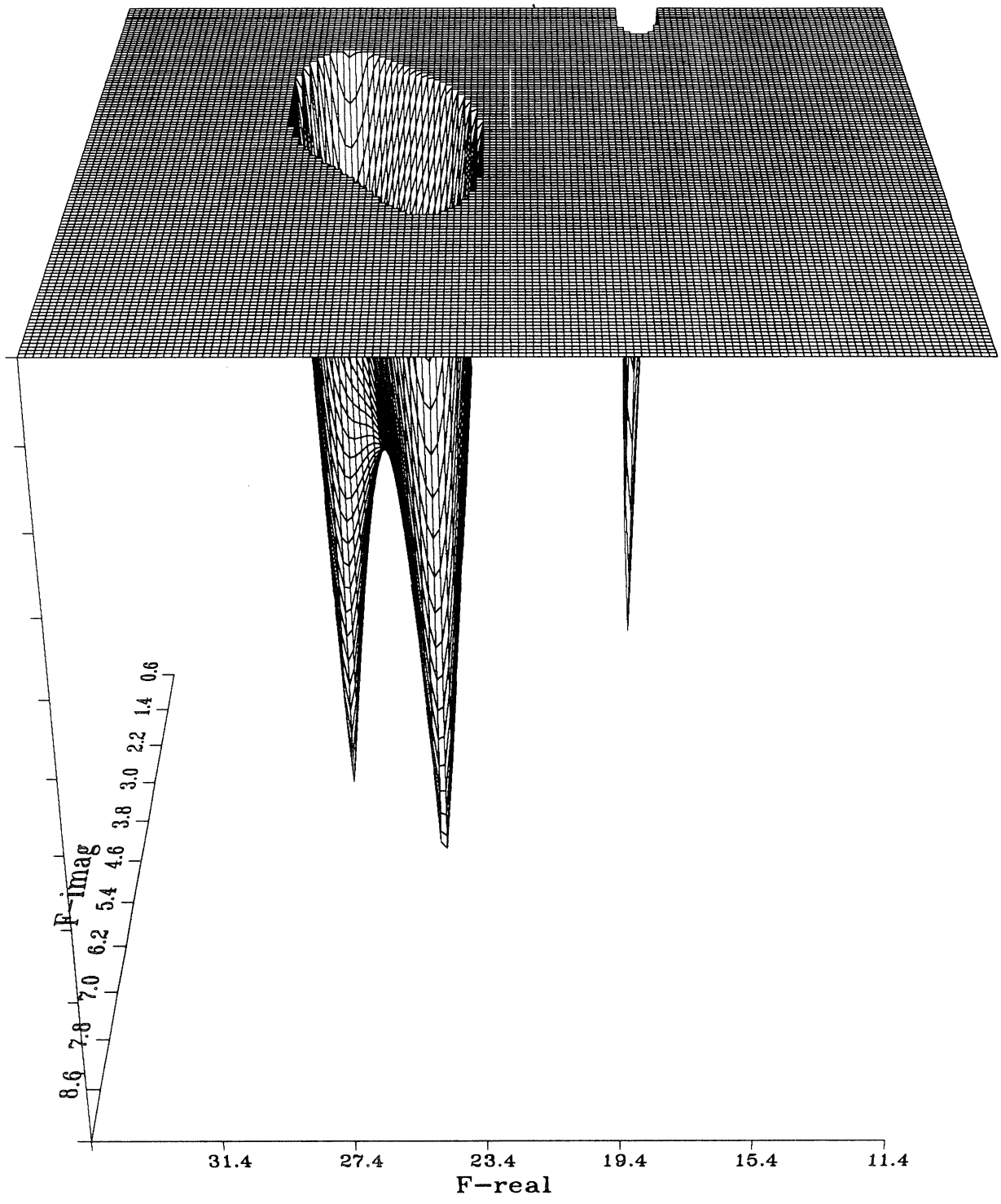

Equation for ~~Epsr~~ tanδ =1.5

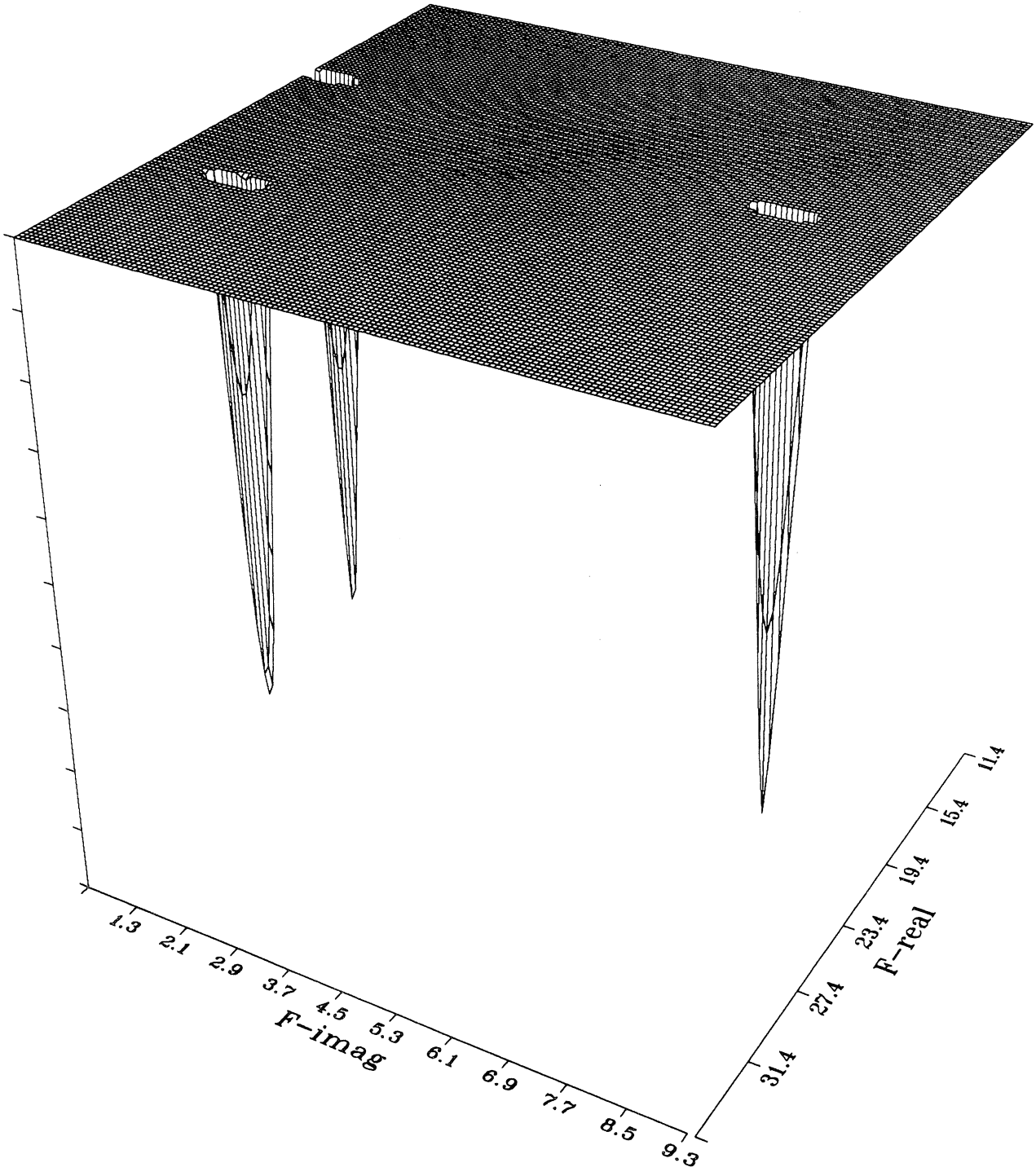

Equation for Epsr=2.0

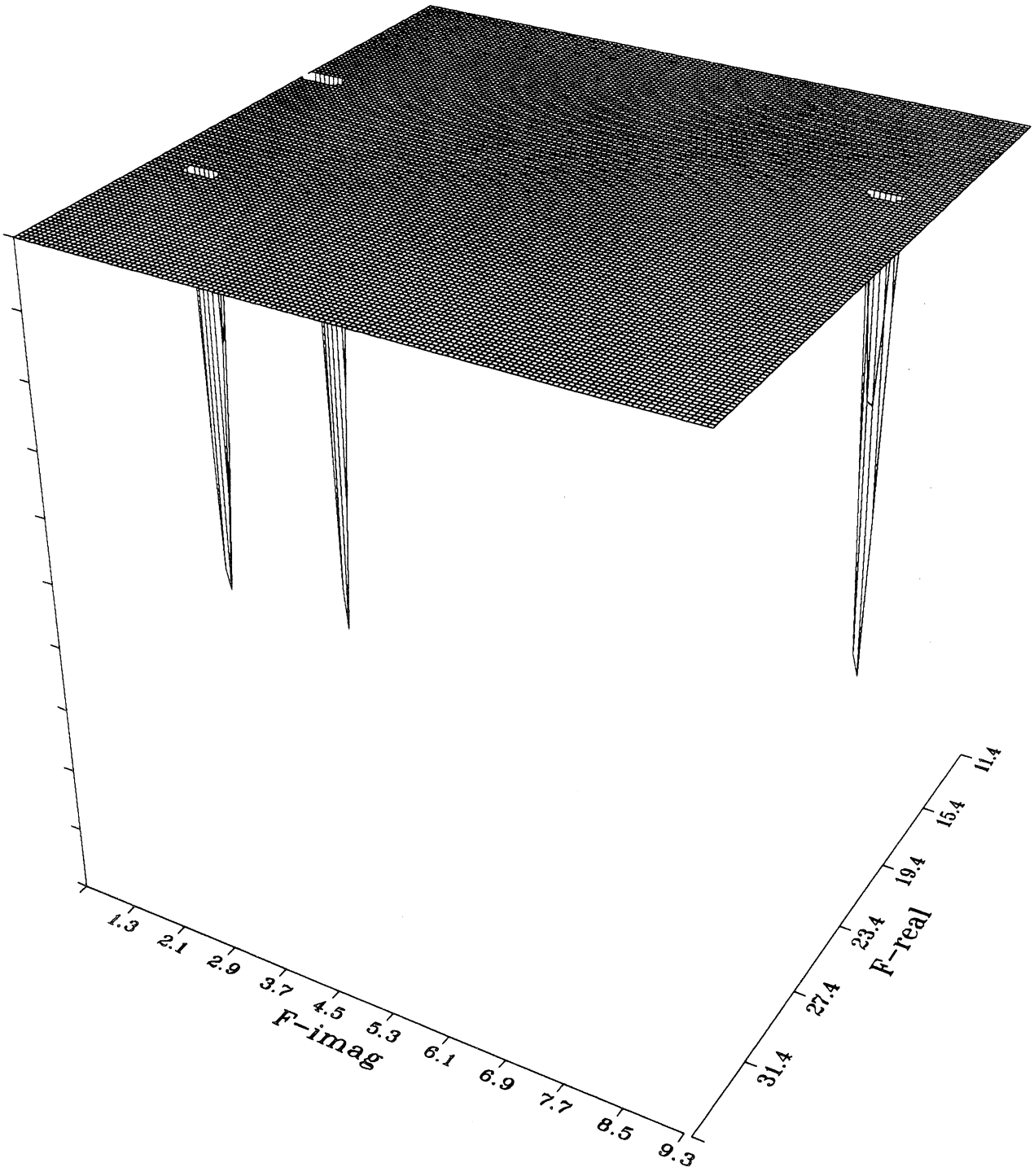

Equation for Epsr=2.5

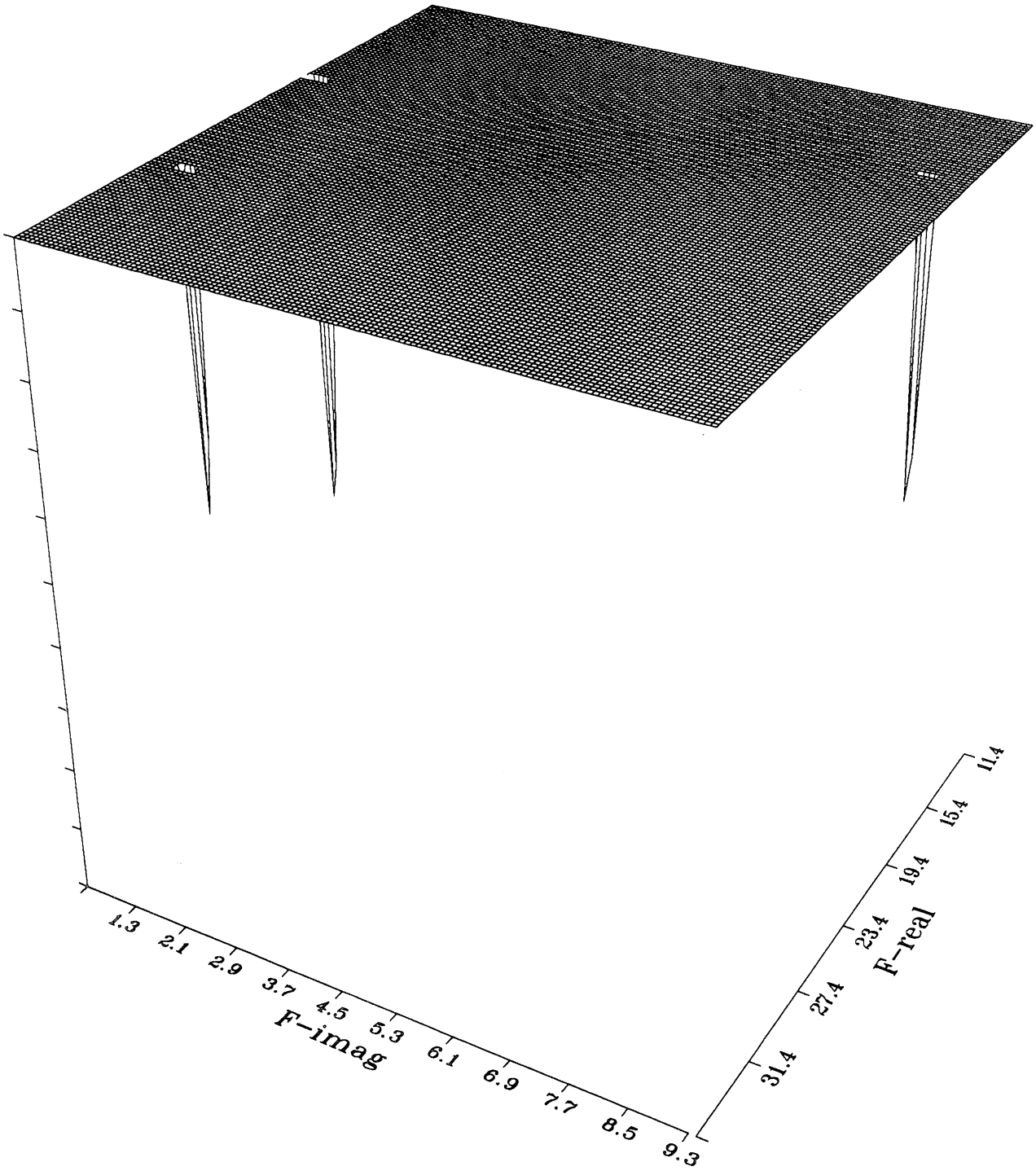

GROUP D

Specs:

Type of Mode = LSE

$k_y = 0.0$
a = 0.305"
b = 0.305"
$\varepsilon_r = 16.0$
h = 0.025"

Observations:

- At first glance, one might sense a problem with these plots. The specs are nearly the same with those of Group A, #5 which shows no mode crossover. Yet it is clear from these plots that the dominant LSE mode is replaced as tand is increased.
- The difference between this curve and the corresponding one in Group A is in k_y.

Equation for tand=0.005 (LSF

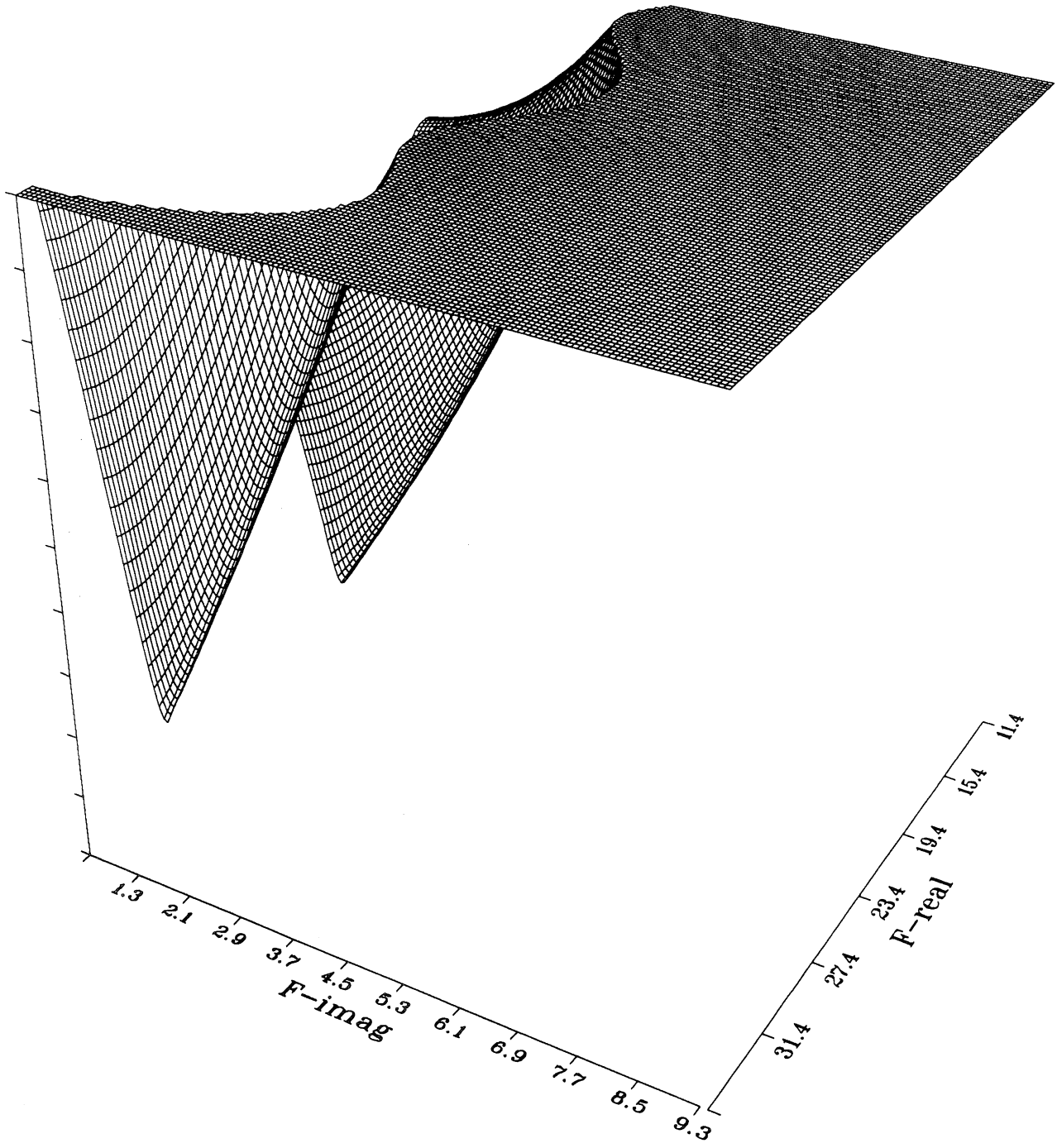

Equation for tand=0.01 (LSE)

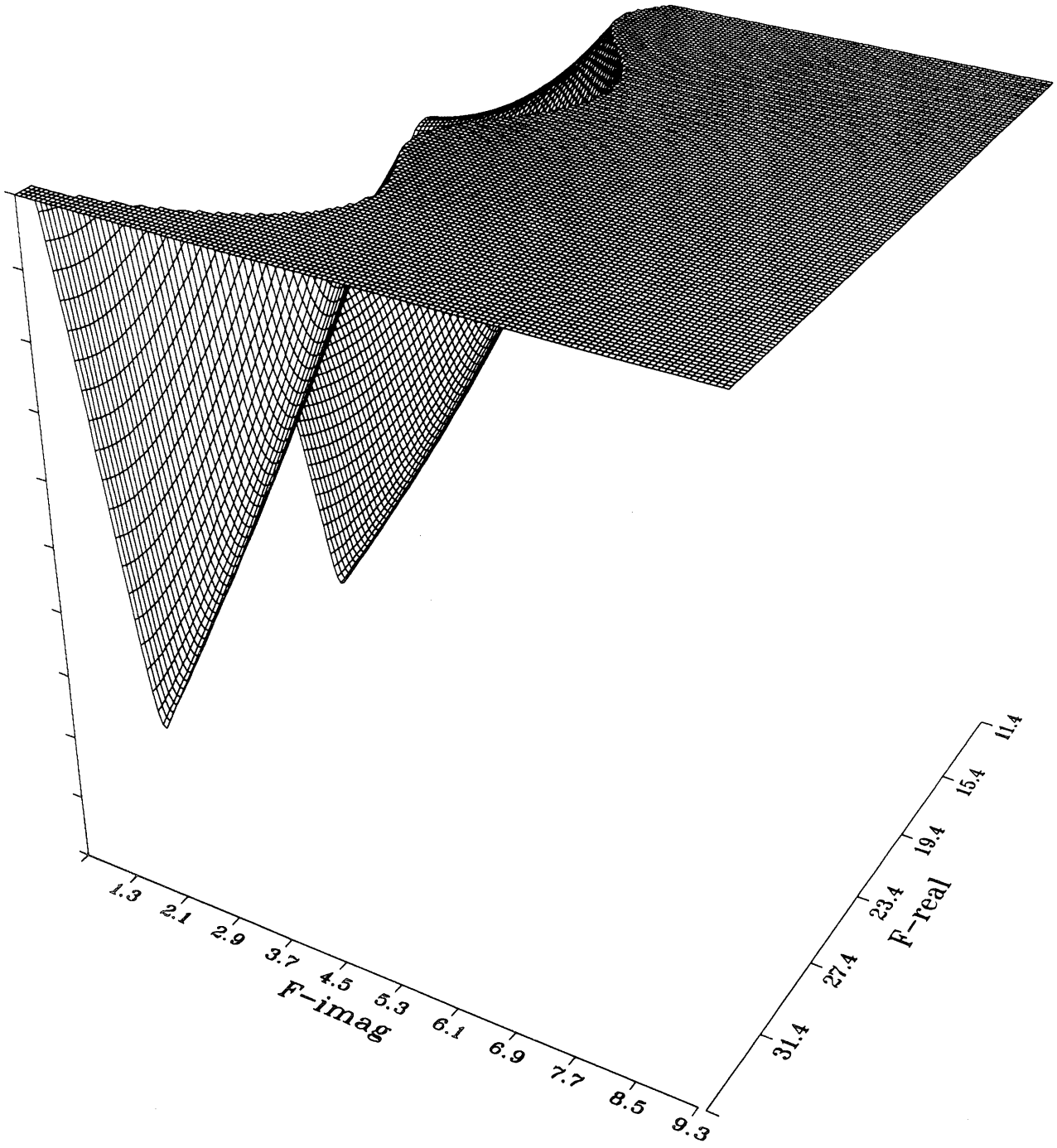

Equation for tand=0.05 (LSE

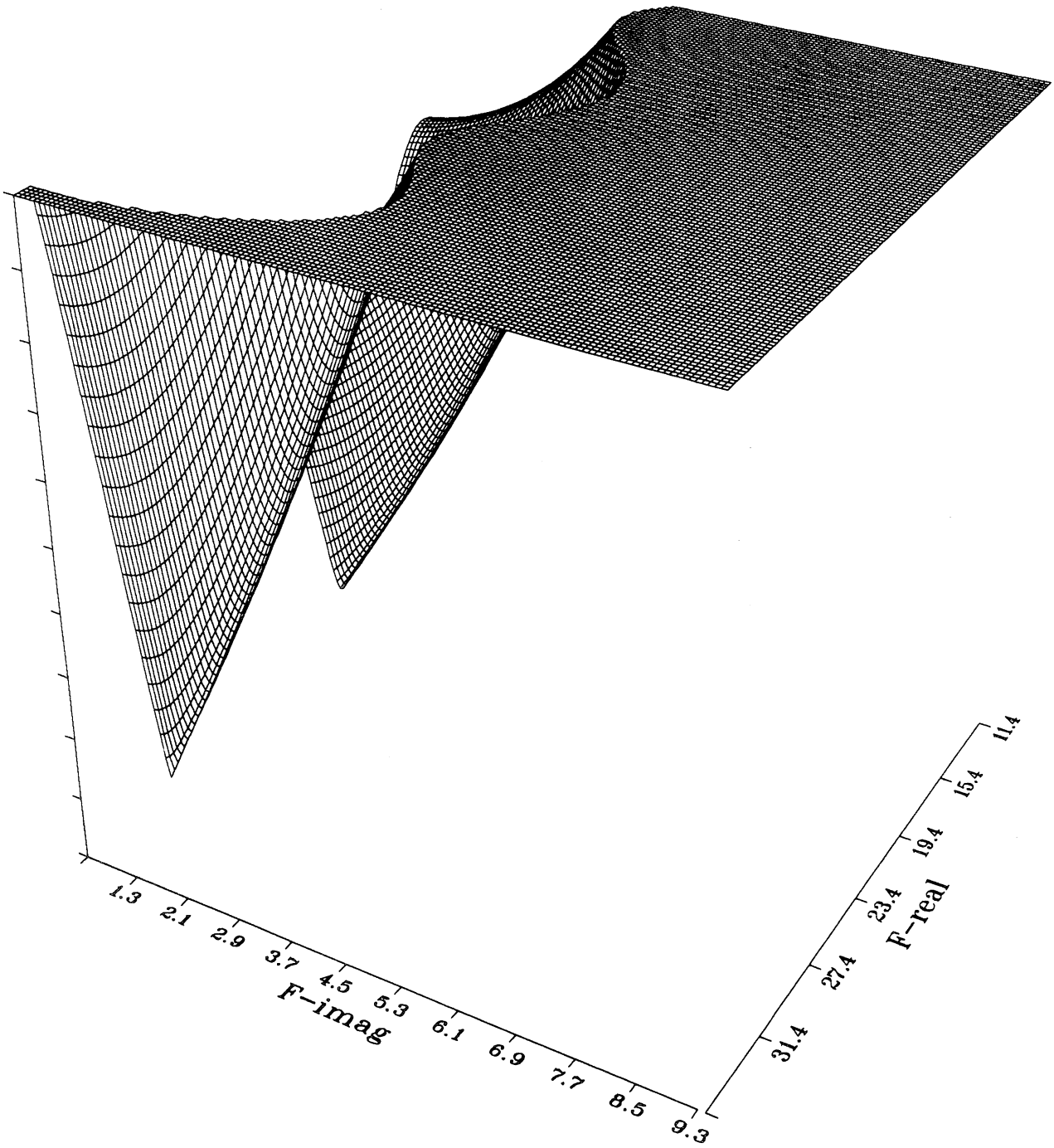

Equation for tand=0.1 (LSE)

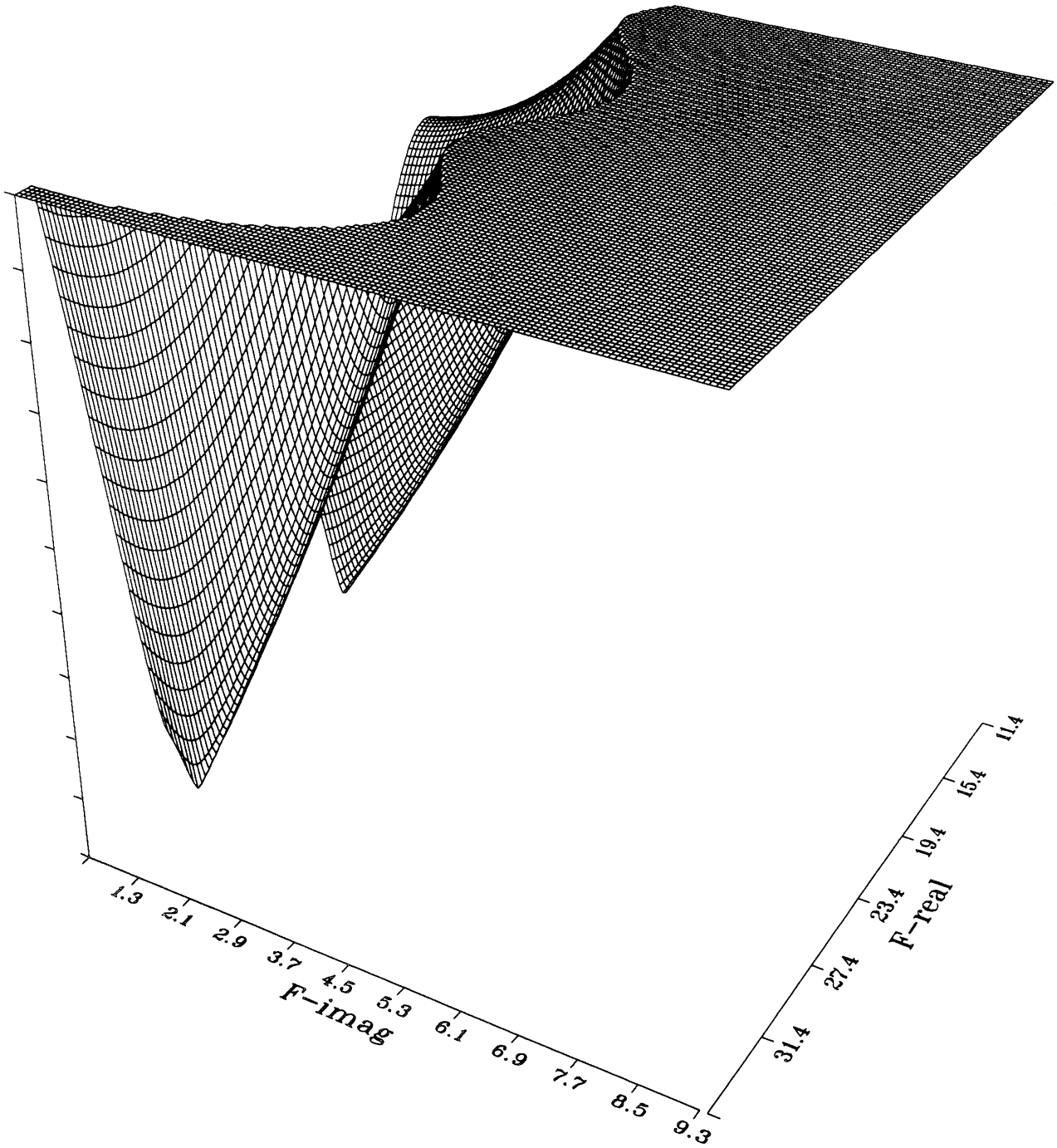

Equation for tand=0.3 (LSE)

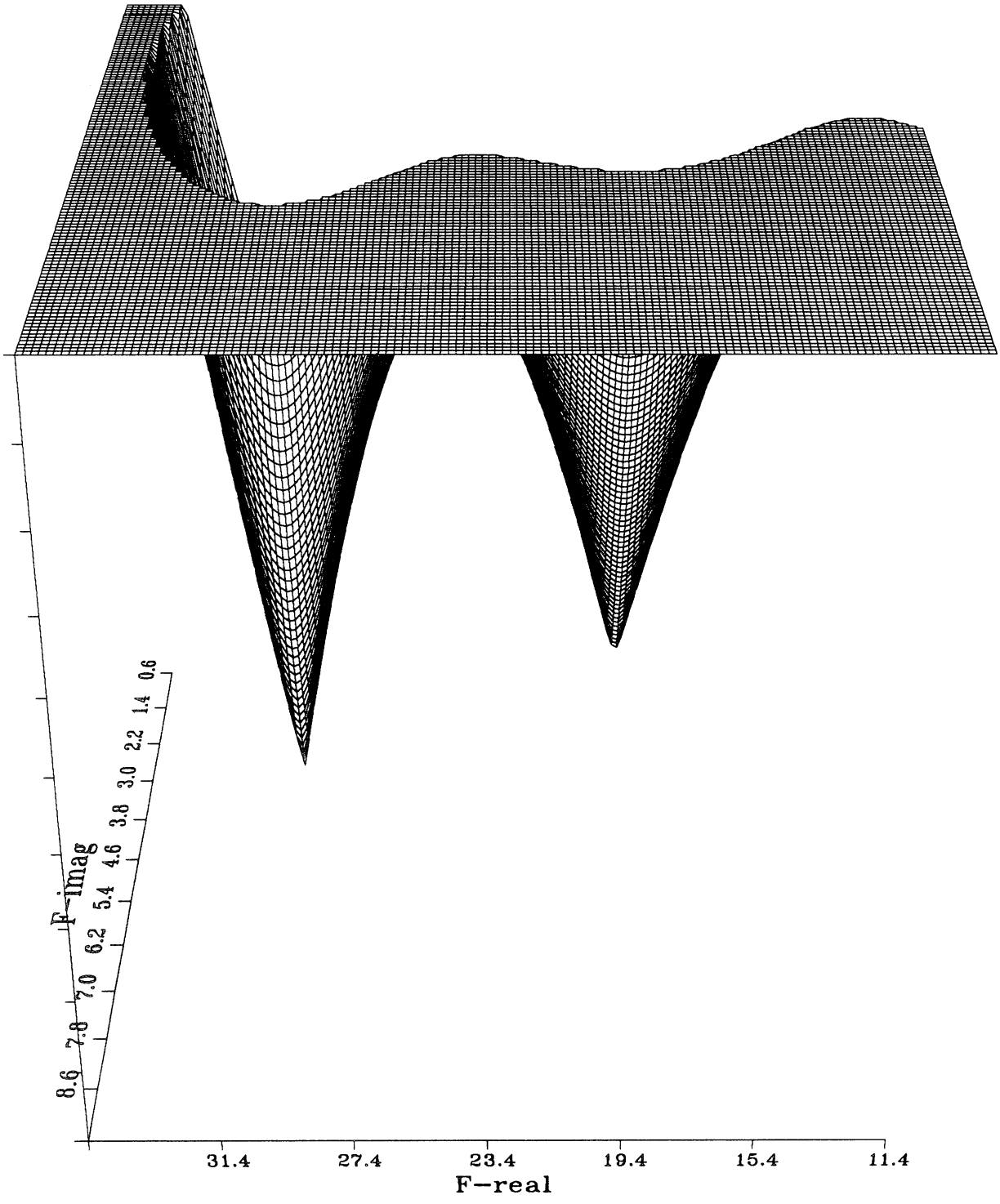

Equation for tand=0.5

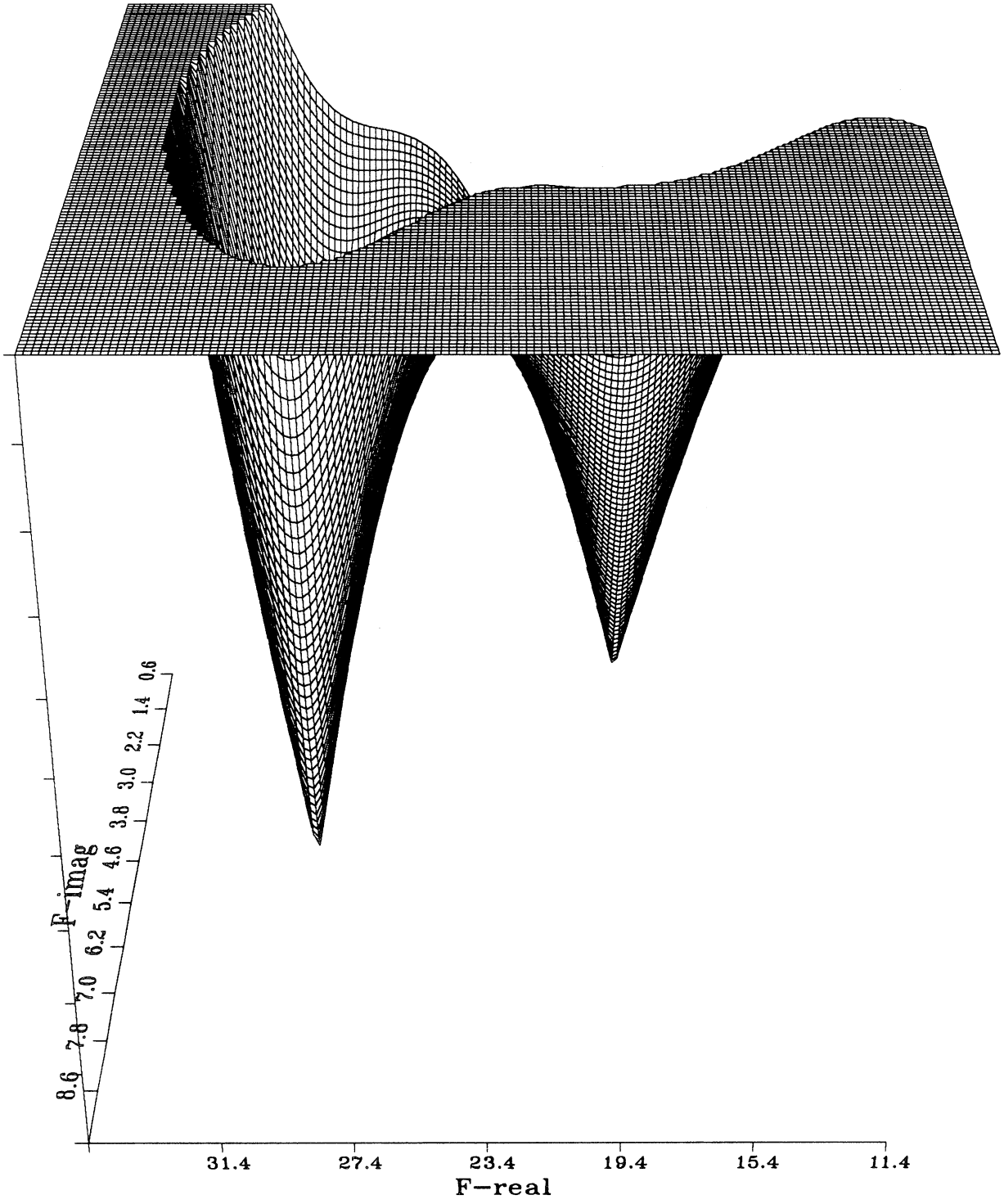

Equation for tand=1.0

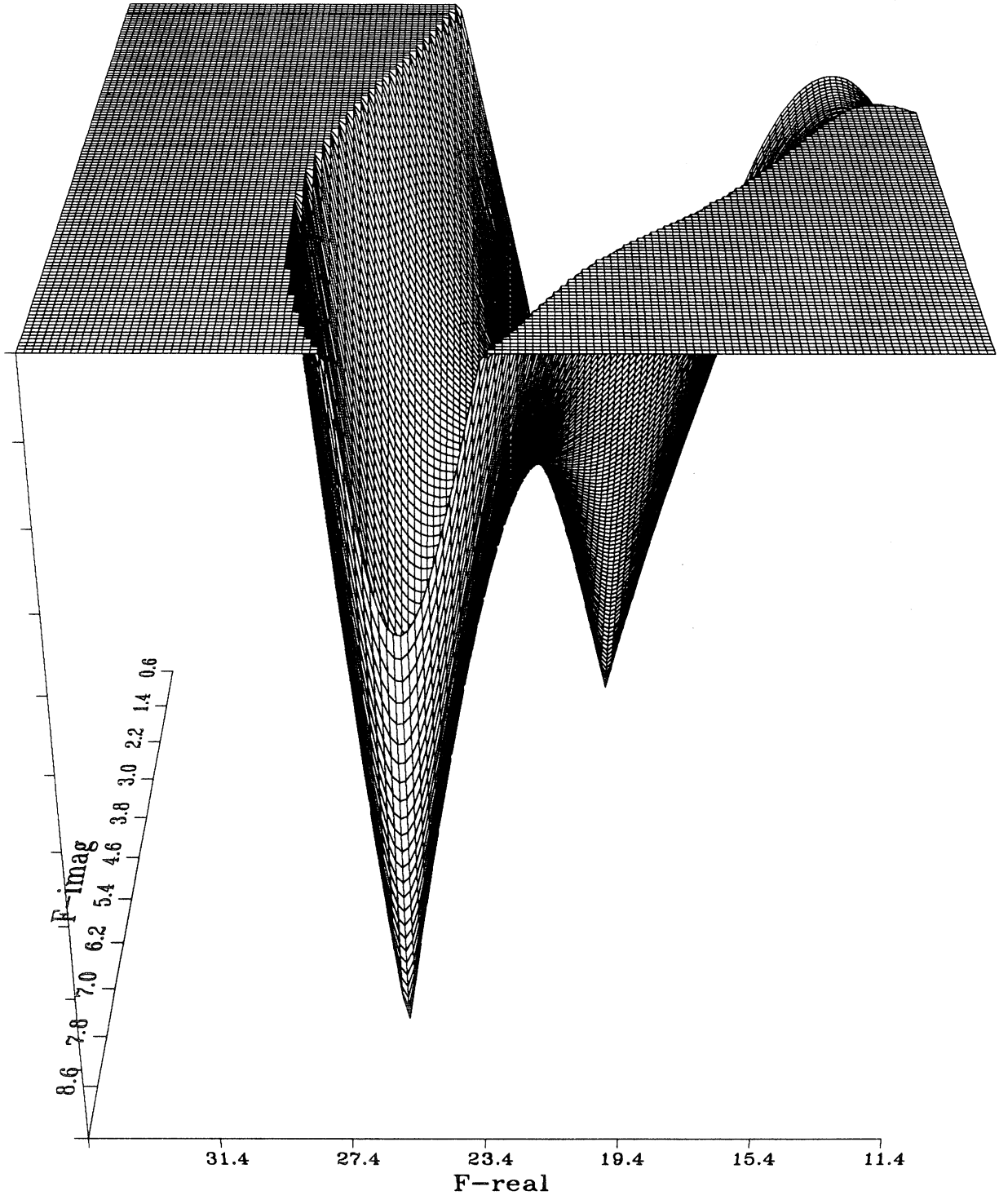

Equation for tand=1.5

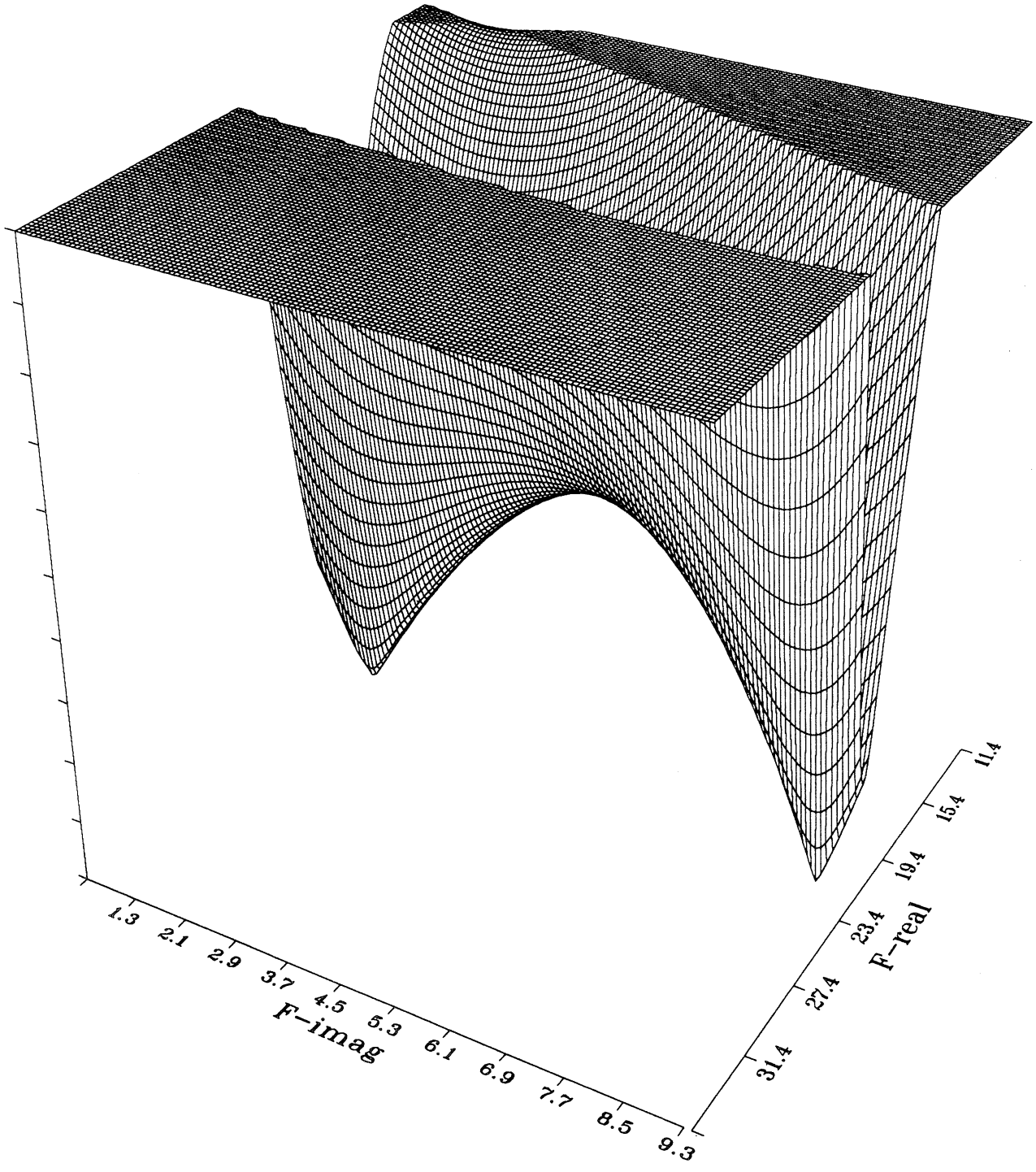

Equation for tand=2.0

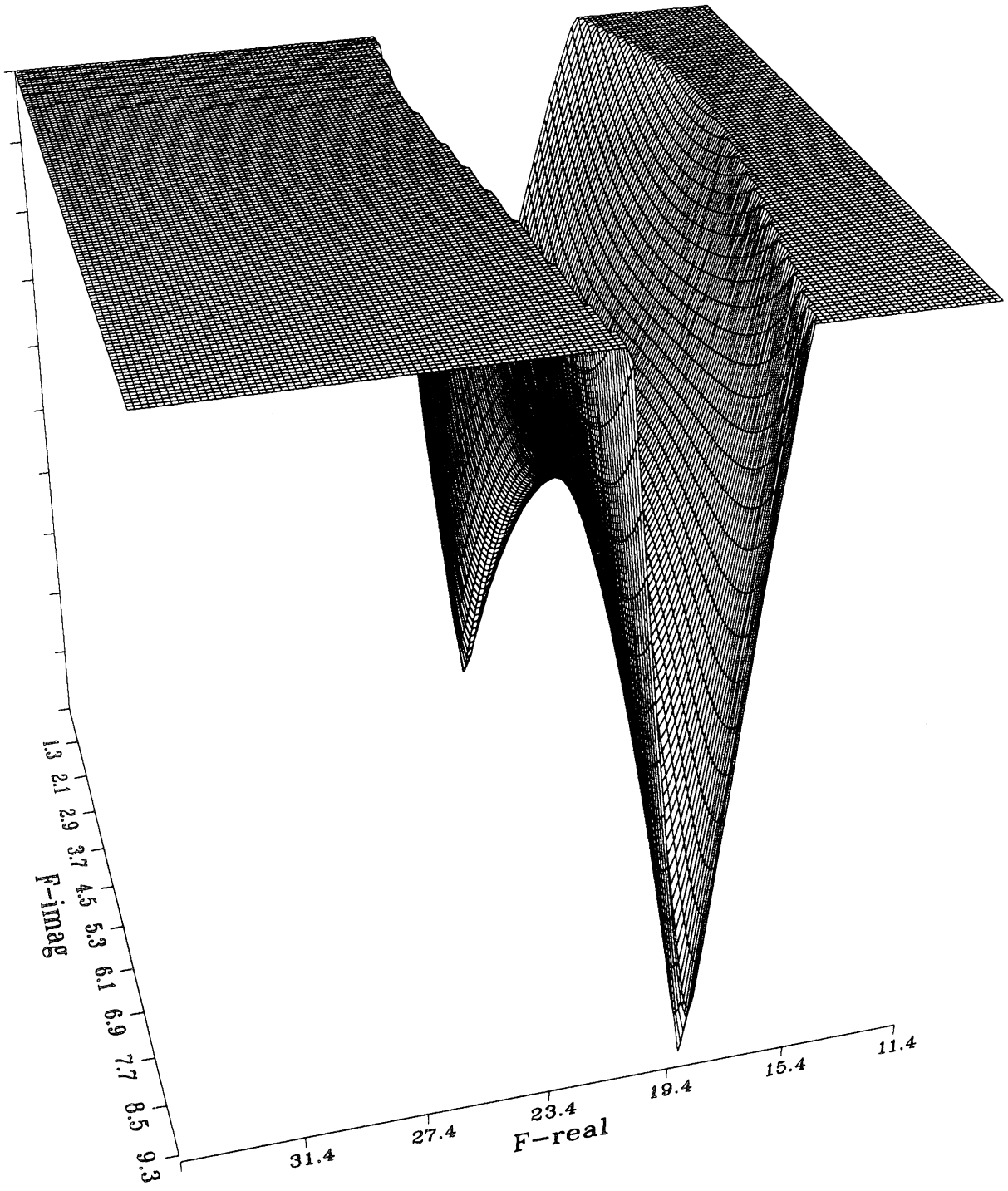

GROUP E

Specs:

Type of Mode = LSE

$k_y = \pi/b$
a = 0.305"
b = 0.305"
$\varepsilon_r = 16.0$
h = 0.025"

Observations:

- Following the progression of these plots, it is clear that there is a mode which remains nearly fixed for increasing tand. This would be the LSE_2 mode which appears in #5 from Group A. It also appears that another higher order mode is cutting across.

Equation for tand=0.1 (LSE)

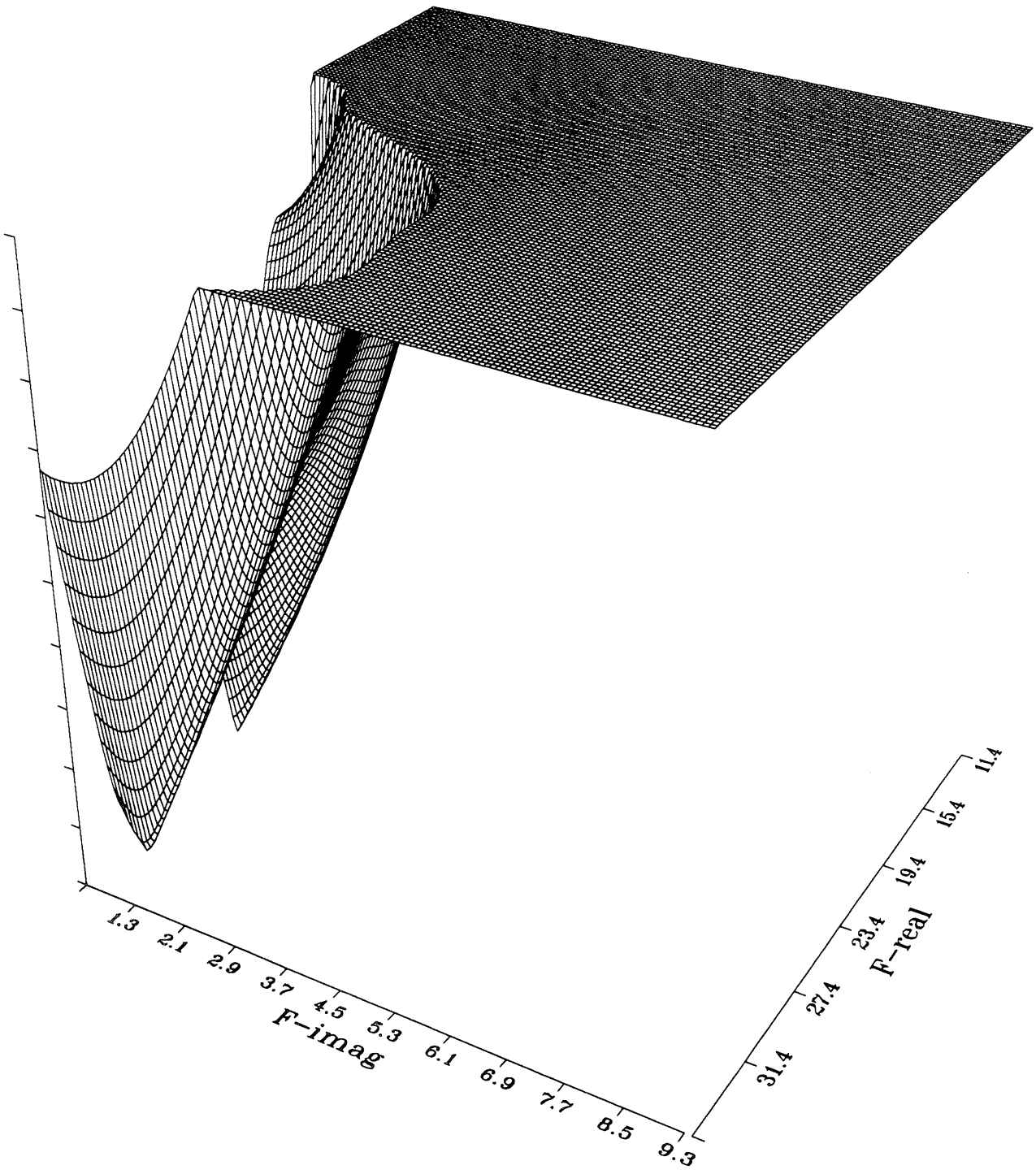

Equation for tand=0.5 (LSE)

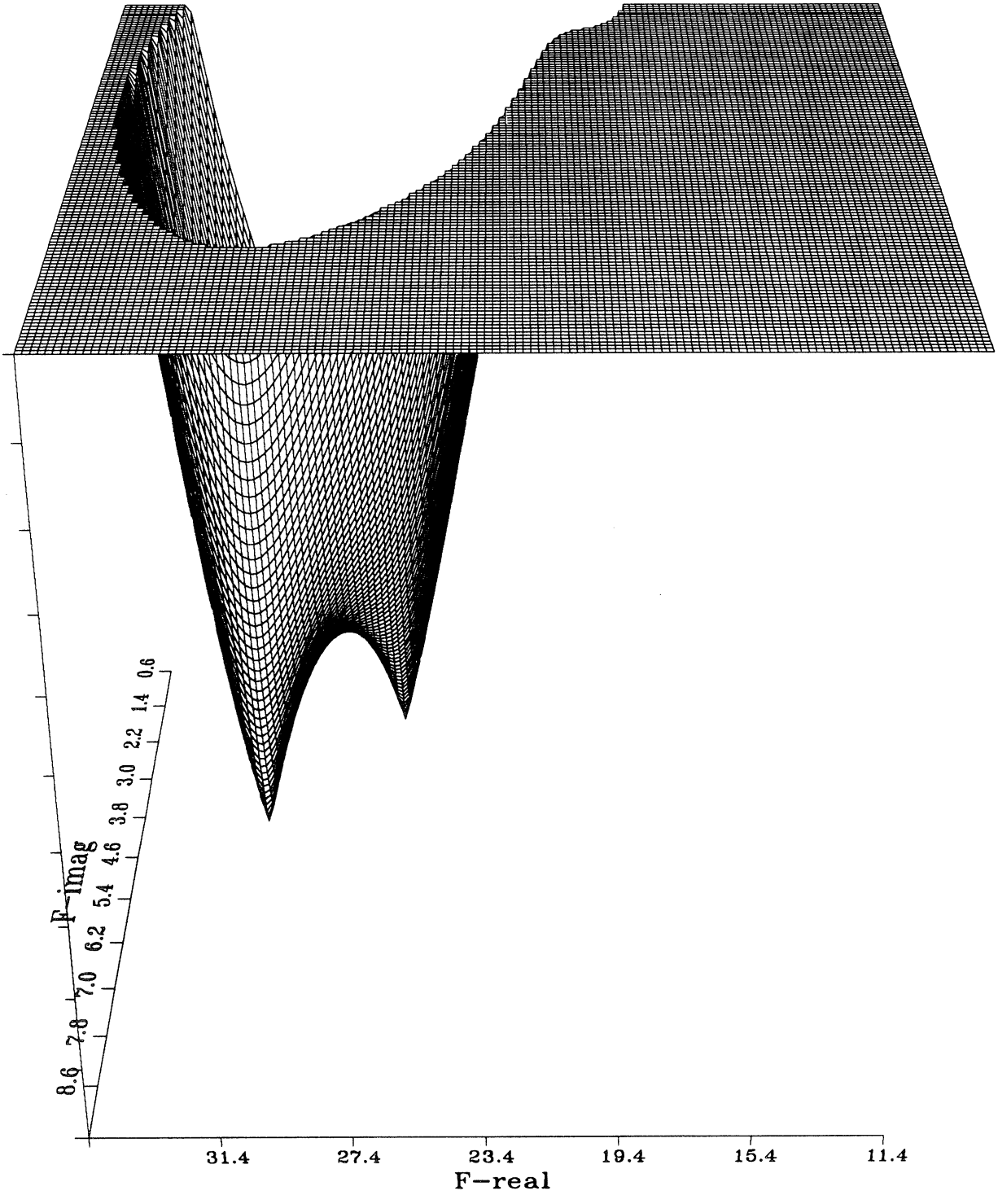

Equation for tand=1.0 (LSE)

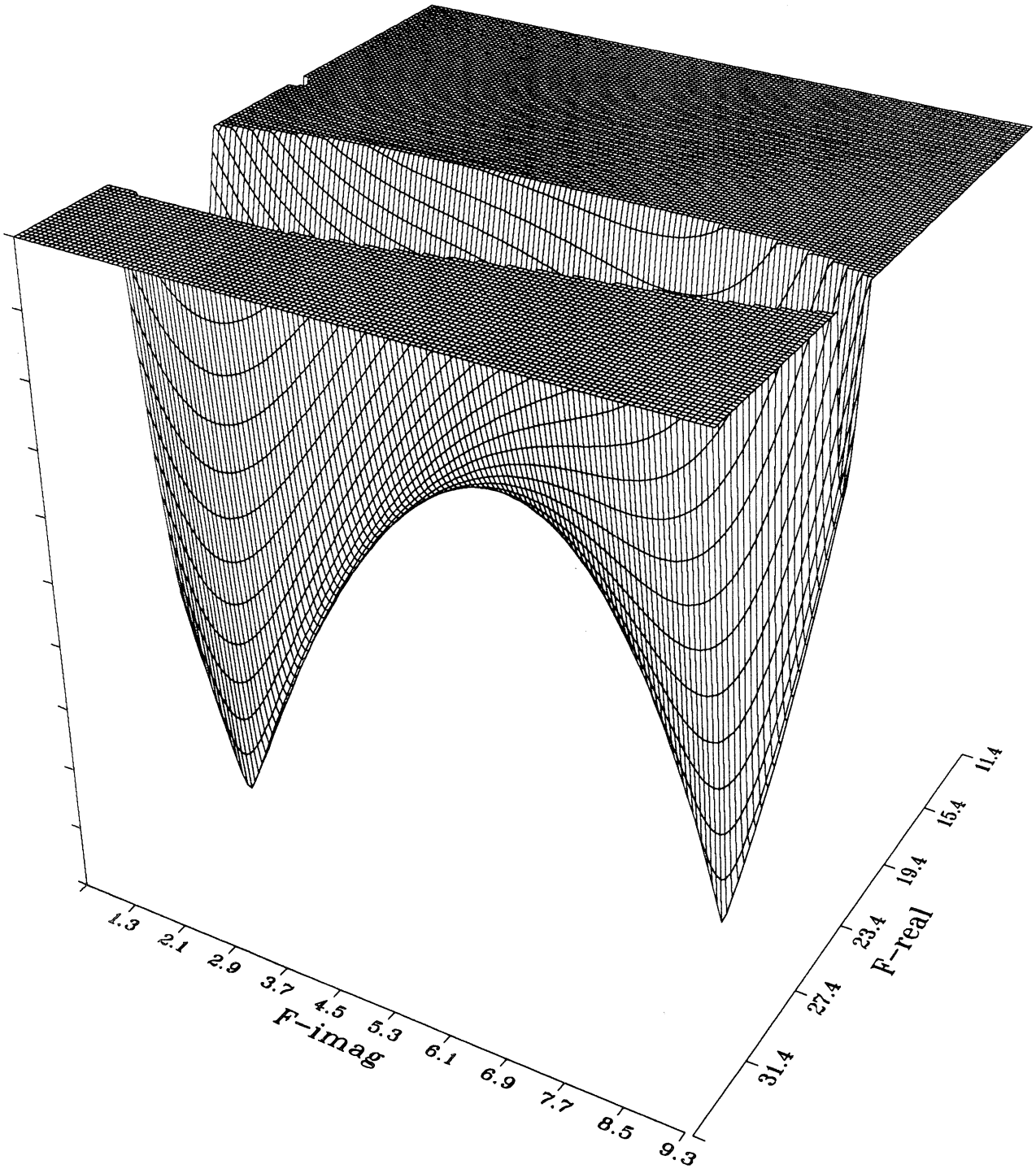

Equation for tand=1.5 (LSE)

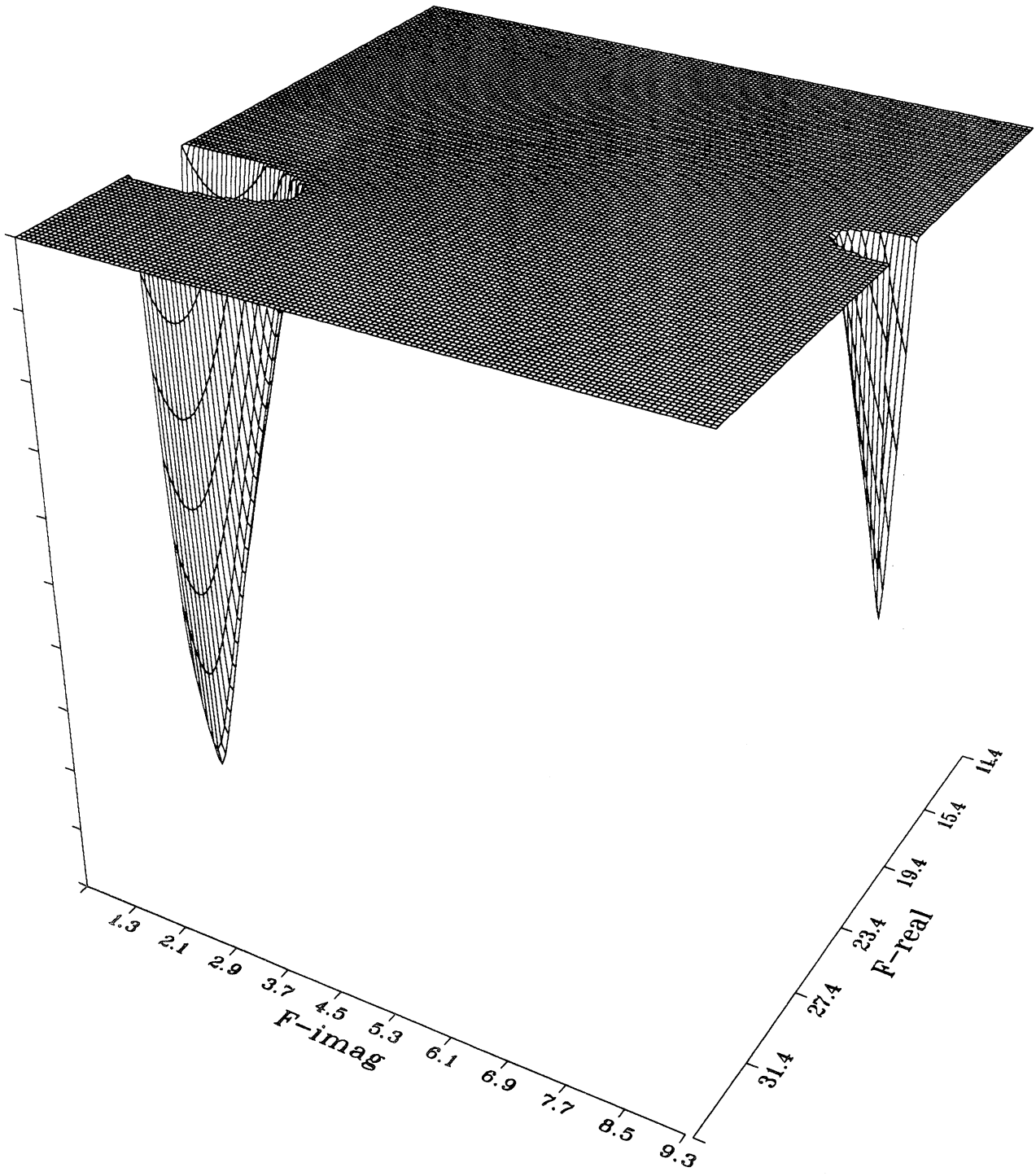

Equation for tand=2.0 (LSE)

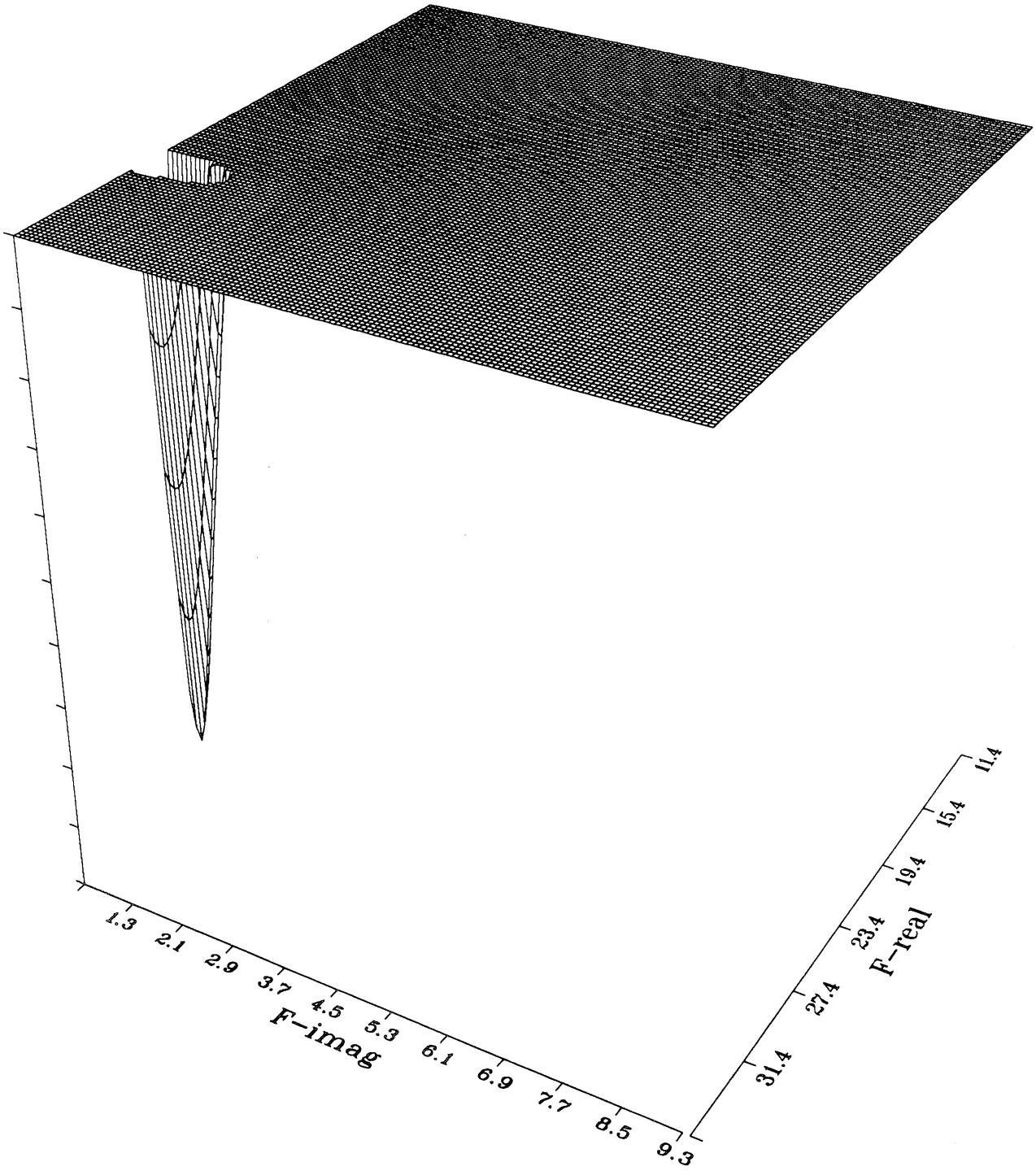

GROUP F

Specs:

Type of mode = LSM

$k_y = \pi/b$
a = 0.305"
b = 0.305"
h = 0.025"
$\varepsilon_r = 12.0$

Observations:

- By changing ε_r from 16.0 to 12.0 we can observe much greater stability in the relationship between LSM_1 and LSM_2. Note, however, that a higher order mode is still seen to be moving to the dominant position.

Equation for tand=0.5 (LSM)

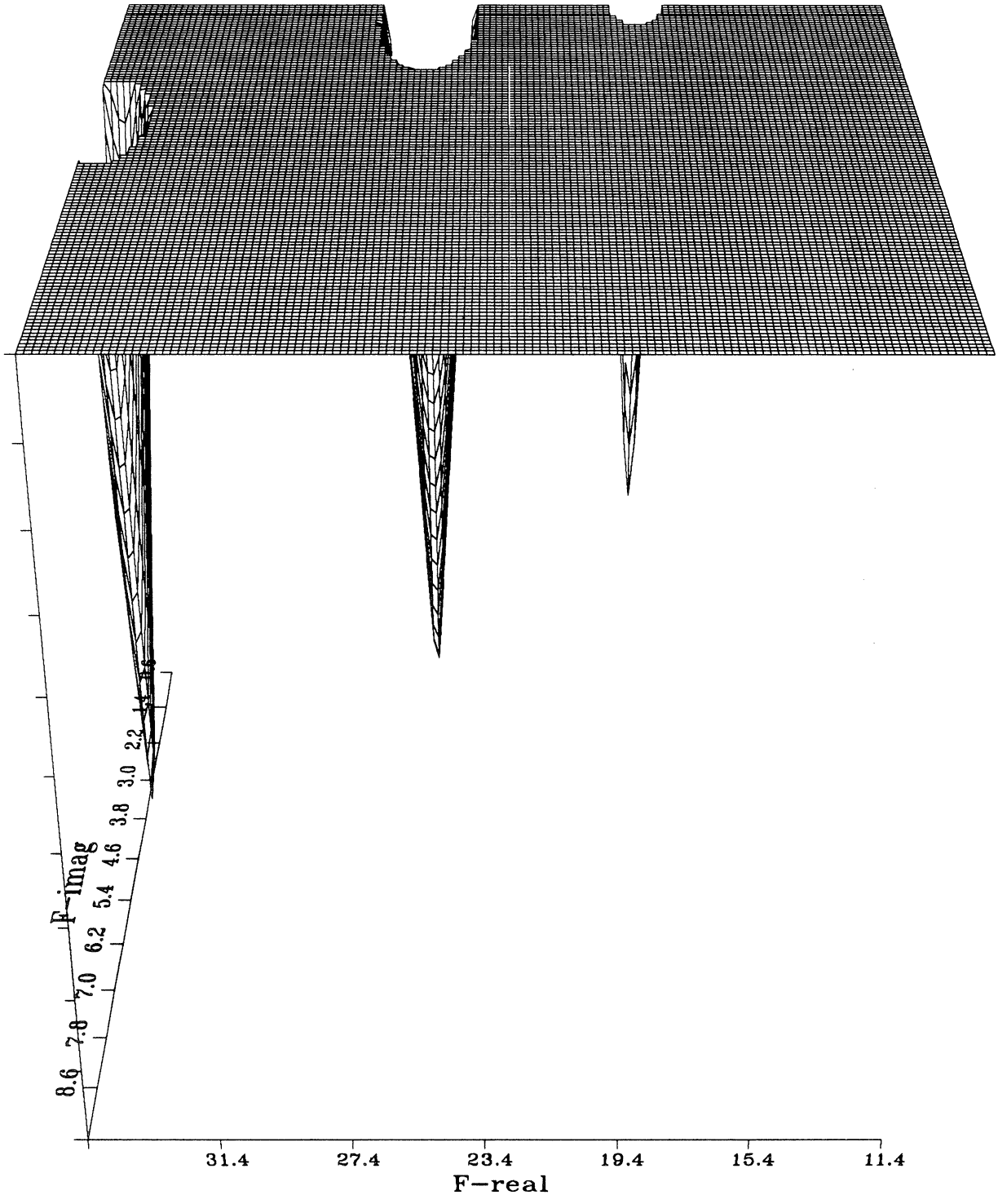

Equation for tand=1.0 (LSM)

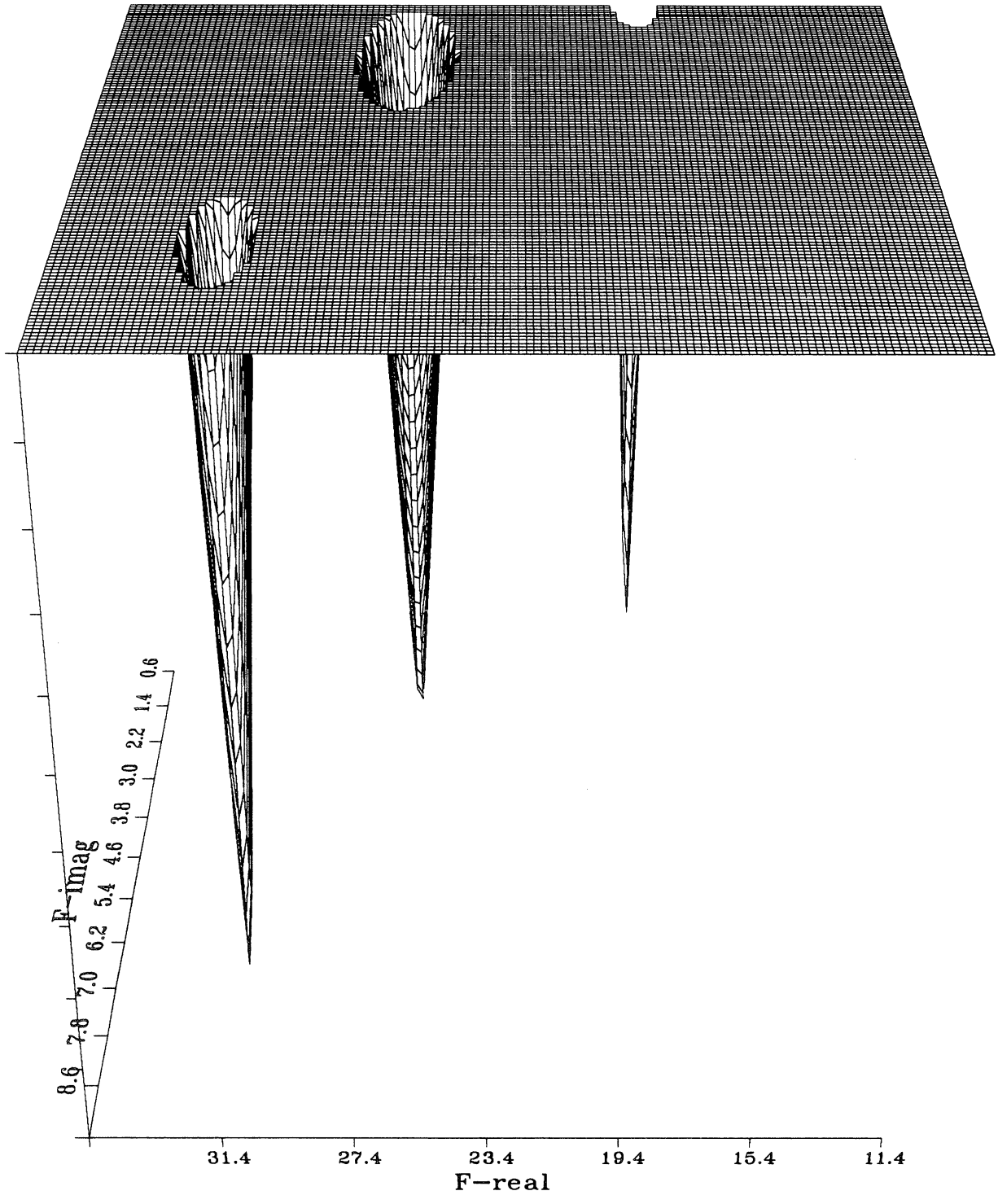

Equation for tand=1.5 (LSM)

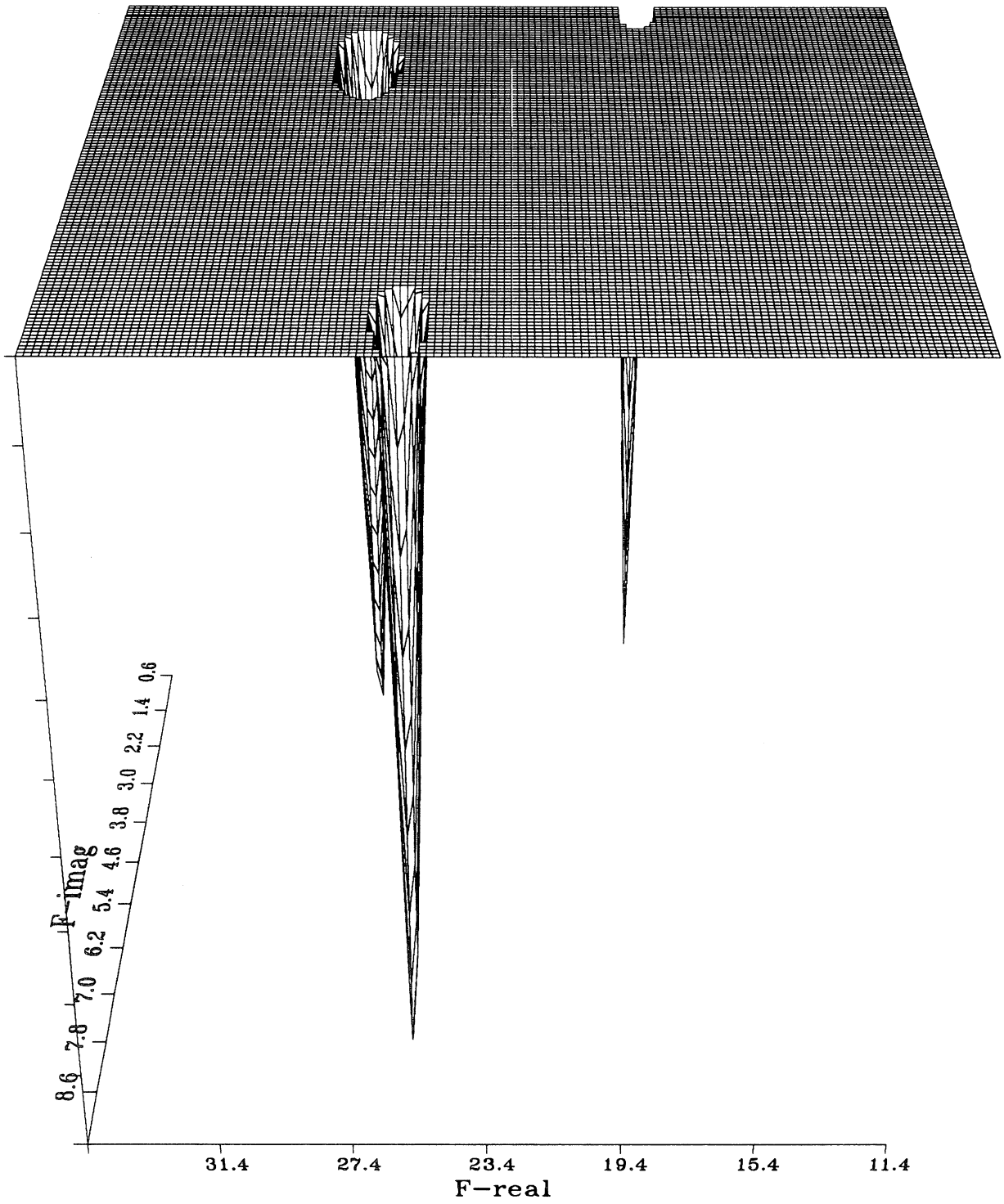

Equation for tand=2.0 (LSM)

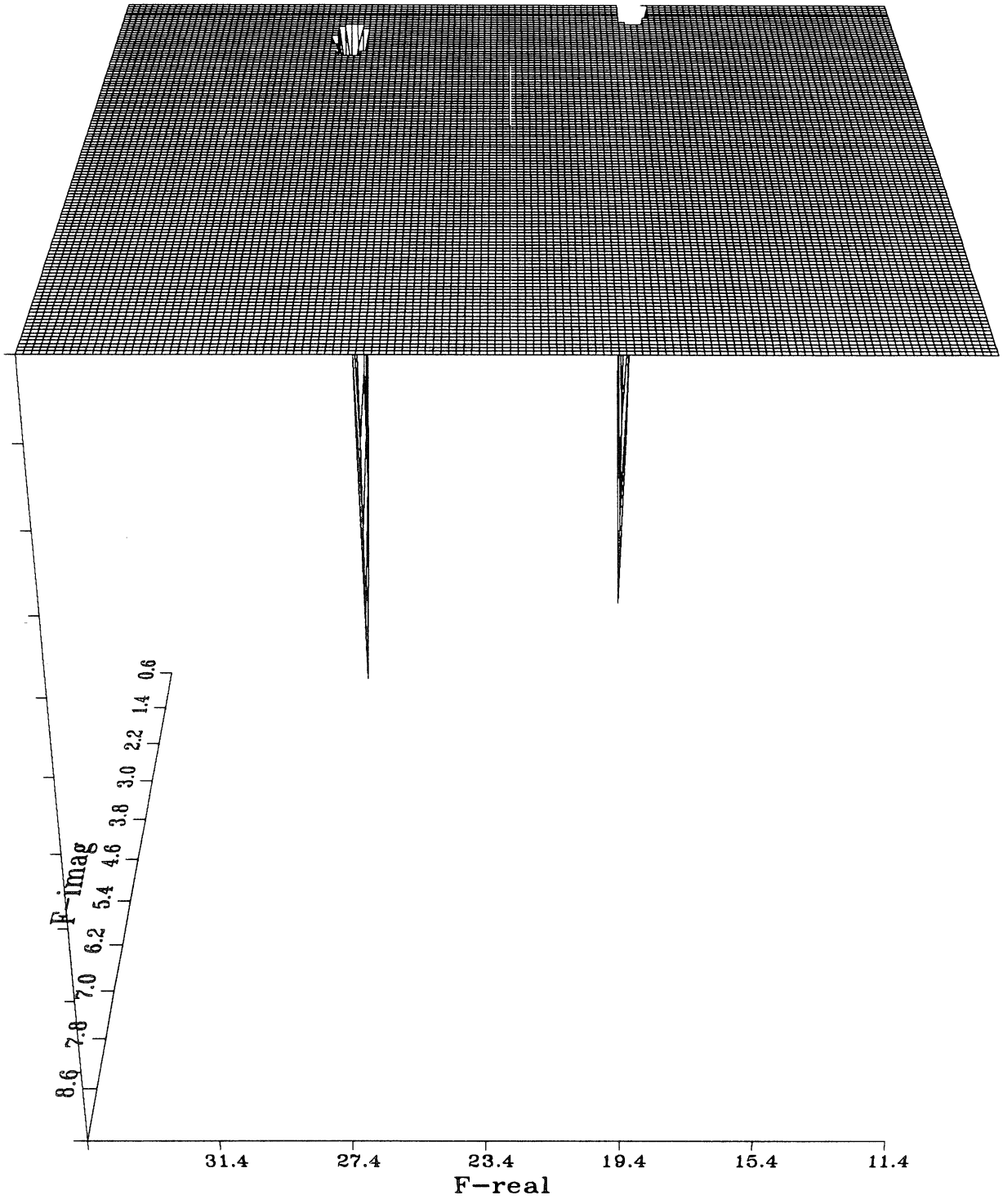

REFERENCES

1. L.P. Dunleavy and P.B. Katehi, "Shielding Effects in Microstrip Discontinuities - Part I: Theory." It has been submitted for publication in IEEE Trans. on Microwave Theory and Techniques.

2. L.P. Dunleavy and P.B. Katehi, "Shielding Effects in Microstrip Discontinuities - Part II: Applications." It has been submitted for publication in IEEE Trans. on Microwave Theory and Techniques.

3. E. Yamashita and K. Atsuki, "Analysis of Microstrip-Like Transmission Lines by Nonuniform Discretization of Integral Equations." IEEE Trans. Microwave Theory and Techniques, vol. MTT-24, No. 4, pp. 195-200, April 1976.

4. M. Hashimoto, "A Rigorous Solution for Dispersive Microstrip." IEEE Trans. on Microwave Theory and Techniques, vol. MTT-33, pp. 1131-1137, Nov. 1985.

5. C.J. Railton and T. Rozzi, "Complex Modes in Boxed Microstrip." IEEE Trans. on Microwave Theory and Techniques, vol. MTT-366, pp. 865-874, May 1988.